

Remote Sensing of the ocean

Cédric Jamet

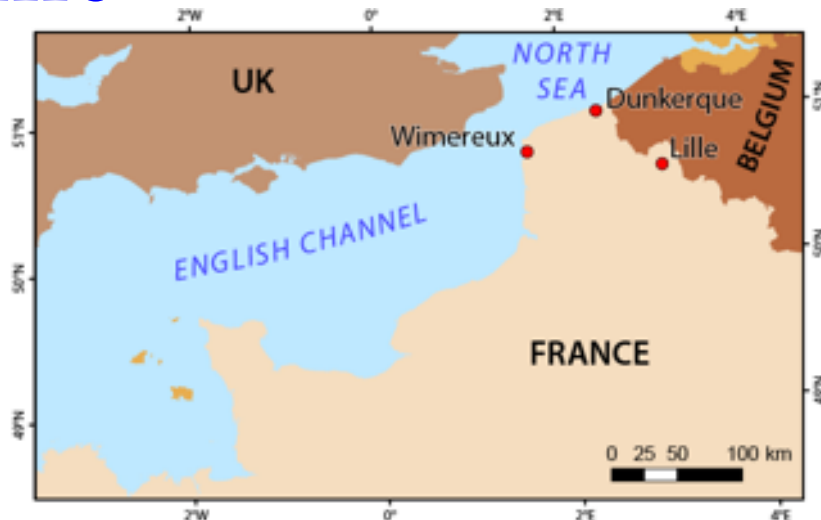
Laboratoire of Oceanology and Geosciences

Summer School ML4Oceans

cedric.jamet@univ-littoral.fr

About me

- PhD « Atmospheric correction of SeaWiFS images »: jan. 2004
- Associate professor since sept. 2006 at the Université du Littoral-Côte d'Opale and the Laboratory of Oceanology and Geosciences
- Chairman of an IOCCG WG on Evaluation of atmospheric correction algorithms over optically-complex waters
- Evaluation and improvements of atmospheric correction over optically-complex waters
- Retrieval of ocean color parameters using optimization and neural networks algorithms
- Lidar for ocean color



Inter-disciplinaries studies

- *observation/experimentation/modelling*
- *Focused on coastal and littoral environments*
- *From bacteria to satellite*
- *From micro-scale to climate scale*

Old marine station (1874), new lab created in 2008:

- *60 full-time permanent scientists*
- *30 PhD students*
- *130 members in total*



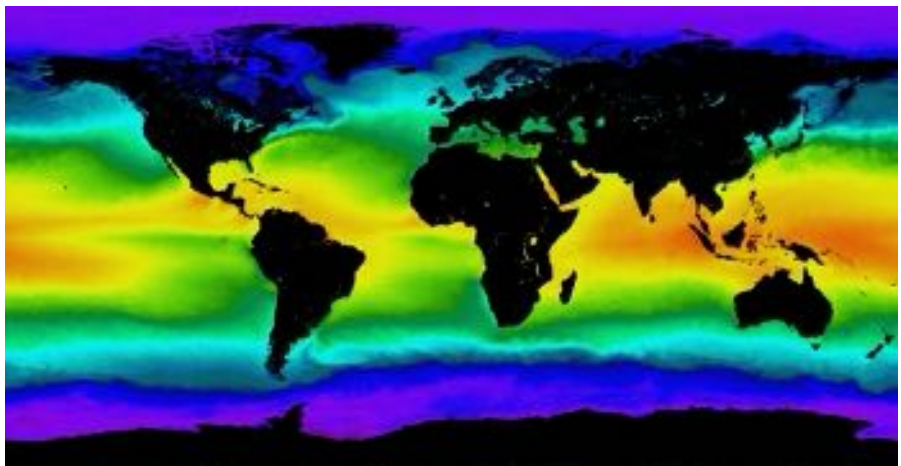
Content

- 101 Remote Sensing
- Sea-surface temperature
- Sea surface height
- Ocean Color Radiometry
- Vertical profiles of the upper ocean

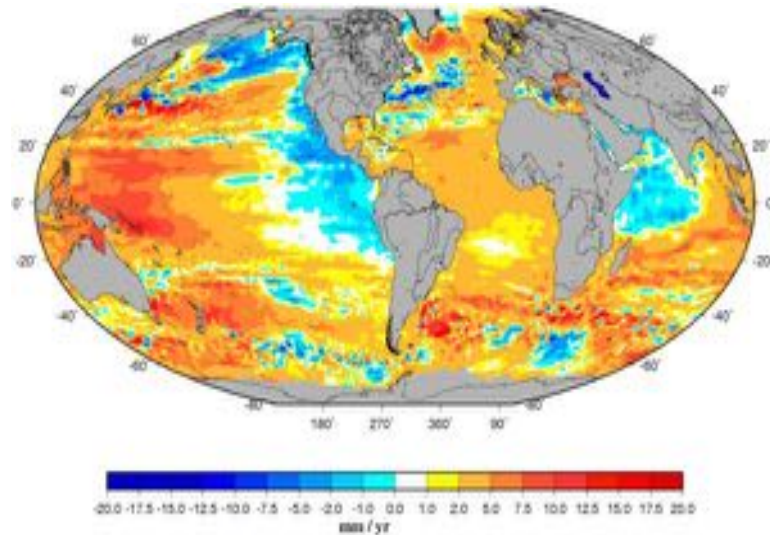
Content

- 101 Remote Sensing
- Sea-surface temperature
- Sea surface height
- Ocean Color Radiometry
- Vertical profiles of the upper ocean

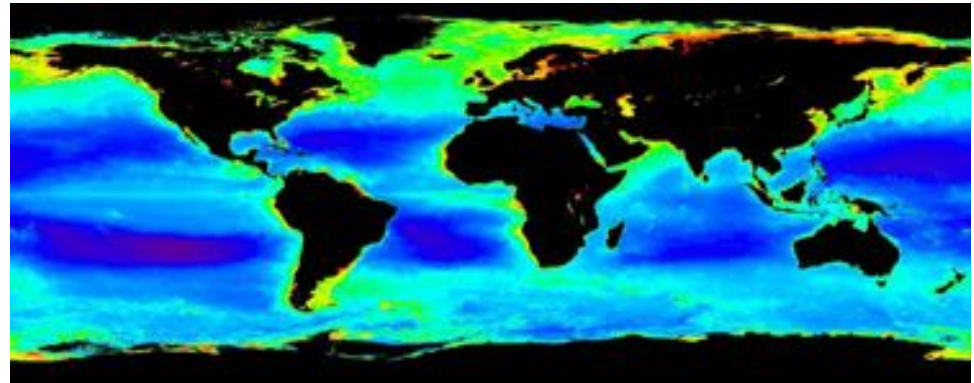
Space measurements



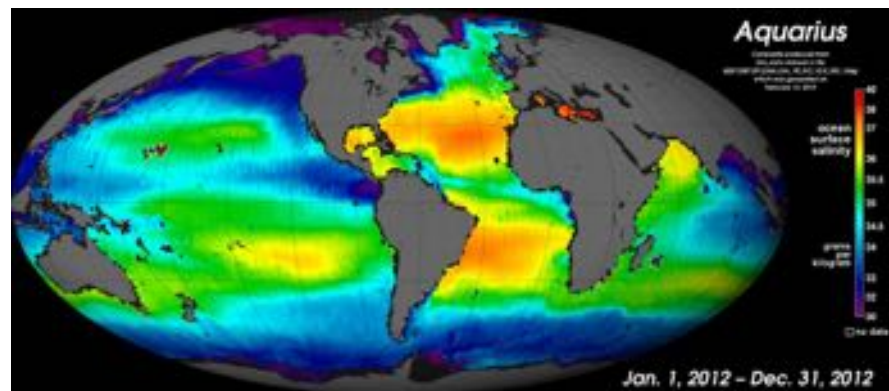
Mean annual SST in 2004 from MODIS (NASA)



Spatial distribution of the SSH variation between 1993 and 2006 from Topex/Poseidon and Jason-1



Mean annual chlorophyll-a concentration in 2002 from SeaWiFS



Mean annual salinity from AQUARIUS

What is remote sensing ?



Collecting and interpreting data on some properties of something by a recording device not in physical contact with it.



Field measurements



Airplane, or balloon

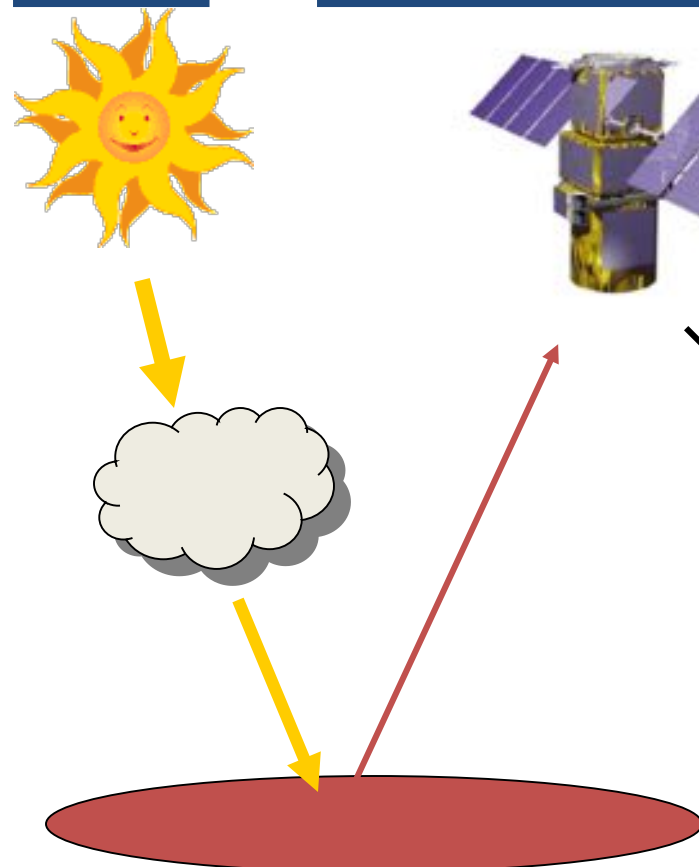


Satellite

Remote sensing: involves multiple steps

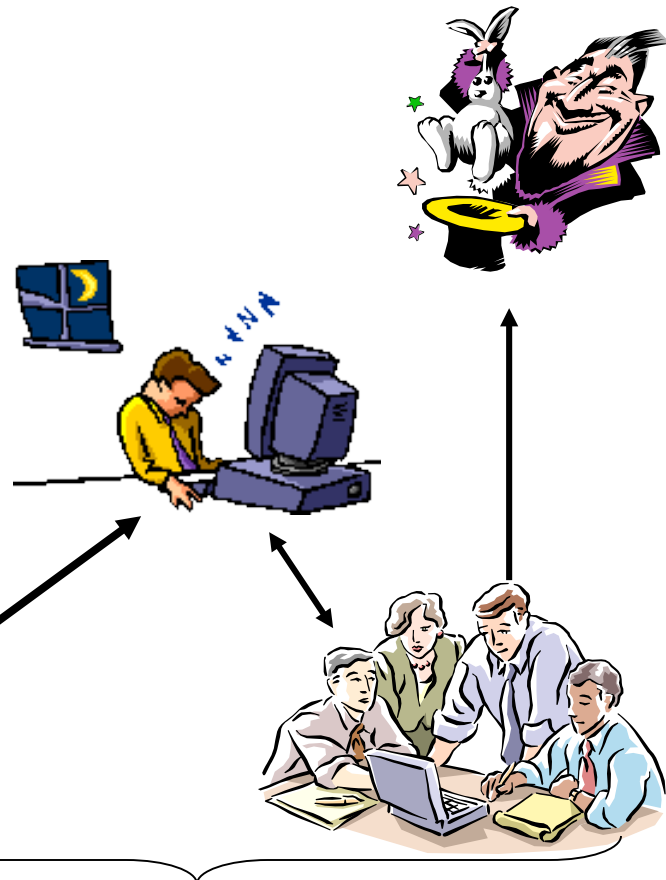
Source

Recording by the sensor

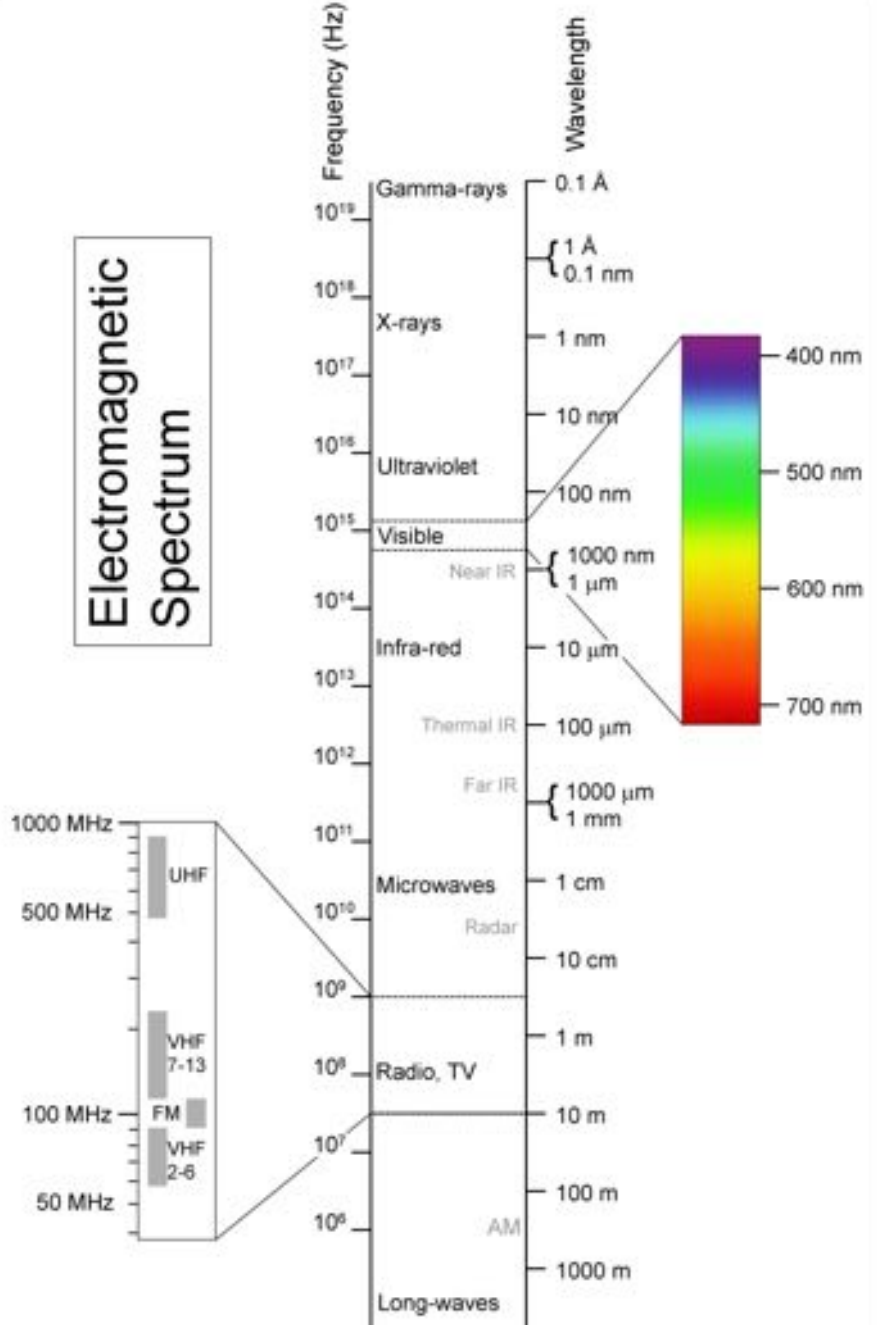


Interaction with the Target

Transmission, processing, analysis, and interpretation of the data



Electromagnetic Spectrum



Spectral ranges for some remote sensing applications

Ocean Color Radiometry
(400-865 nm)

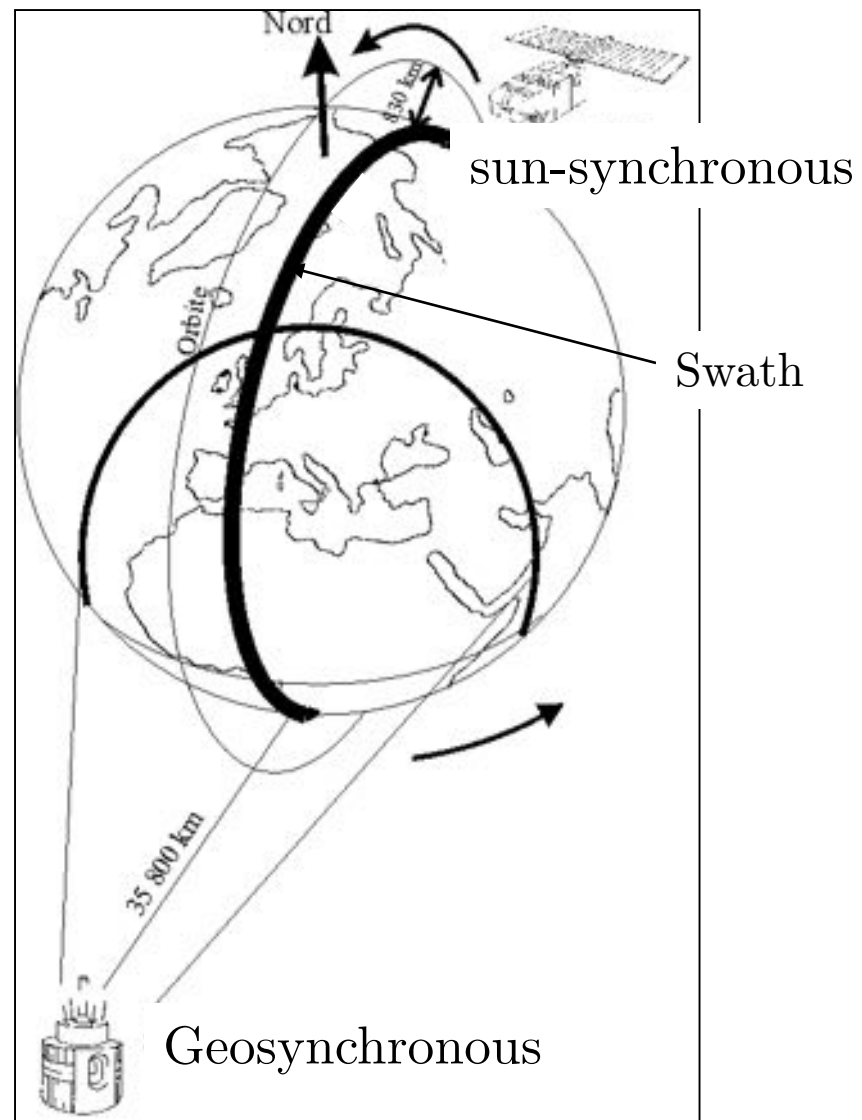
Atmospheric applications
(700-3500 nm)

Sea Surface Temperature
(3,5-20 mm)

Sea surface Height
(K_u Band, 13,6 GHz;
C band at 5.3 GHz)

Name of satellite orbits

orbit figure	circular orbit	$e = 0$
	ellipsoid orbit	$0 < e < 1$
	parabolic orbit	$e = 1$
	hyperbolic orbit	$1 < e$
inclination	equator orbit	$i \approx 0$
	slant orbit	$0 < i < 90^\circ$
	polar orbit	$i \approx 90^\circ$
period	earth synchronous	
	sun synchronous	
recurrency	recurrent orbit	
	semi-recurrent orbit	



Earth observation satellite orbits:
geosynchronous, sun-synchronous,
near equatorial low inclination.

Classification of sensors

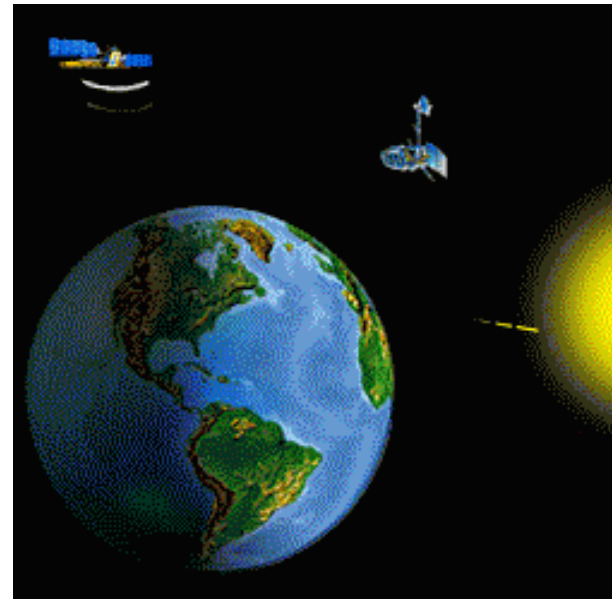
Passive sensors: measure levels of energy that are naturally emitted, reflected, or transmitted by the target object (sun is generally the source; and these sensors record the reflected and/or emitted (NIR) radiations). Some can operate at night (in the NIR).

Active sensors: provide their own energy source for illumination of the target (radar, lidar, scatterometer). Can operate at night, and over clouds cover areas.

Remarks:

Sensors which only records the sun energy reflected by the earth, can only record images while observing the sunlit side of the Earth.

source: <http://ccrs.nrcan.gc.ca>



Spatial, temporal, spectral, and radiometric resolutions

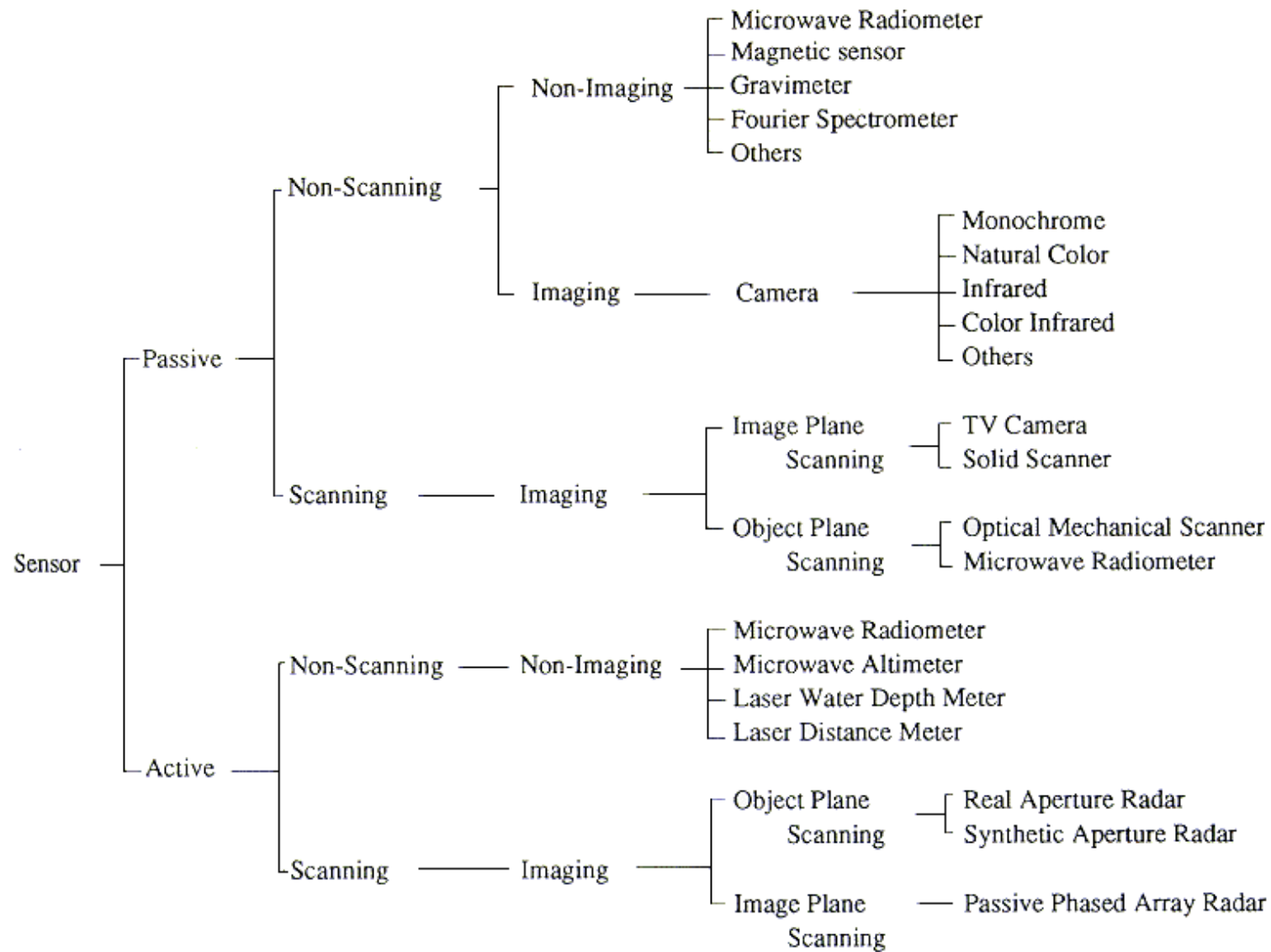
Spatial resolution: the pixel size of satellite images covering the earth surface (ground spatial resolution = IFOV x altitude).

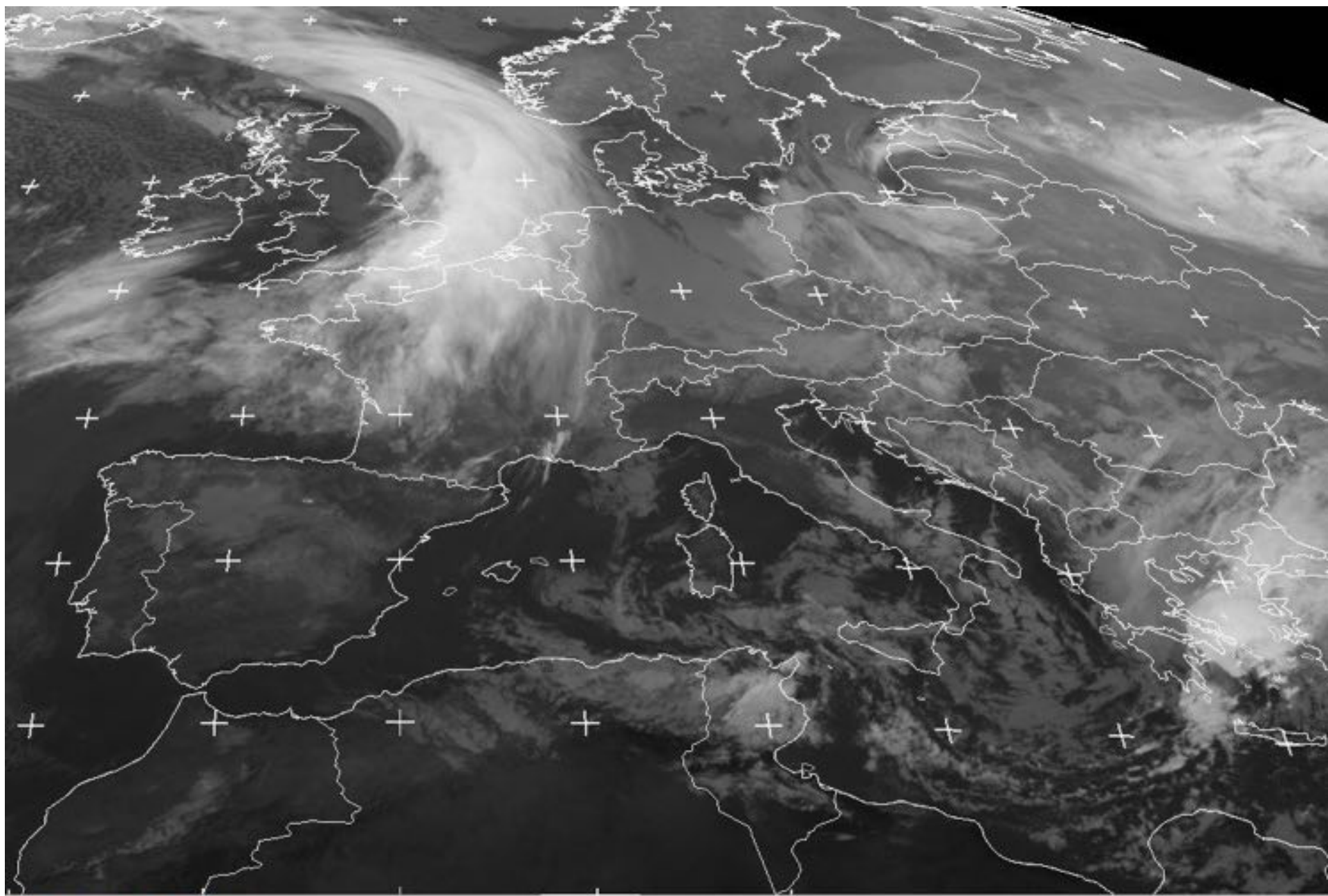
Temporal resolution: repetitive coverage of the ground by the platform

Spectral resolution: band-widths of the Electro-magnetic radiation of the channels used.

Radiometric resolution: the number of discrete levels into which signals may be divided.

Classification of sensors







Vegetation from MODIS true color images – resolution 1 km



Copyright Cnes 1998 - Distribution Spot Image

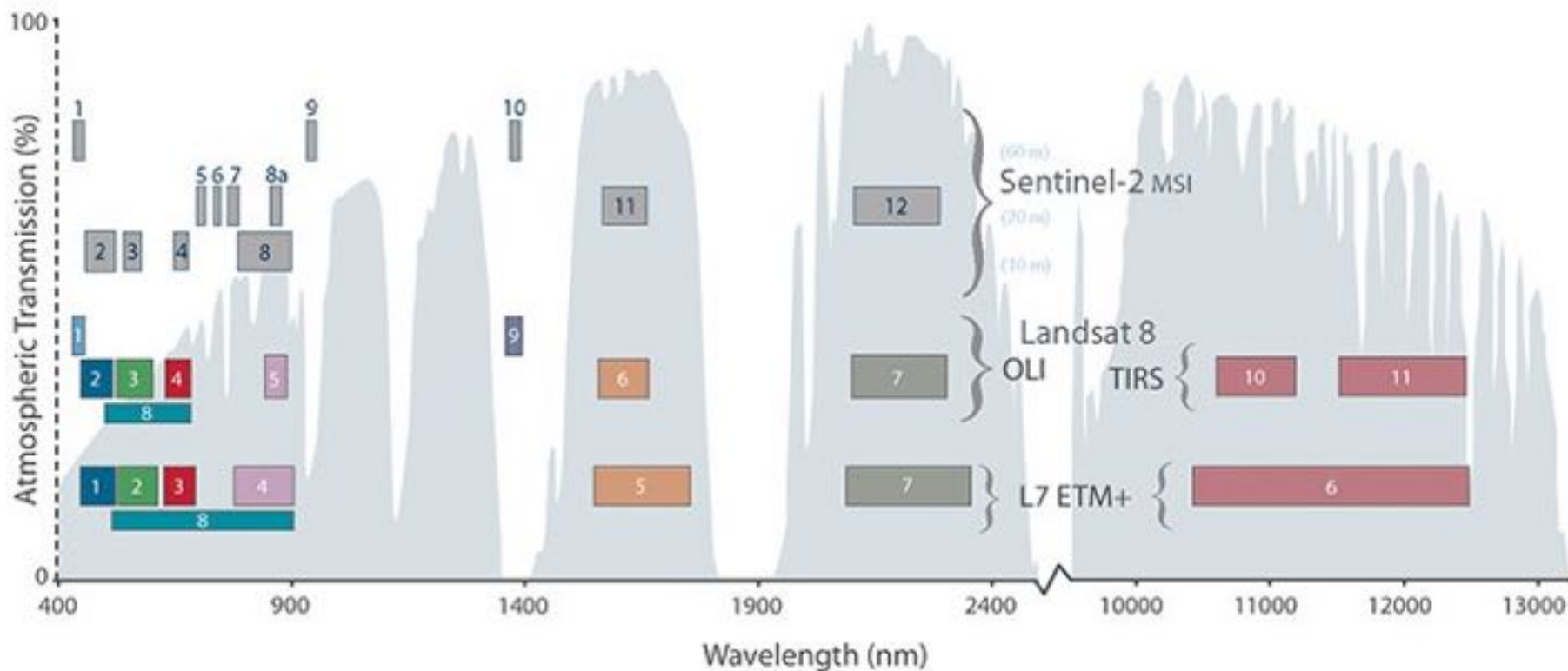
Rhône delta from SPOT4 - resolution 10 m

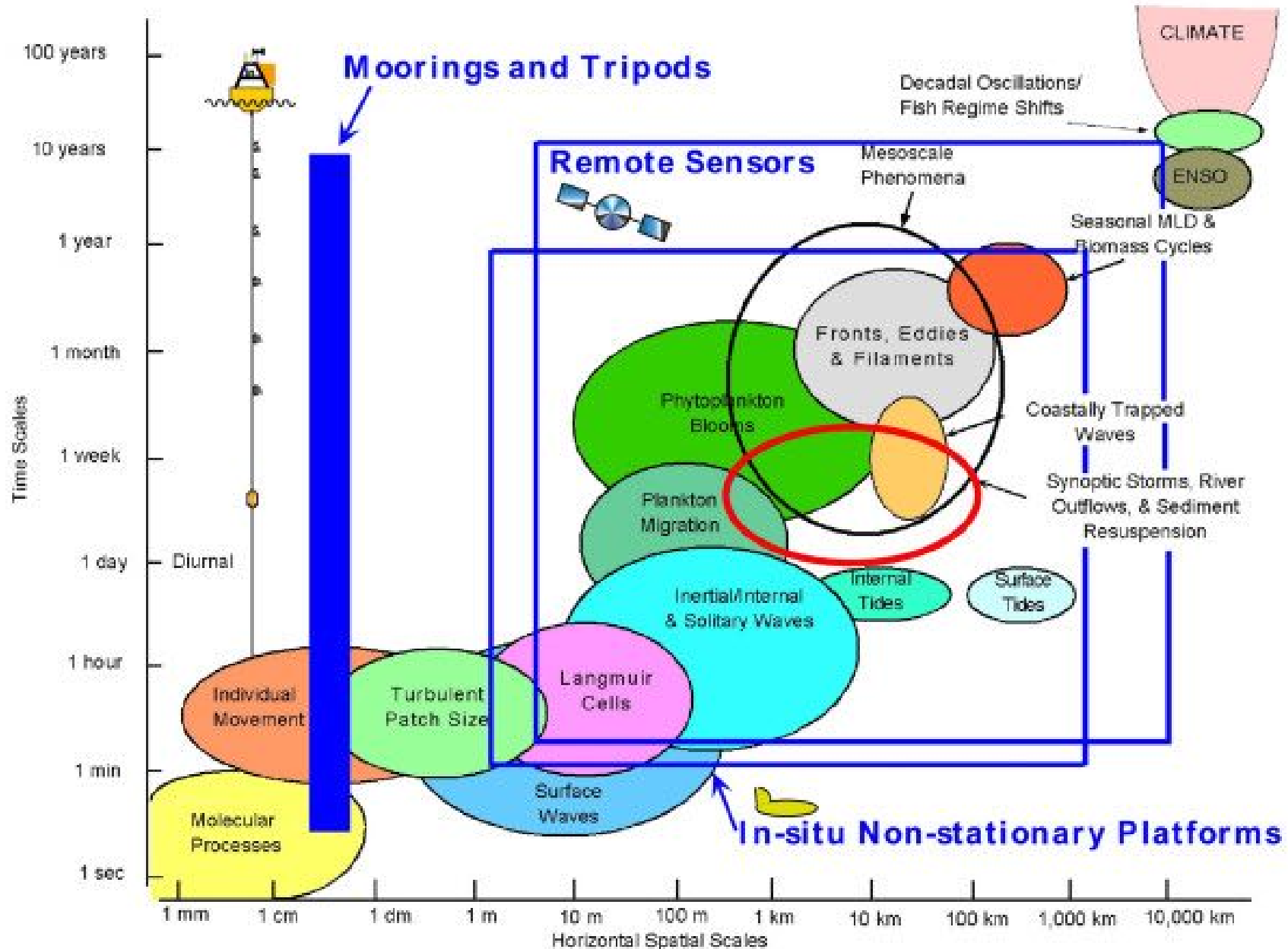
Mission ID	Mission Name Short	Mission Name Full	Mission Agencies	Mission Status	Launch Date	EOL Date
377	ADM-Aeolus	Atmospheric Dynamics Mission (Earth Explorer Core Mission)	ESA	Operational (nominal)	22 Aug 2018	Aug 2022
768	Biomass	Biomass	ESA	Approved	oct-22	Apr 2028
529	CryoSat-2	CryoSat-2 (Earth Explorer Opportunity Mission)	ESA	Operational (nominal)	08 Apr 2010	Dec 2020
580	EarthCARE	EarthCARE	ESA, JAXA	Approved	sept-22	sept-25
836	FLEX	Fluorescence Explorer	ESA	Approved	Apr 2024	Apr 2027
917	GOMX4	GomSpace Express-4	ESA, NSO	Operational (nominal)	02 Feb 2018	Dec 2020
260	Meteosat-10	Meteosat Second Generation-3	EUMETSAT, ESA	Operational (nominal)	05-juil-12	sept-30
451	Meteosat-11	Meteosat Second Generation-4	EUMETSAT, ESA	Operational (nominal)	15-juil-15	Dec 2033
229	Meteosat-8	Meteosat Second Generation-1	EUMETSAT, ESA	Operational (nominal)	28 Aug 2002	janv-22
259	Meteosat-9	Meteosat Second Generation-2	EUMETSAT, ESA	Operational (nominal)	22 Dec 2005	janv-25
261	Metop-A	Meteorological Operational Polar Satellite - A	EUMETSAT, NOAA, CNES, ESA	Operational (nominal)	19-oct-06	Dec 2021
230	Metop-B	Meteorological Operational Polar Satellite - B	EUMETSAT, NOAA, CNES, ESA	Operational (nominal)	17-sept-12	sept-24
231	Metop-C	Meteorological Operational Polar Satellite - C	EUMETSAT, NOAA, CNES, ESA	Operational (nominal)	07-nov-18	sept-23
557	METOP-SG A1	EUMETSAT Polar System, Second Generation	EUMETSAT, DLR, COM, CNES, ESA	Approved	oct-23	Apr 2031
838	METOP-SG A2	EUMETSAT Polar System, Second Generation	EUMETSAT, DLR, COM, CNES, ESA	Approved	nov-30	May 2038

Status	Sensor type	Platform	Sensor	Spatial Resolution=Pixel size	Spectral bands (400–1000 nm)	Revisit frequency (at equator)	Launch (end)	Water quality variables					
								Chl	CYP	TSM	CDOM	Kd	Turb/ SD
Defunct	Sun-sync	SeaStar	SeaWiFS	4 and 1 km	8	2 days	1997-(2010)						
		Envisat	MERIS	1.2 km and 0.3 km	15	2 days	2002-(2012)						
Current	Sun-sync	Terra/Aqua	MODIS-A&T	1 km	9	daily	1999/2000						
		Oceansat-2	OCM-2	300 m	8	2-3 days	2009						
		Suomi/NOAA-20	VIIRS	750 m	7	daily	2011/2017						
		Sentinel 3 A/B	OLCI	300 m	21	Daily (with 2 satellites)	2016/18						
	GEO	GCOM-C	SGI-2	250 m	9	2-4 days	2017						
		KOMPSAT	GOI	500 m	8	Half hourly	2010						
		Himawari-8&9, GOES-R	AHI	500 m–2 km	4	10 min	2014						
Future	Sun-sync	JPSS-2, JPSS-3	VIIRS	750 m	7	daily	2017, 2022,						
		Sentinel 3 C/D	OLCI	300 m	21	Daily (with 2 satellites)	>2022						
		Oceansat-3	OCM-3	300 m	13	2-3 days	2020						
		Sabia-MAR	MUS	200/800 m	13	1-2 days global							
		PACE	OCI	1 km	Hyperspectral; 5 nm (340–800 nm)	Daily	2022						
	GEO	KOMPSAT-3B	GOI	500 m	8s	Half hourly	2019						

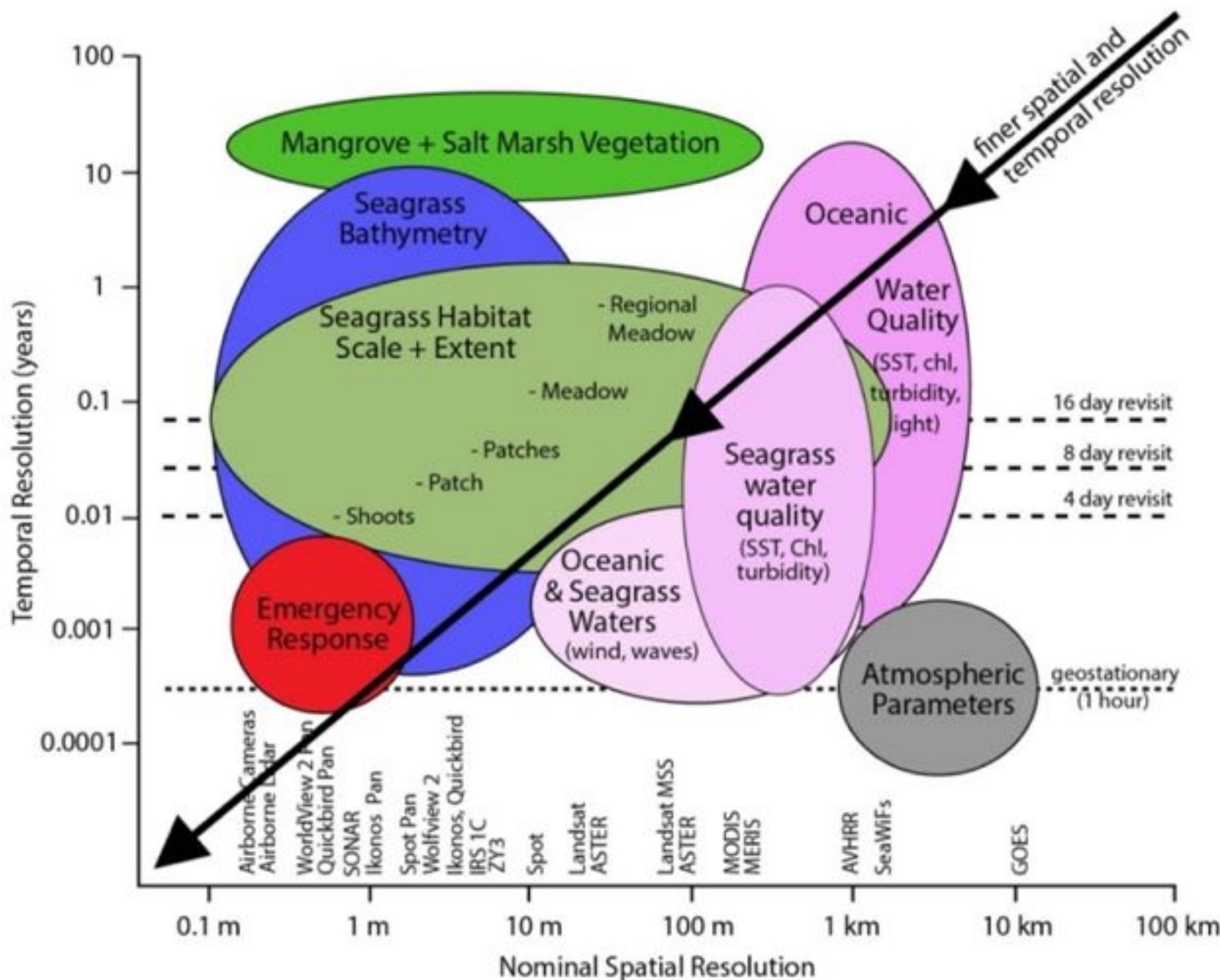
■: highly suitable, ■: suitable, ■: potential, ■: not suitable, Chl, Chlorophyll; CYP, cyanobacterial pigments (S denotes surface blooms); TSM, total suspended matter; CDOM, coloured dissolved organic matter; Kd, diffuse attenuation coefficient (or attenuation coefficient of diffuse light); Turb, Turbidity / SD, Secchi Disk Depth.

Comparison of Landsat 7 and 8 bands with Sentinel-2





Spatial and Temporal Resolution for Selected Parameters

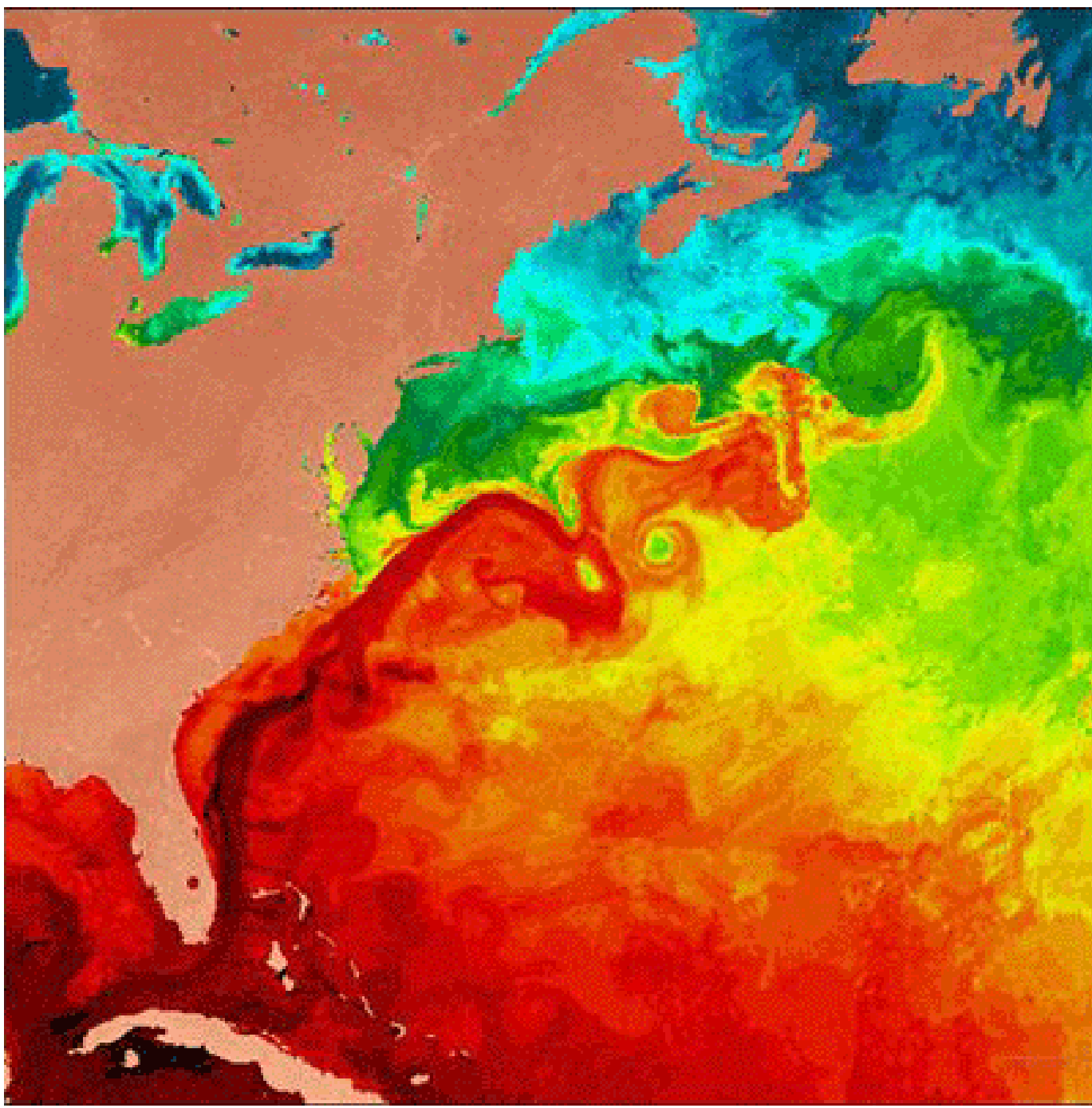


Content

- 101 Remote Sensing
- **Sea-surface temperature**
- Sea surface height
- Ocean Color Radiometry
- Vertical profiles of the upper ocean

Why studying Sea Surface Temperature (SST)?

- Satellite Obs.: Understanding of regional and global variabilities of climate change
 - Spatial and temporal patterns of water vapor and heat atmospheric fluxes: $f(\text{SST})$
 - SST proportional to heat capacity of ocean surface
- Obs. large variety of oceanic movements



Why studying Sea Surface Temperature (SST)?

- Satellite Obs.: Understanding of regional and global variabilities of climate change
 - Spatial and temporal patterns of water vapor and heat atmospheric fluxes: $f(\text{SST})$
 - SST proportional to heat capacity of ocean surface
- Obs. large variety of oceanic movements
- Impact on biodiversity
- Impact on marine life

What is SST?

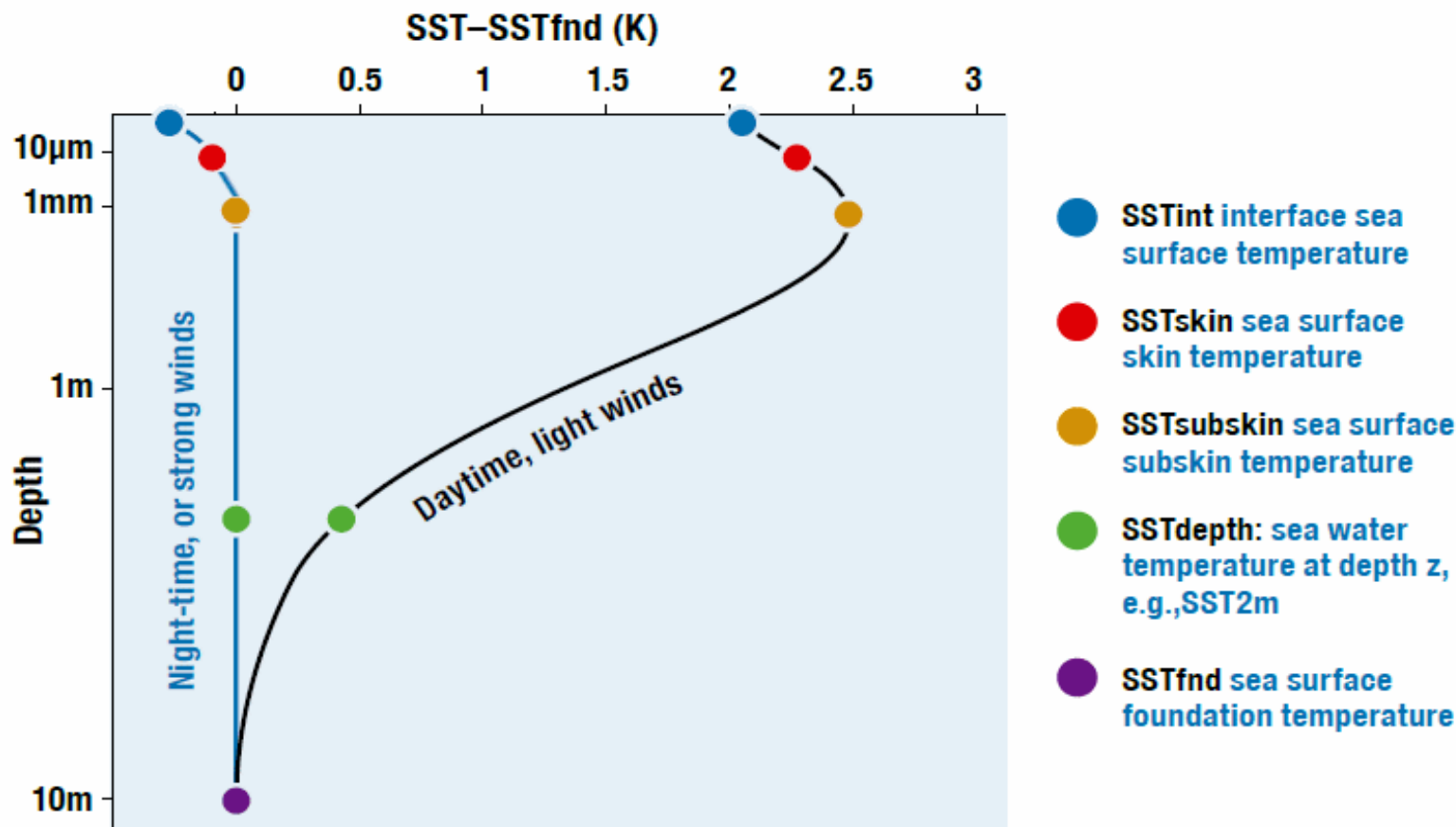


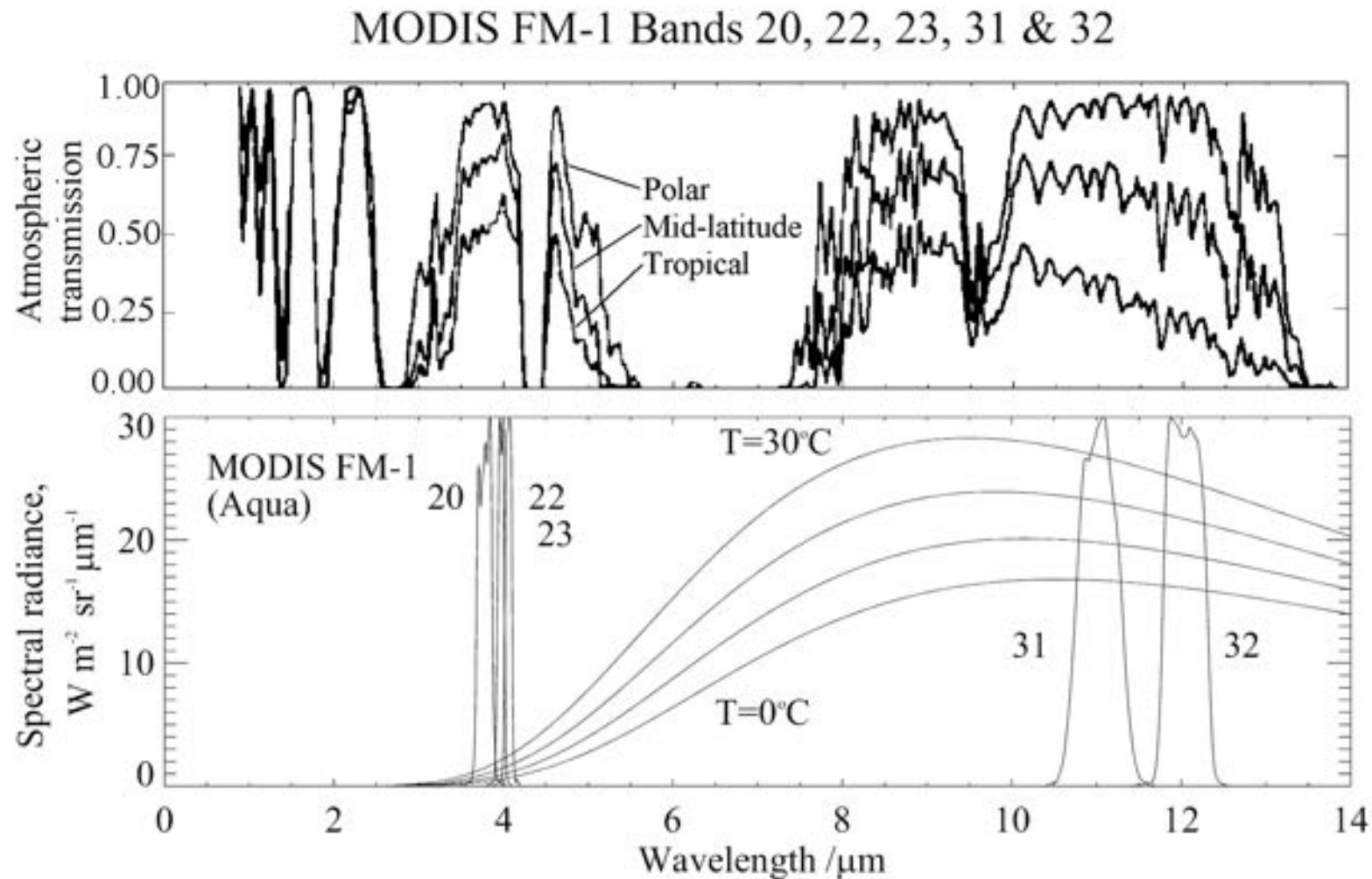
Figure 1: The hypothetical vertical profiles of temperature for the upper 10m of the ocean surface in high wind speed conditions or during the night (red) and for low wind speed during the day (black).

What is SST?

- Ocean infrared emission: <1mm of the ocean – **skin layer**
- Ocean-to-atmosphere heat flow through the skin layer is by molecular conduction: this causes, and results from, a temperature gradient through the skin layer
- Classic measurements of SST from in-water thermometers - **“bulk” T**
- T_{depth} : no impacted by diurnal heat- **“foundation” temperature.**

Infra-red measurements of SST

Based on the brightness temperature at two bands (black body)



$$L(\lambda_i, z_H) = L_0(\lambda_i) t_i^{\sec \theta} + f_P(\bar{T}, \lambda_i) (1 - t_i^{\sec \theta})$$

- i: # bande
- Left part: radiance measured by the satellite
- 1st right term: attenuated surface radiance
- 2nd right term: atmospheric radiance
- $\underline{1} - t$: atmospheric emissivity
- \bar{T} : mean température moyenne of low troposphere
- Can be simplified by using Planck's function
 - Hyp.: $e=1 \rightarrow L_0$ emitted by surface is $f_P(T_s, \lambda_i)$, where f_P is the Planck's function est la fonction de Planck et T_s , the skin temperature (skin). Same thing for the radiance measured by the satellite

The SST atmospheric correction algorithms

The form of the daytime and night-time algorithm for measurements in the long wave atmospheric window is:

$$SST = c_1 + c_2 * T_{11} + c_3 * (T_{11} - T_{12}) * T_{sfc} + c_4 * (\sec(\theta) - 1) * (T_{11} - T_{12})$$

where T_n are brightness temperatures measured in the channels at $n \mu\text{m}$ wavelength, T_{sfc} is a 'climatological' estimate of the SST in the area, and θ is the satellite zenith angle. This is based on the Non-Linear SST algorithm.

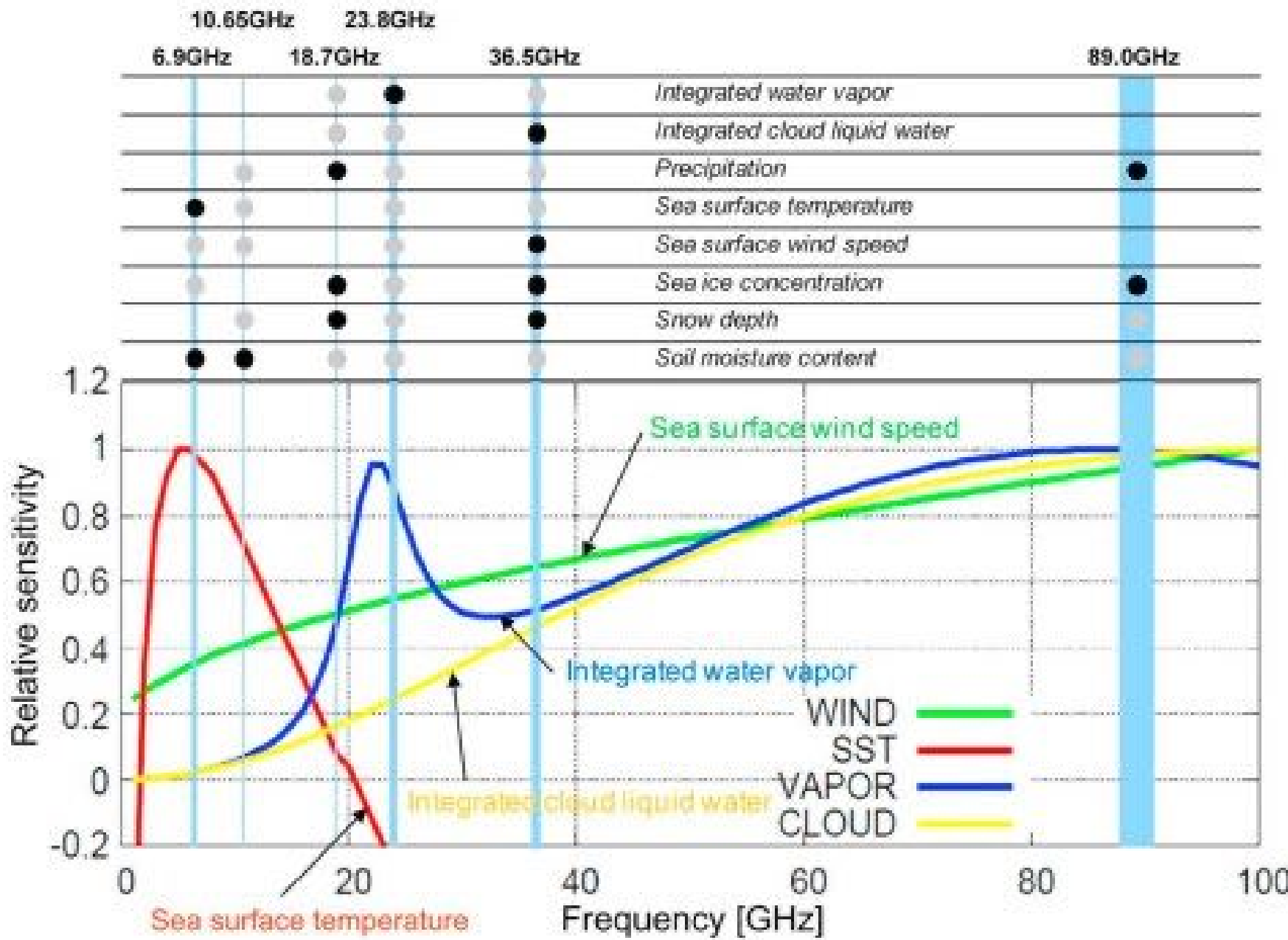
[Walton, C. C., W. G. Pichel, J. F. Sapper and D. A. May (1998). "The development and operational application of nonlinear algorithms for the measurement of sea surface temperatures with the NOAA polar-orbiting environmental satellites." Journal of Geophysical Research **103** 27,999-28,012.]

The MODIS night-time algorithm, using two bands in the $4\mu\text{m}$ atmospheric window is:

$$SST4 = c_1 + c_2 * T_{3.9} + c_3 * (T_{3.9} - T_{4.0}) + c_4 * (\sec(\theta) - 1)$$

Note, the coefficients in each expression are different. They can be derived in three ways:

- empirically by regression against SST values derived from another validated satellite instrument
- empirically by regression against SST values derived from surface measurements from ships and buoys
- theoretically by numerical simulations of the infrared radiative transfer through the atmosphere.



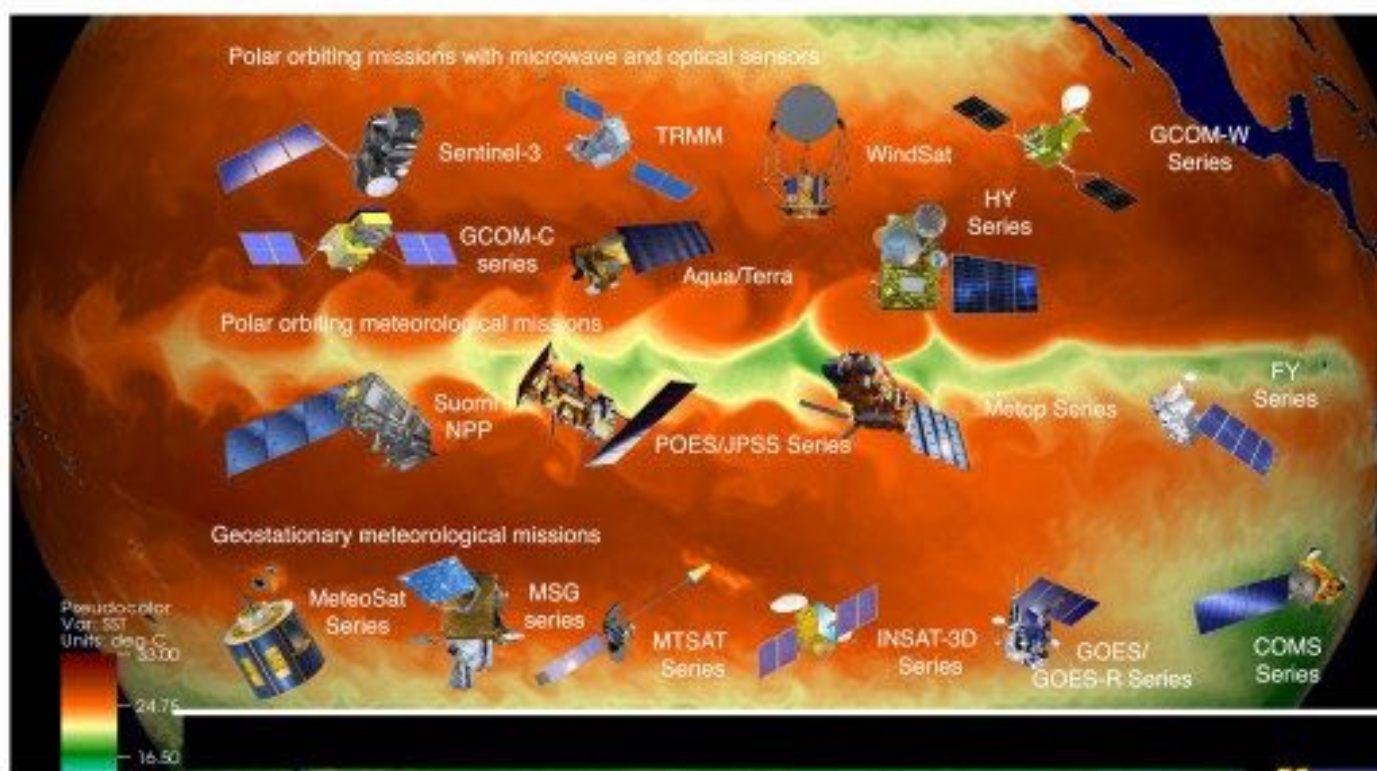


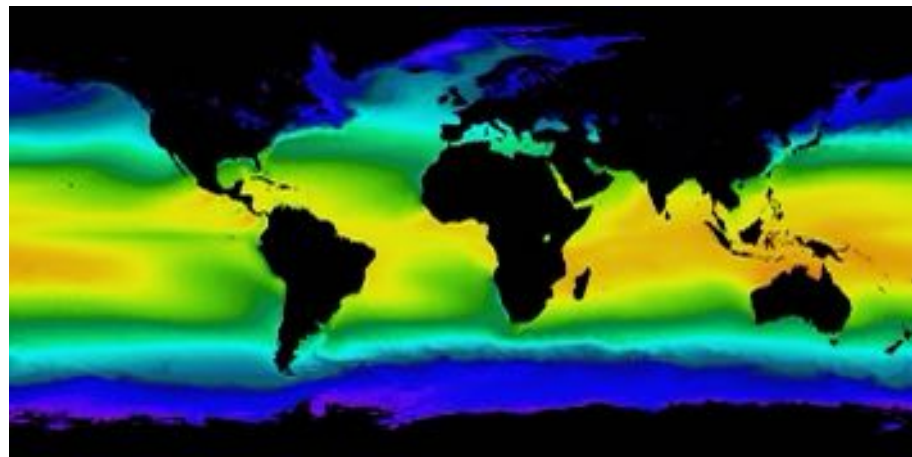
FIGURE 1 | The main satellite missions contributing to the current SST constellation. (Reproduced by permission under CC BY 4.0 from <http://doi.org/10.6084/m9.figshare.7291694>.

TABLE 1 | Current platform and sensor characteristics with capability for sea surface temperature, specifying whether in GEO or LEO; IR or PMW; daily coverage; spatial resolution at nadir; position or orbit and equator crossing time; agency and the expected lifetime till.

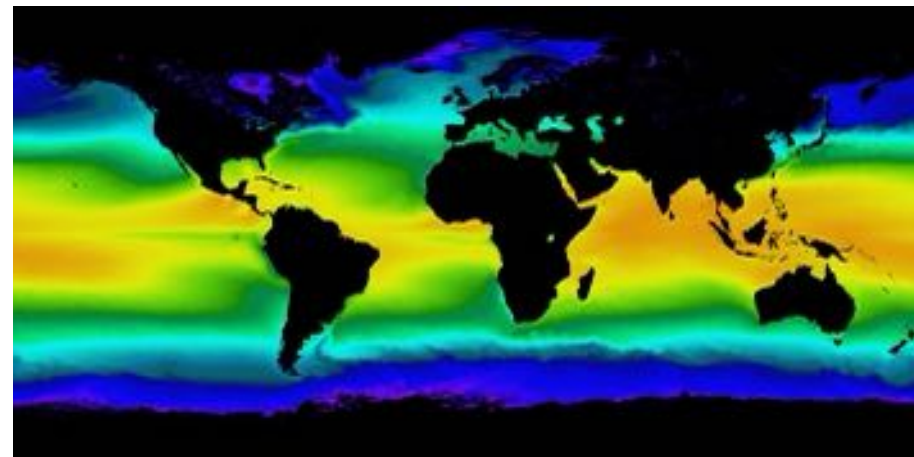
Platform	Sensor	GEO/LEO	IR/PMW	Coverage	Spatial resolution at nadir (SST channels)	Position/orbit (equator crossing time)	Agency	Expected lifetime till
Meteosat ¹	SEVIRI	GEO	IR	Full disk 15 min	3 km	0°	EUMETSAT	2024
GOES-R (S/T/U)	ABI	GEO	IR	Full disk 10 min	2 km	E: 72.5°W W: 137.2°E	NOAA	2036
Himawari	AHI	GEO	IR	Full disk 10 min	2 km	140.7°E	JMA	2031
FY-2	S-VISSR	GEO	IR	Full disk 30 min	5 km	86.5°E	CMA	2022
FY-4	AGRI	GEO	IR	Full disk 15 min	4 km	105°E	CMA	2040
Electro-L	MSU-GS	GEO	IR	Full disk 15–30 min	4 km	76°E	RosHydroMet	2039
GEO-KOMPSAT	AMI	GEO	IR	Full disk <10 min	2 km	128.2°E	KMA	2031
INSAT-3D	Imager	GEO	IR	Full disk 30 min	4 km	82°E	ISRO	2029
Terra	MODIS	LEO	IR	Global 2 days	1 km	Sun-synchronous 10:30	NASA	2022
Aqua	MODIS	LEO	IR	Global 2 days	1 km	Sun-synchronous 13:30	NASA	2025
Sentinel-3	SLSTR	LEO	IR	Global 1–2 days	1 km	Sun-synchronous 10:00	EU	2031
EPS ²	AVHRR/3 IASI	LEO	IR	Global twice per day/near global twice per day	1.1 km/12 km IFOV	Sun-synchronous 09:30	EUMETSAT	2024
S-NPP	VIIRS	LEO	IR	Global twice per day	750 m	Sun-synchronous 13:30	NASA & NOAA	2025
JPSS (NPP/N20 and J2/3/4)	VIIRS	LEO	IR	Global twice per day	750 m	Sun-synchronous 13:25	NOAA	2038
Meteosat-M	MSU-MR	LEO	IR	Global twice per day	1 km	Sun-synchronous 15:09	RosHydroMet	2030
GCOM-C	SGI	LEO	IR	Global in 3 days (day-night)	250 m/1 km	Sun-synchronous 10:30	JAXA	2022
HY-2	MWII	LEO	PMW	Daily global	80 × 120 km IFOV at 6.6 GHz	Sun-synchronous 06:00	NSOAS	2023
GPM-Core	GMI	LEO	PMW	Near-global in 2 days <70° latitude	19 × 32 km IFOV at 10.65 GHz	Drifting, 65° inclination	NASA/JAXA	2019
GCOM-W	AMSR-2	LEO	PMW	Global once per day	35 × 62 km IFOV at 6.9 GHz	Sun-synchronous 13:30	JAXA	2019
Coriolis	WindSat	LEO	PMW	Global in 1.5 days	39 × 71 km IFOV at 6.8 GHz	Sun-synchronous 06:00	US/NASA	2019
FY-3	VIRR/MERSI-2/MWRI	LEO	IR/PMW	Global twice per day	250 m/51 × 85 km IFOV at 10.65 GHz	Sun-synchronous 06:00/14:00	CMA	2029

¹Meteosat Third Generation (MTG) will follow-on from MSG until 2036. ²EUMETSAT Polar System-Second Generation (EPS-SG) will follow-on from EPS until 2043.

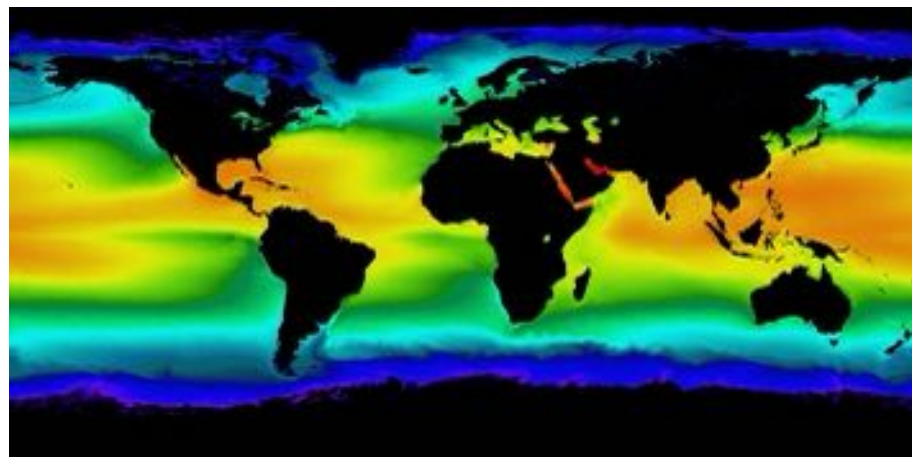
Winter



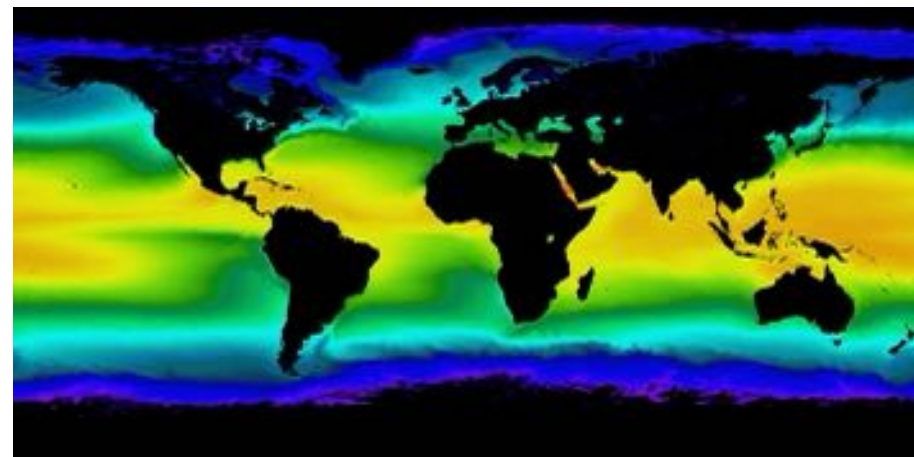
Spring



Summer



Fall



Seasonal climatology of SST between 2002 and 2015 from MODIS/NASA sensor at 4 μ m during nighttime

https://cfs.climate.esa.int/index.html#/stories/story-16/2?tags=sea-surface-temperature&globe=SI-41.64I34.93I25009995.54I360.00I-89.82I0.00I586465940422.00I0.00Isst.analysed_sstI

<https://cfs.climate.esa.int/index.html#/stories?globe=SI-23.75I20.83I15088309.07I360.00I-89.87I0.00I0.00I0.00II>

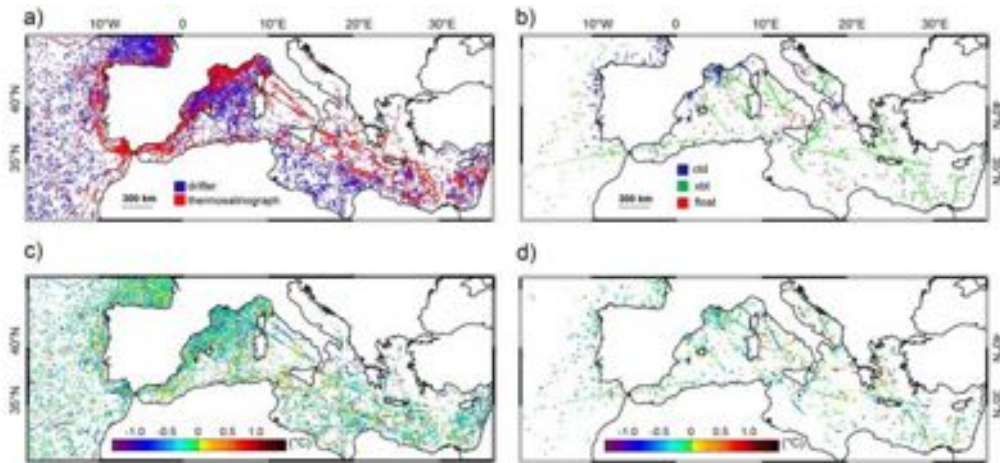


Fig. 6. Spatial distribution of matchup points between PFV52 and (a) drifter and TSG measurements; (b) CTD, XBT and ARGO float measurements, PFV52 minus in situ differences for (c) drifter and TSG matchups and (d) CTD, XBT and ARGO float matchups. Average depth chosen for vertical profile data types is 3 m and the validation period in 1982–2012.

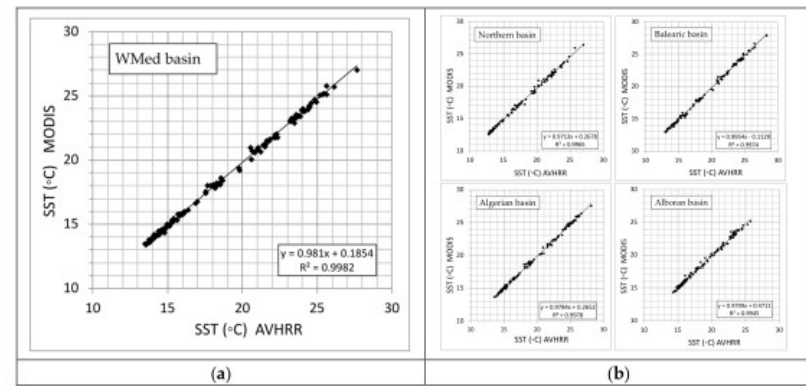
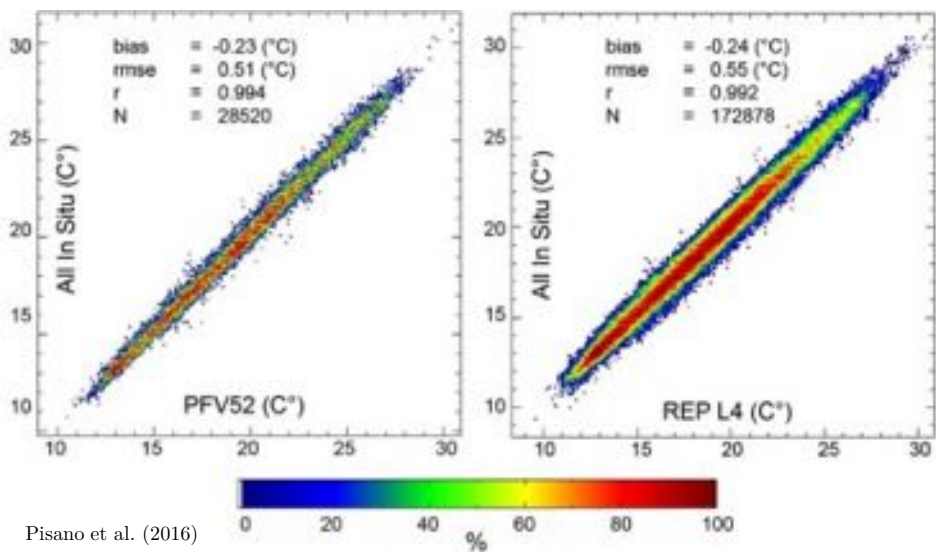


Figure 4. Correlation between monthly SST obtained from AVHRR and MODIS sensors in different basins: (a) Western Mediterranean and (b) Northern, Balearic, Algerian, and Alboran sub-basins.

Garcia (2020)



Pisano et al. (2016)

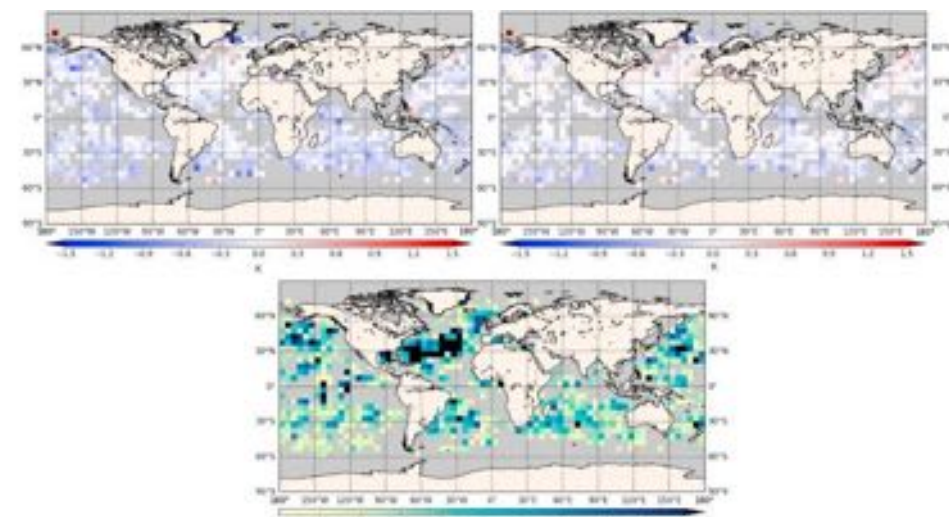


Fig. 14. Maps of the differences between Metop-B AVHRR and drifting buoys temperatures at night for October 2018. Top left: Mean differences (mean = -0.16 K, standard deviation = 0.53 K); top right: Median differences (median = -0.05 K, robust standard deviation = 0.38 K); bottom: number of matchups in 5° latitude \times longitude bins - bins with < 5 matchups are excluded from the analysis. There are 14,560 cases. (Data produced by the OSI SAF; quality index data from 3 to 5 have been used.)

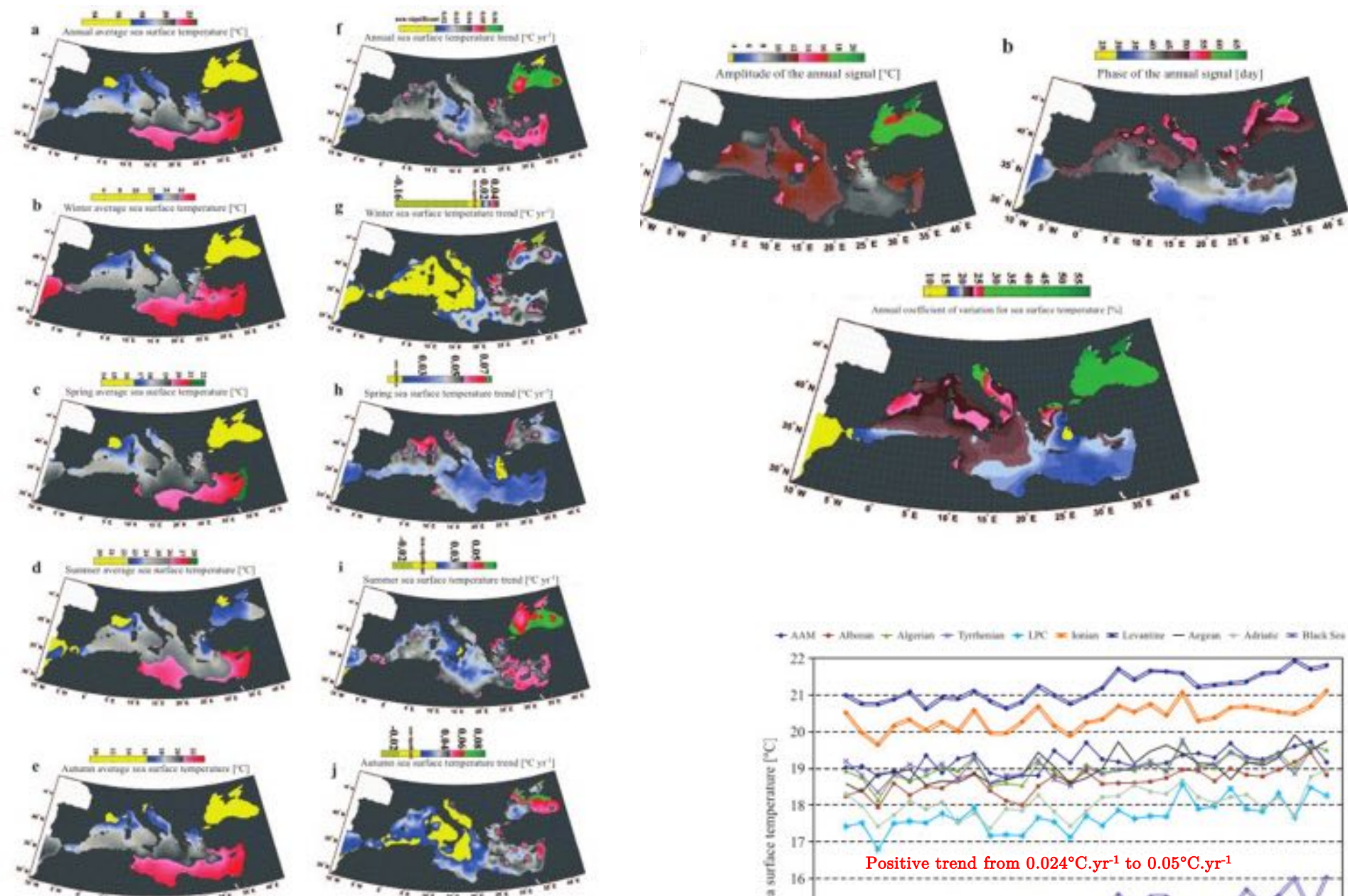
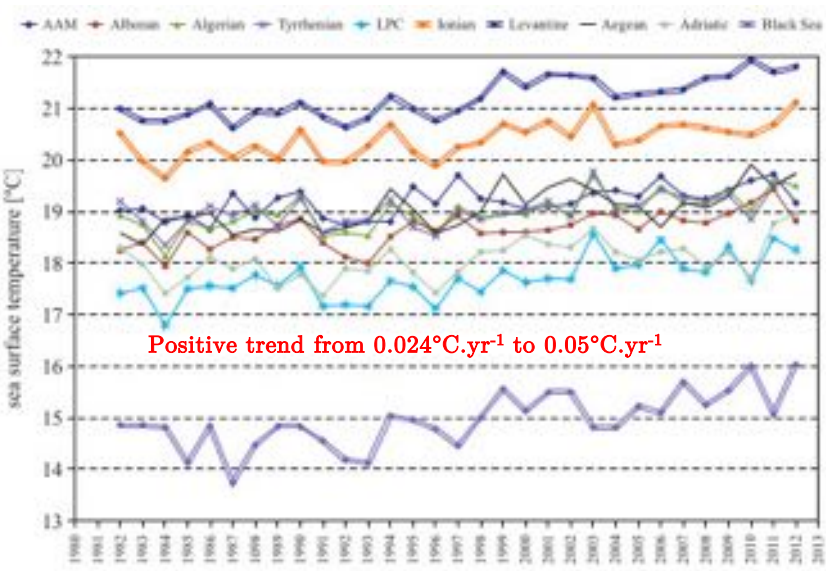
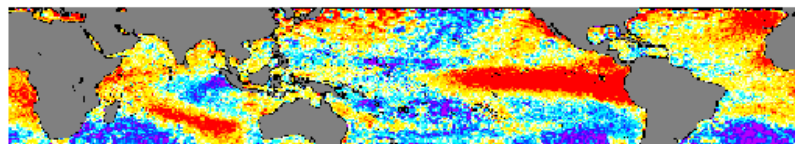


Figure 2. Spatial distribution of annual/seasonal SST means and trends over the 1982–2012 period; green in the left (right) panels (*continued on next page*)

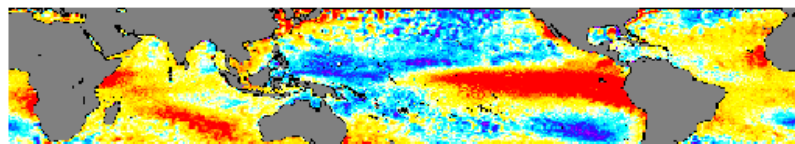


1997/1998 EL NINO

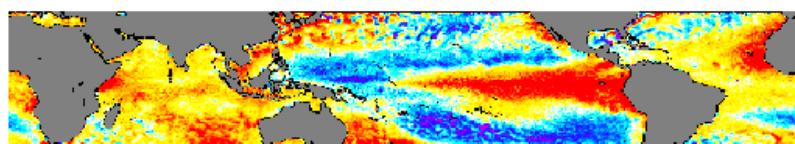
December 1997



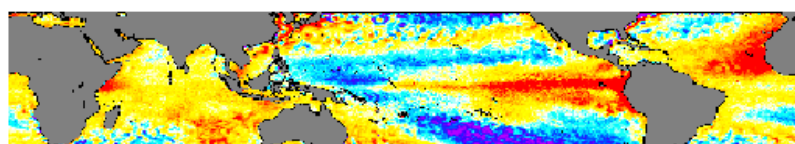
January 1998



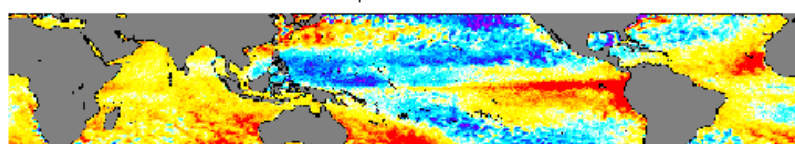
February 1998



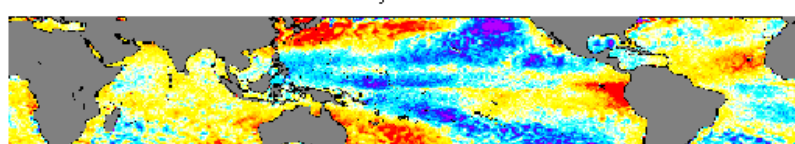
March 1998



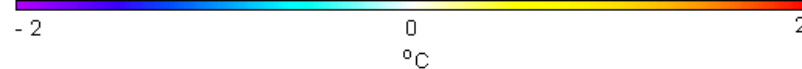
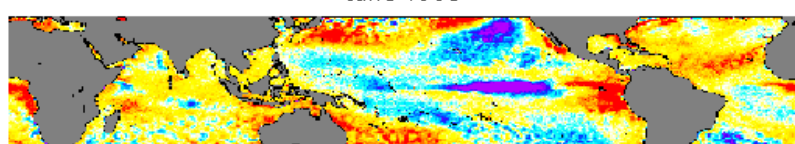
April 1998



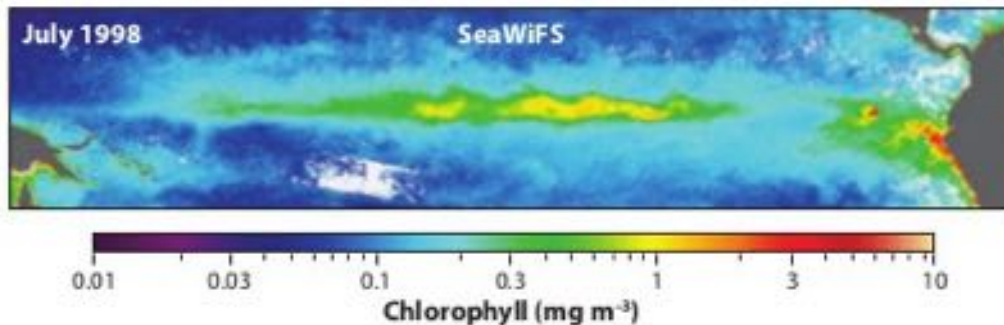
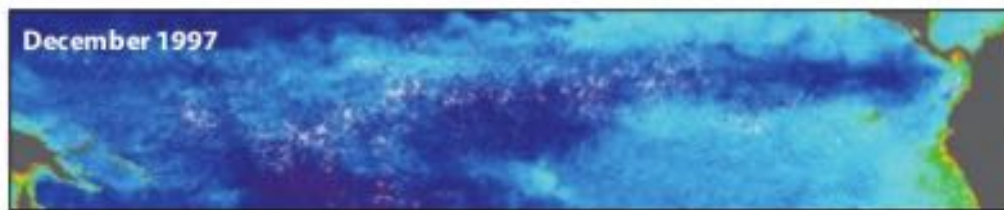
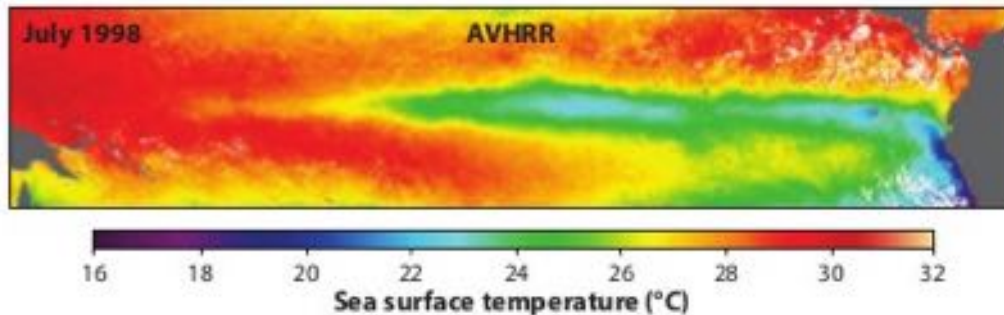
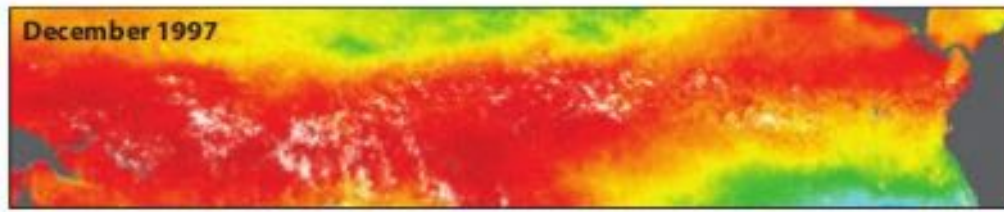
May 1998



June 1998



Correlation between SST and chlorophyll-a concentration during 1997/1998 ENSO event



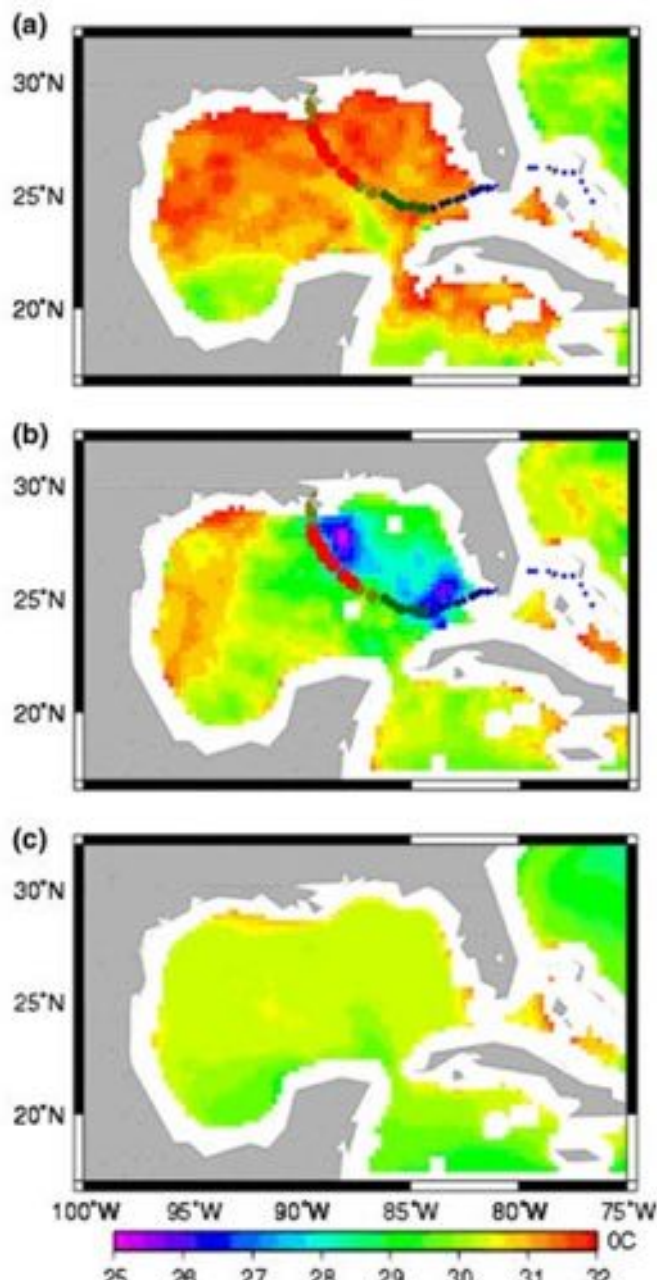
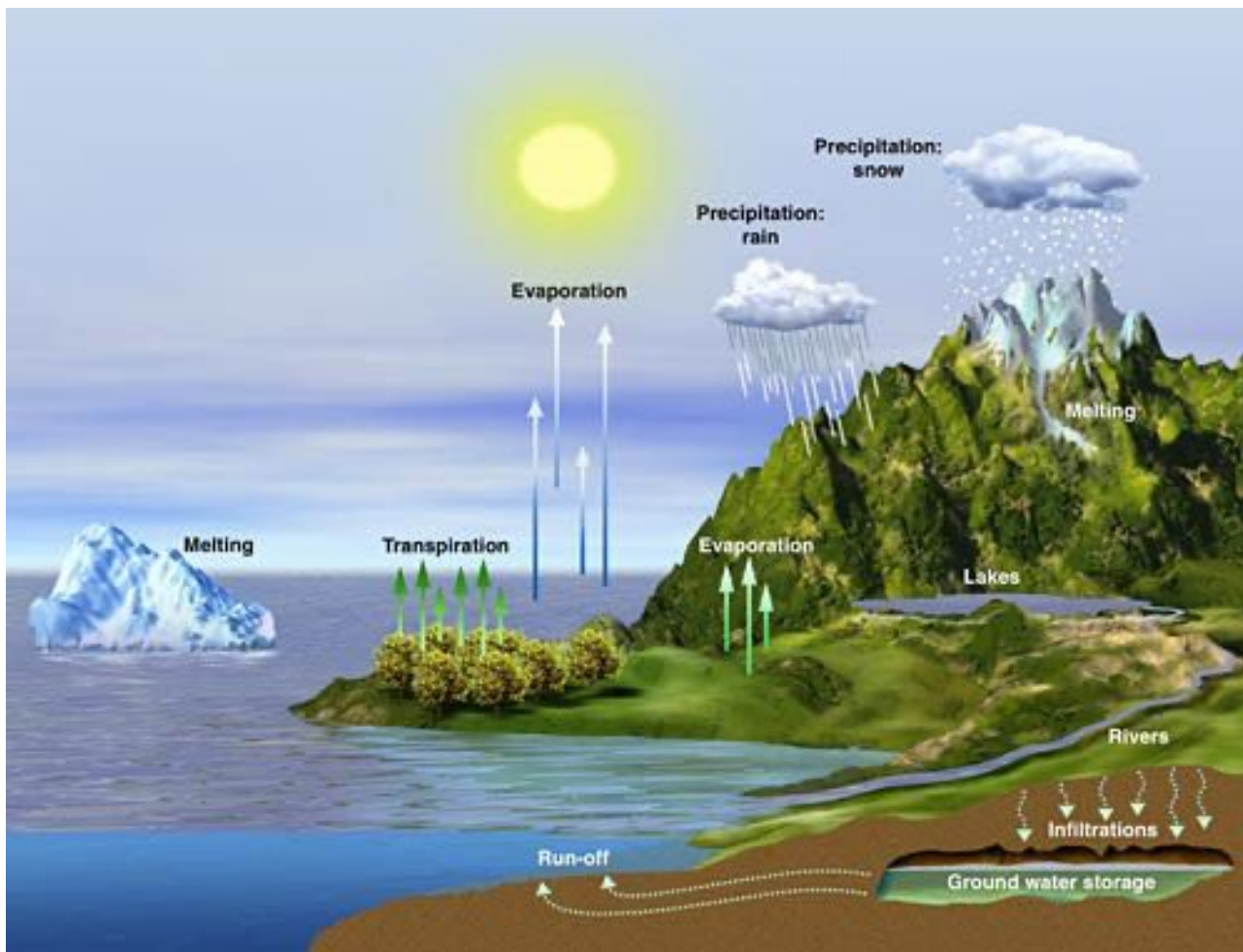


Fig. 3 TMI SST on: (a) 26 August 2005 for two days prior to the storm, and (b) 30 August 2005 for one day after the storm, and (c) 8-year (1998–2005) averaged monthly mean SST in August. The color bars in (a) and (b) is the same as in (c). The circles of different colors indicate the track and intensity of Hurricane Katrina

Content

- 101 Remote Sensing
- How to observe the ocean from space?
- Sea-surface temperature
- **Sea surface height**
- Ocean Color Radiometry
- Vertical profiles of the upper ocean

Water cycle



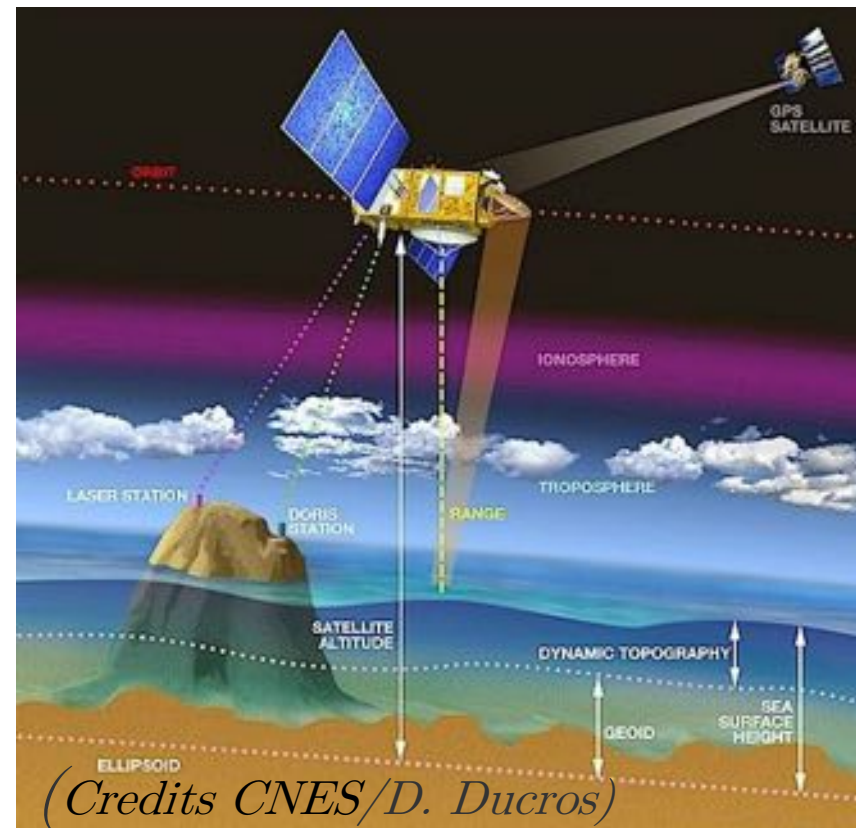
Sea-surface height (altimetry)

Objective: To determine the variation of the sea surface height of the oceans (SSH), from geostrophic currents, tides and other oceanic phenomena

How: Use of radar altimeter that transmits short microwave pulses vertically to the ocean surface

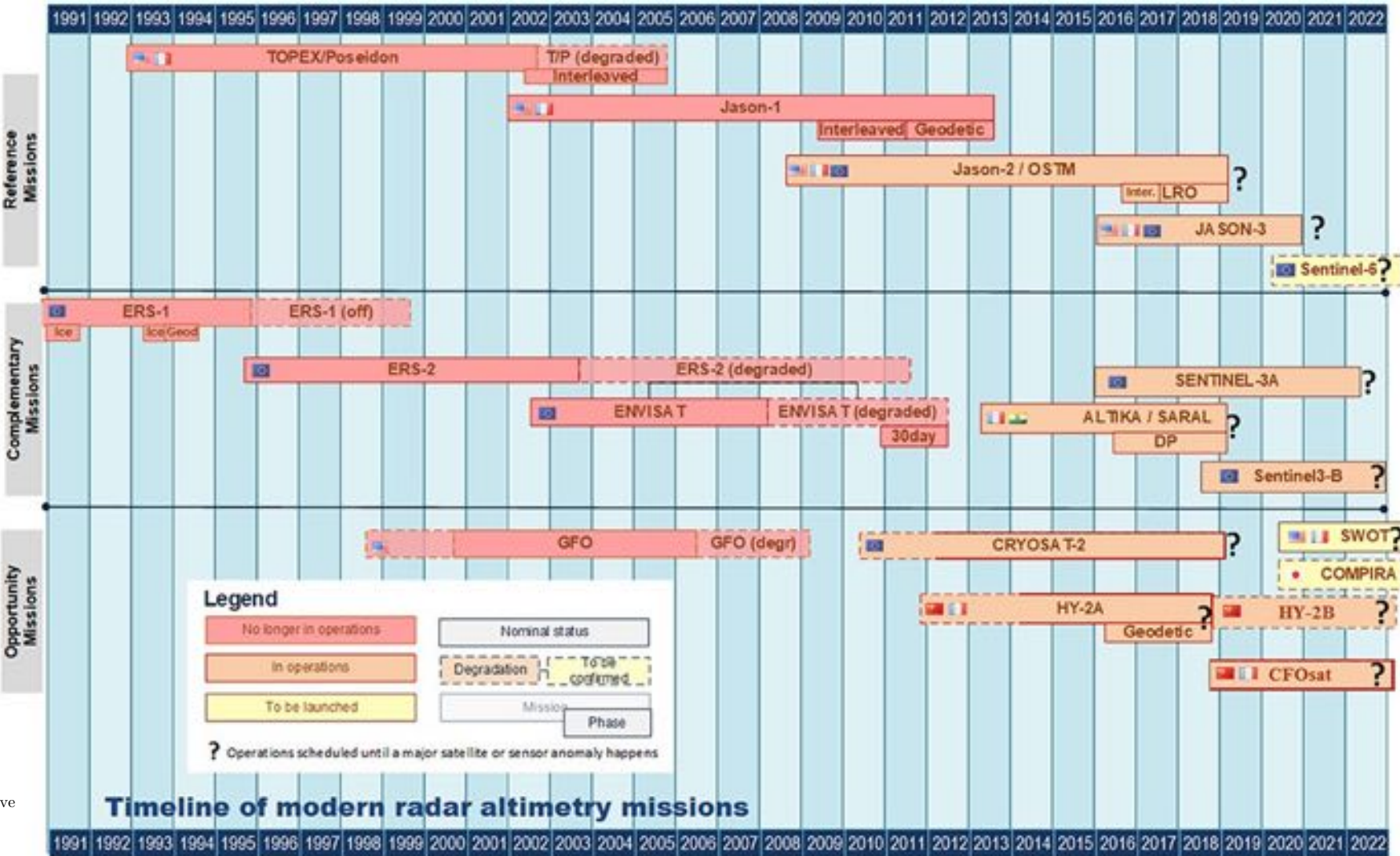
Main problems to solve:

- Exact position of the satellite on its orbit
- Reference surface (geoid)



Satellite measurements

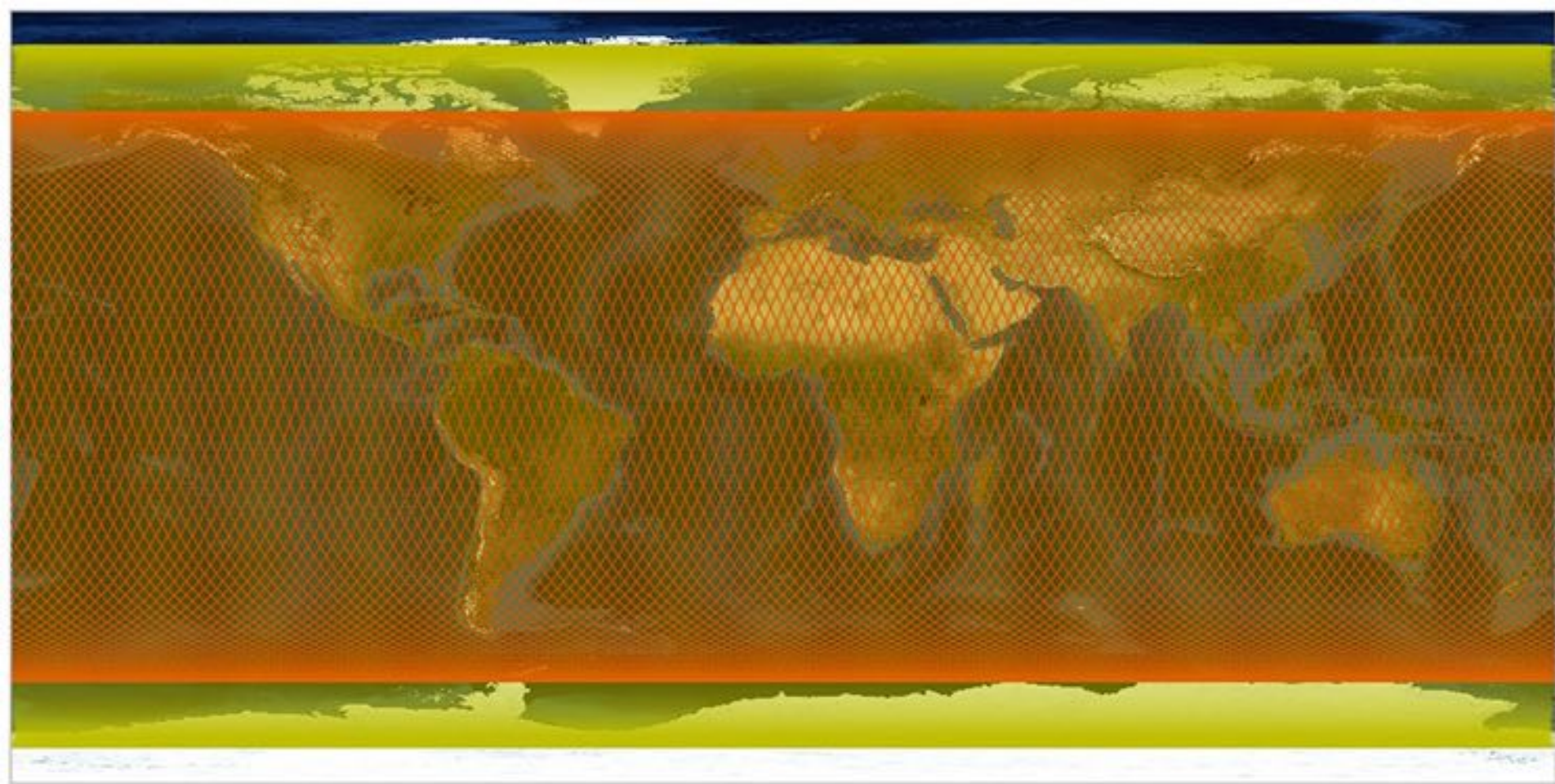
- Operational satellite for the past 25 years
- Global observations of SSH
- Direct measurement of the absolute SSH relative to the mass center of Earth
- Main satellites:
 - Topex/Poséïdon (1992-2006)
 - Jason series (1: 2001-2013; 2: 2008-; 3: 2016-)
- Orbital cycle of 10 days



Sea surface height

Choice of the orbit:

No Sun-synchronous orbit (to avoid perturbations from tides or from daylight) and high altitudes to reduce atmospheric effects



Cazenave et al. (2019)

Sea surface height

Choice of the orbit:

No Sun-synchronous orbit (to avoid perturbations from tides or from daylight) and high altitudes to reduce atmospheric effects

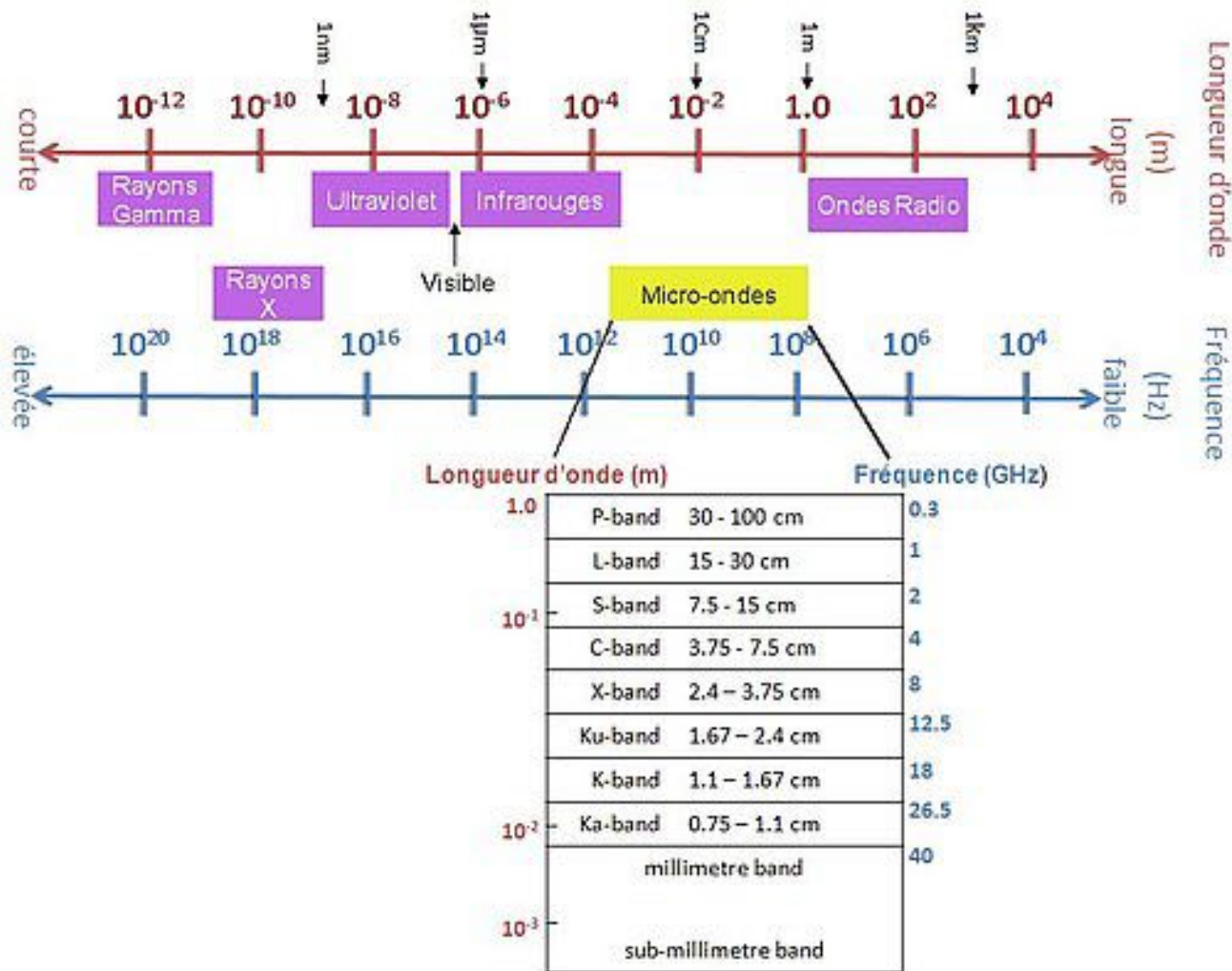
Choice of frequency

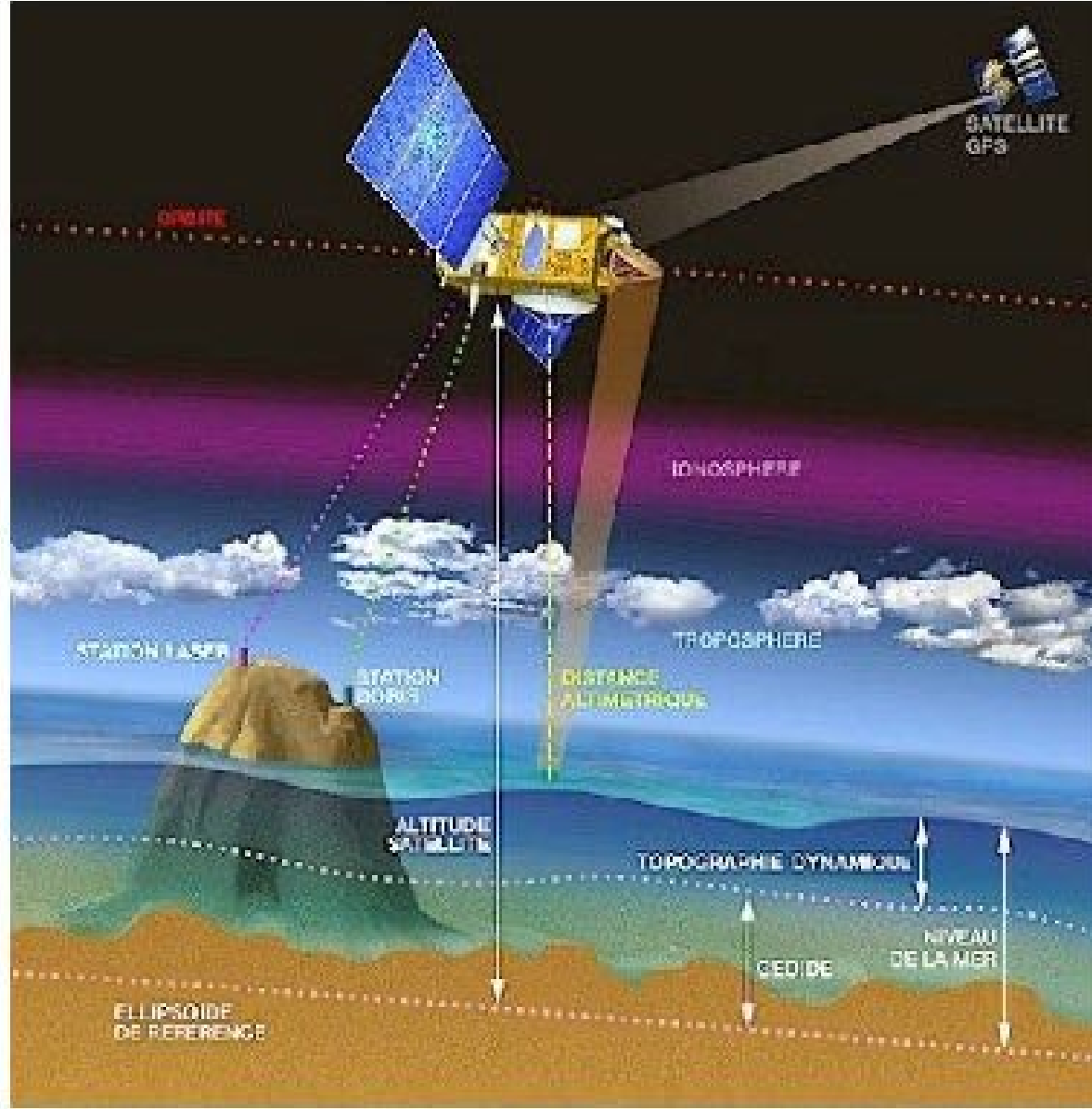
K_u band at 13.6 GHz (or $\lambda=2$ cm) is the most common frequency (Topex/Poseidon, Jason-1, Envisat, ERS, etc).

C band at 5.3 GHz (or $\lambda=6$ cm) is known for being more sensitive than K_u band to ionospheric perturbations and less sensitive to effects of atmospheric liquid water. Use to correct the ionospheric shift, combined with measurements with Ku band



Advantage of dual-band altimeters





Principle of the altimetric measurements of Topex-Poseidon

Sea surface height (altimetry)

- position of satellite on its orbit (accuracy: centimeter)

Combination of three embedded system (on Topex/Poseidon):

- ✓ One reflecting laser matrix (target for the laser measurements from the ground)
- ✓ One embedded GPS (to determine the position of the satellite by triangulation)
- ✓ A DORIS system (by using the measurements of the Doppler shift at two ultra-stable frequencies)

Need models of orbits more and more accurate

(including detailed knowledge of the satellite and its variations due to maneuvers, fuel consumption, solar panels orientation, ...)

Processing of the measurements(1/2)

- Need to eliminate variations dues to the waves
- Problem of reference point: fixed pt used at the origin for the measurements
- Definition of a geodesic reference: ensemble of pts for which the coordinates are perfectly known

Processing of the measurements(2/2)

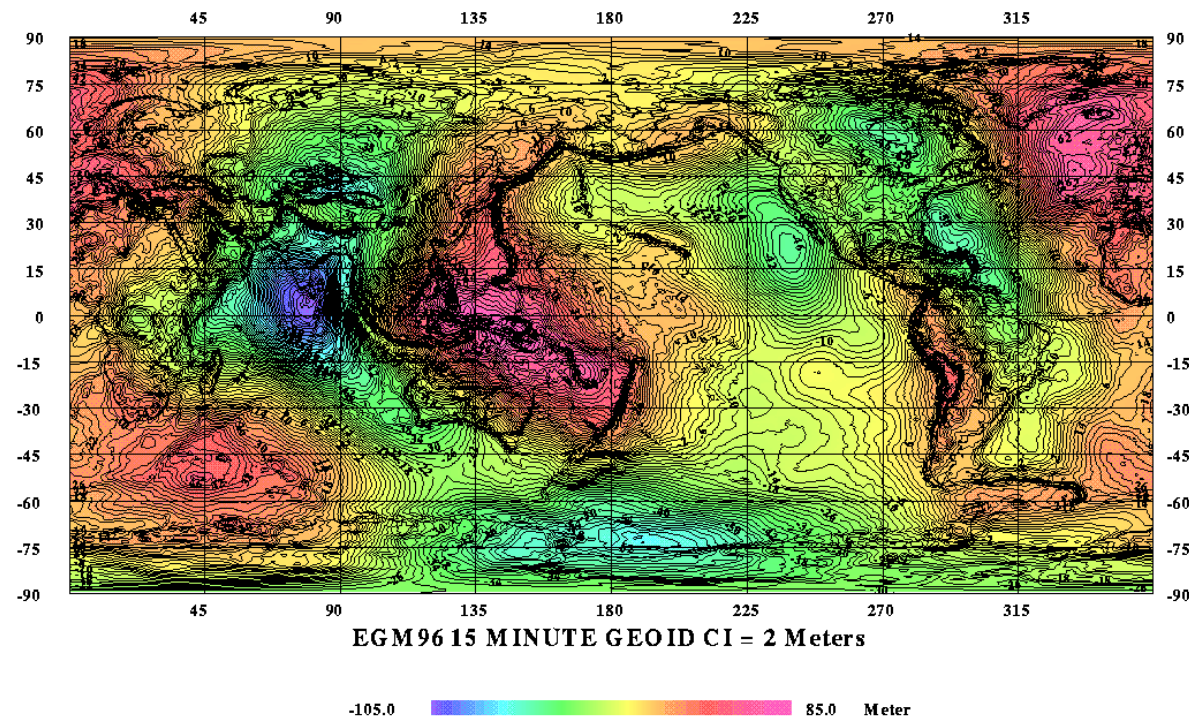
- High sea: definition needs a reference geoid → surface covering the entire globe
- With external forces, sea level == geoid
- Real life: no → diff. pression, T, salinity, marine currents
- Global scale: level not cst and variations +/- 2m

Sea surface height (altimetry)

- Reference surface (geoid): the shape of the sea surface with the hypotheses of total absence of forces. It represents the gravitational field of the Earth that varies as a function of the Earth's mass distribution

The height of the geoid varies of ~ 200 m, and SSH must be Estimated with an accuracy of cm.

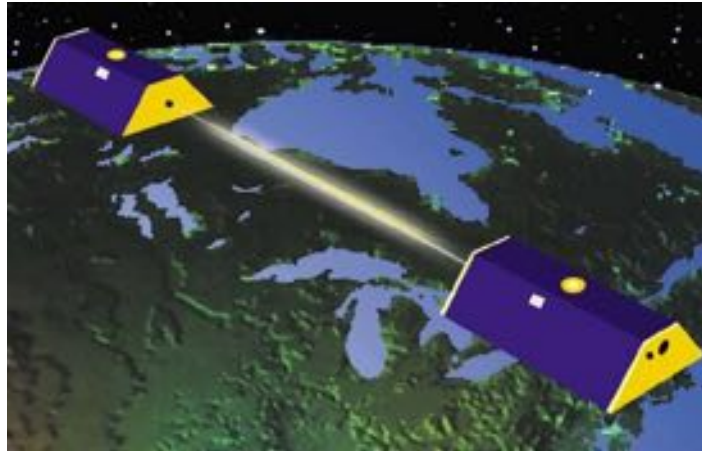
Error of EGM96: ~ 6 - 10 cm above ocean and max max of 50 cm above land (Lemoine et al., 1998).



EGM96 is a geopotential model of the Earth combining data from airborne gravity studies, satellite missions (GEOSAT Geodetic Mission; ERS1 altimeter derived anomalies; TOPEX/POSEIDON), new topographic data) from NASA/TP-1998-206861

Sea surface height (altimetry)

GRACE (2002-): Gravity Recovery and Climate Experiment detects changes in the Earth gravity field by monitoring the changes of the distance between two satellites along their orbit around the Earth



Error of EGM96: ~ 6-10 cm above ocean and max max of 50 cm above land (Lemoine et al., 1998).

GRACE data provide a uniform estimate above land and ocean with a max error of ~ 2 cm (Tapley et al., 2004)

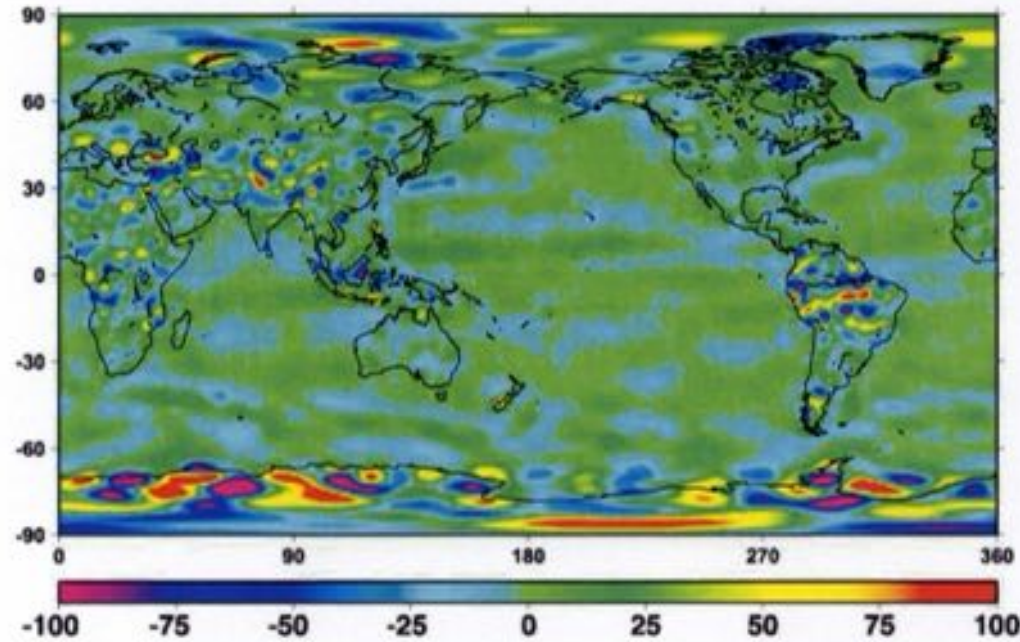
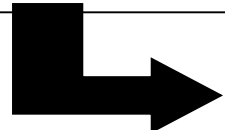


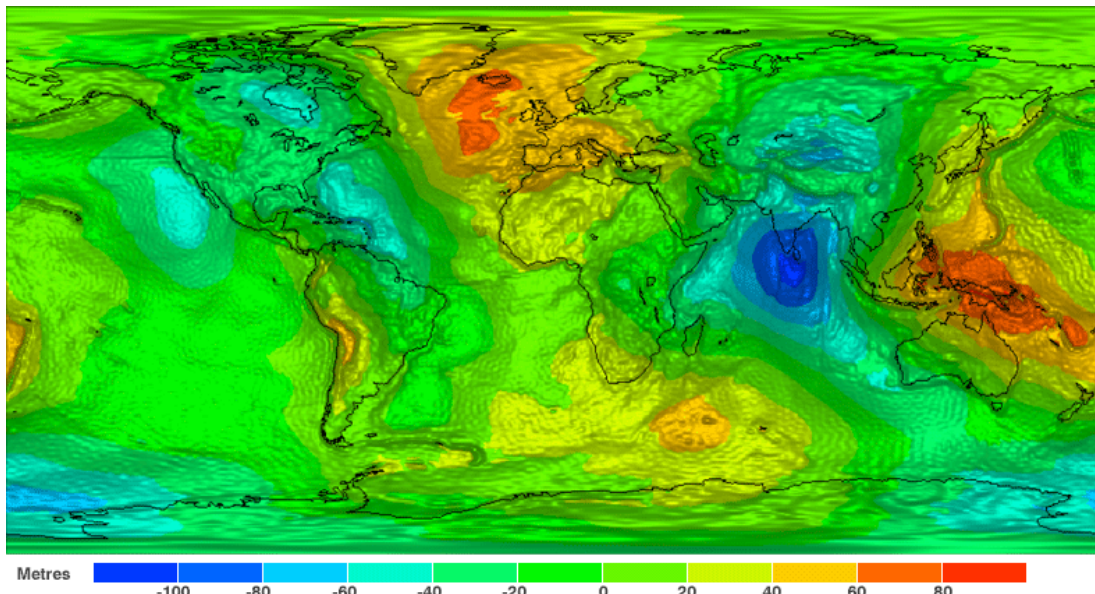
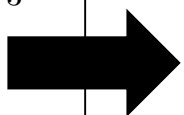
Figure 2. Geoid difference between GGM01S and EGM96 computed to degree and order 90 and smoothed with a 200 km averaging radius. Units are cm.

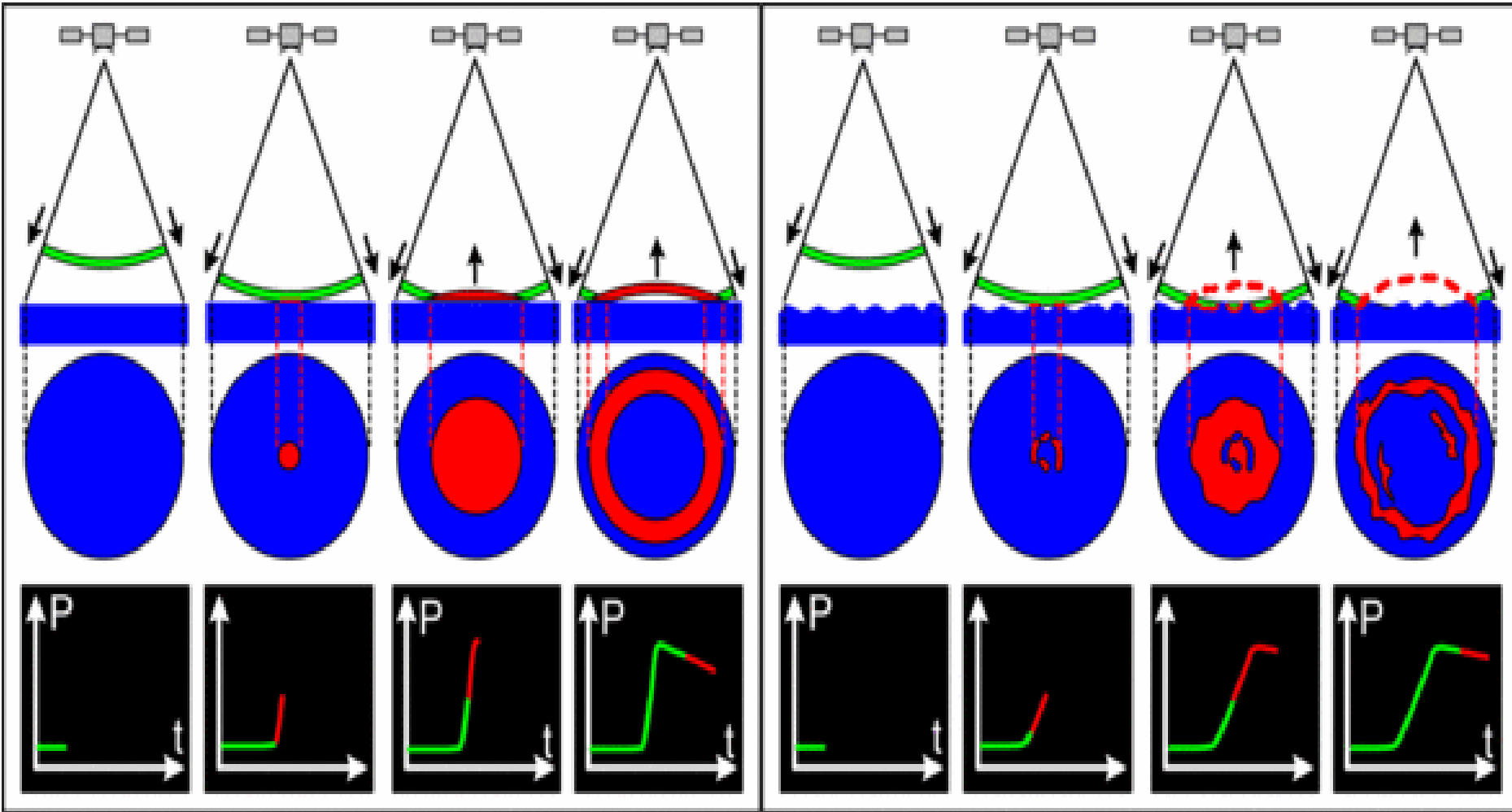
Sea surface height (altimetry)

GOCE (2009-2013): Gravity field and steady-state Ocean Circulation Explorer mapped the Earth geoid with a spatial resolution of de 100 km



GOCE data provides a uniform estimation over land and ocean avec max error of ~ 3 cm
(Pail et al., 2011)

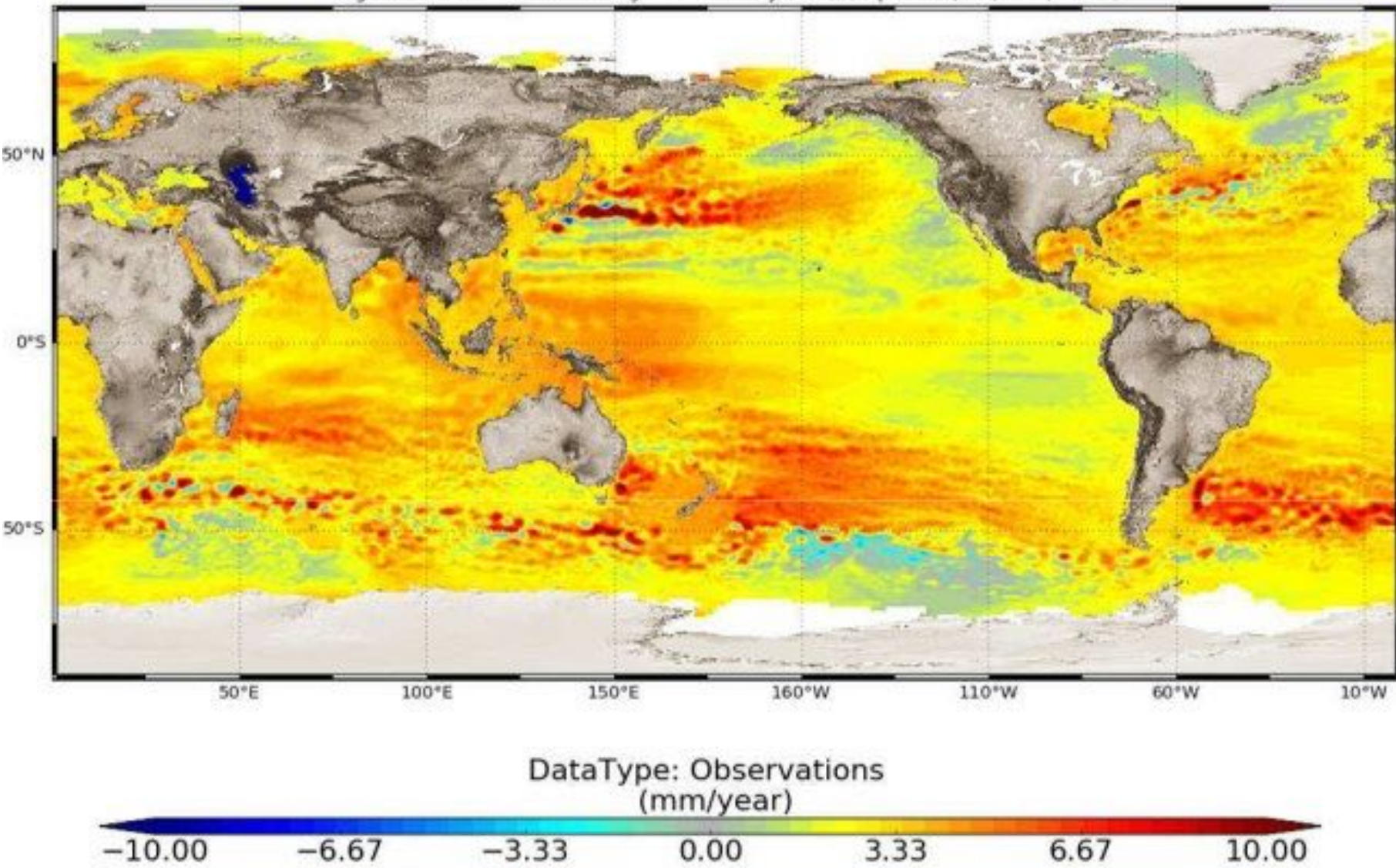


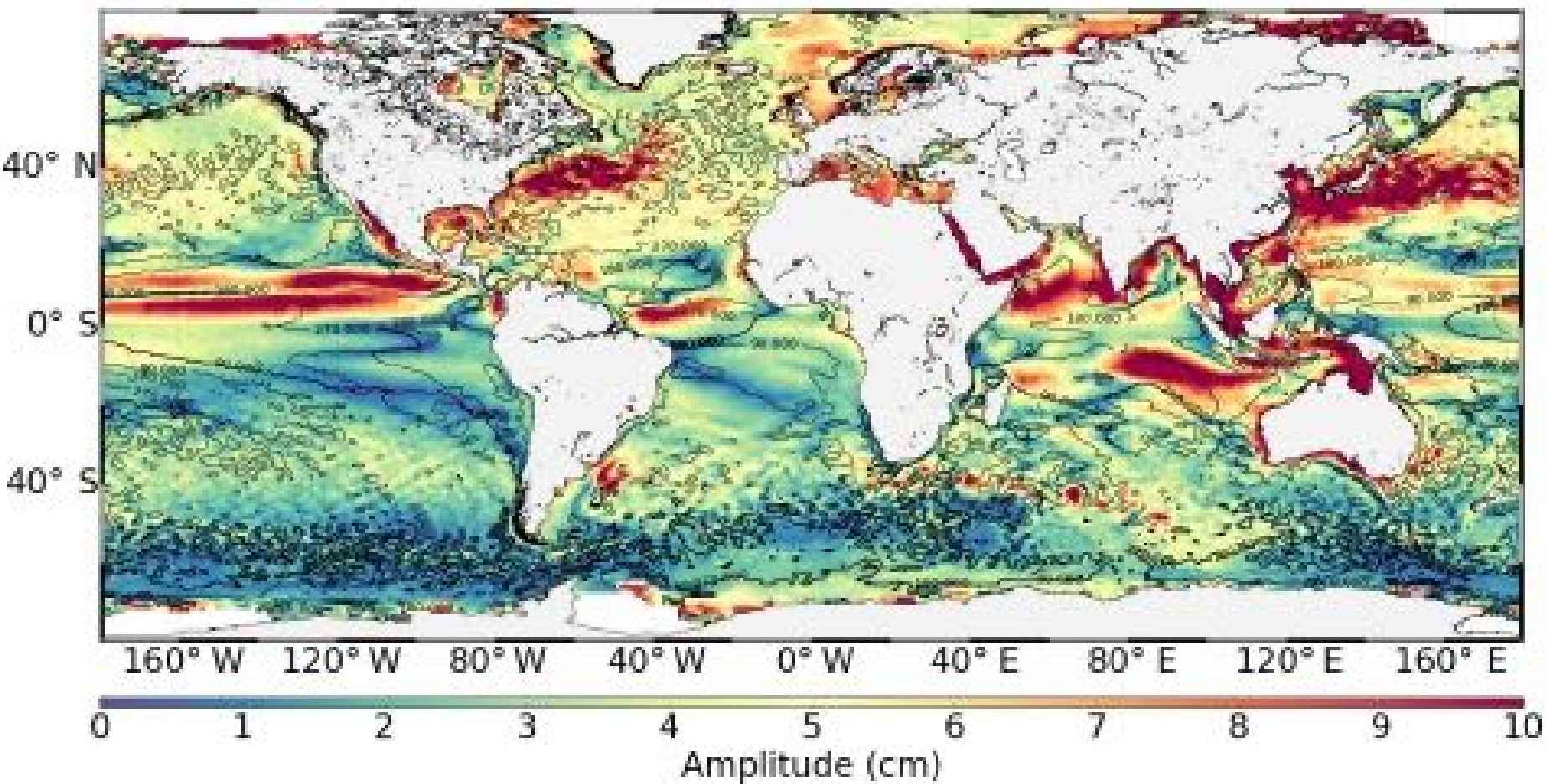


The radar altimeter receives the reflected wave (or echo), which varies in intensity over time. Where the sea surface is flat (a), the reflected wave's amplitude increases sharply from the moment the leading edge of the radar signal strikes the surface. However, in sea swell or rough seas (b), the wave strikes the crest of one wave and then a series of other crests which cause the reflected wave's amplitude to increase more gradually. We can derive ocean wave height from the information in this reflected wave, since the slope of the curve representing its amplitude over time is proportional to wave height.

Regional mean sea level trends over the 1993–2019

Regional Mean Sea Level Trends (Jan-1993 to May-2019). (Copernicus/CLS/CNES/LEGOS)





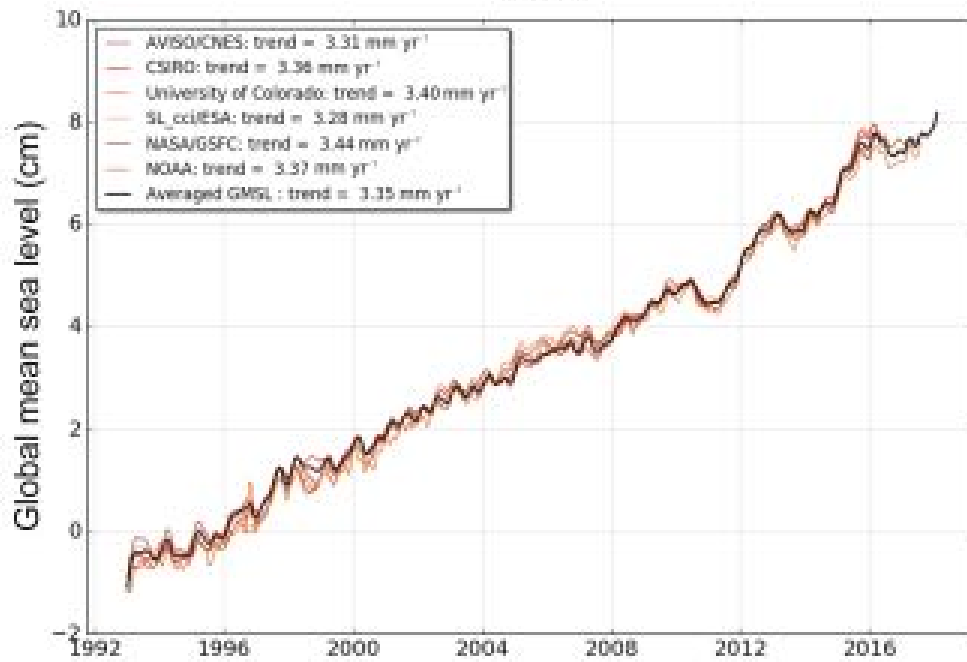
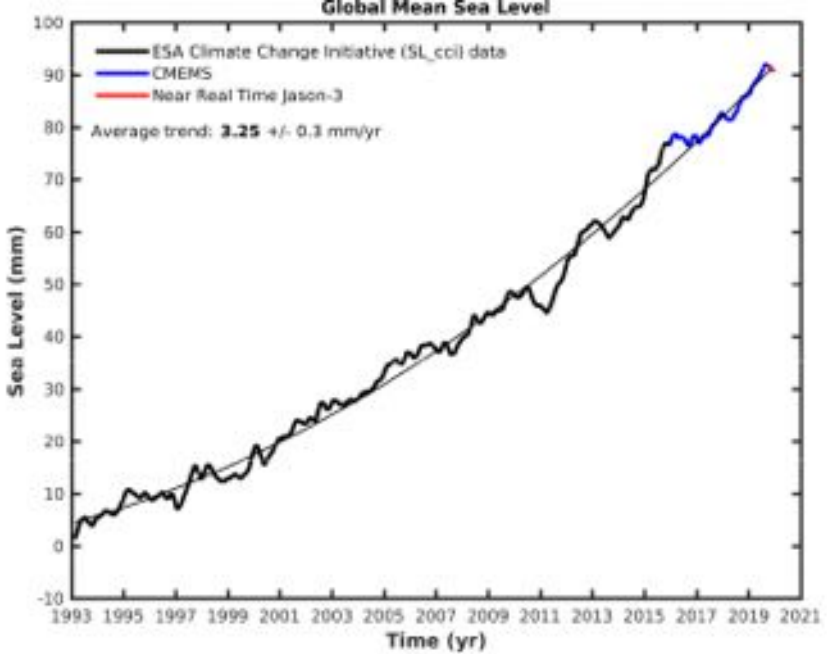
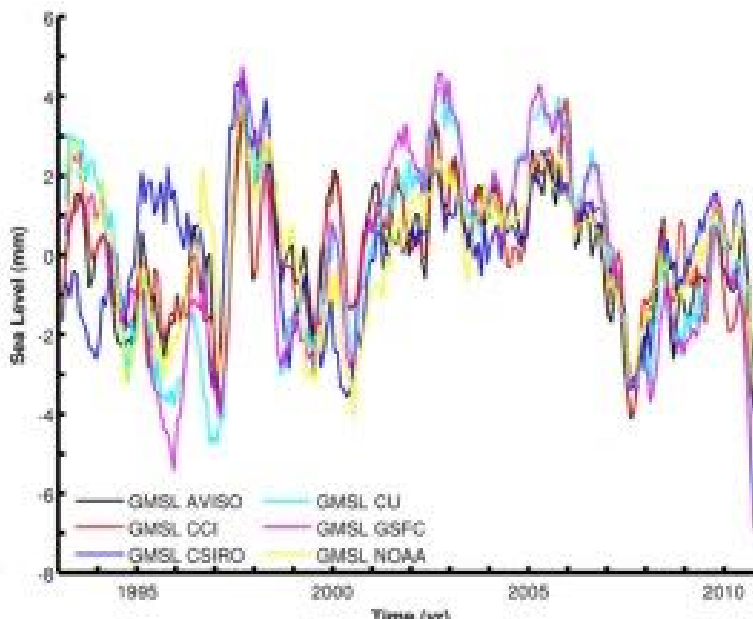
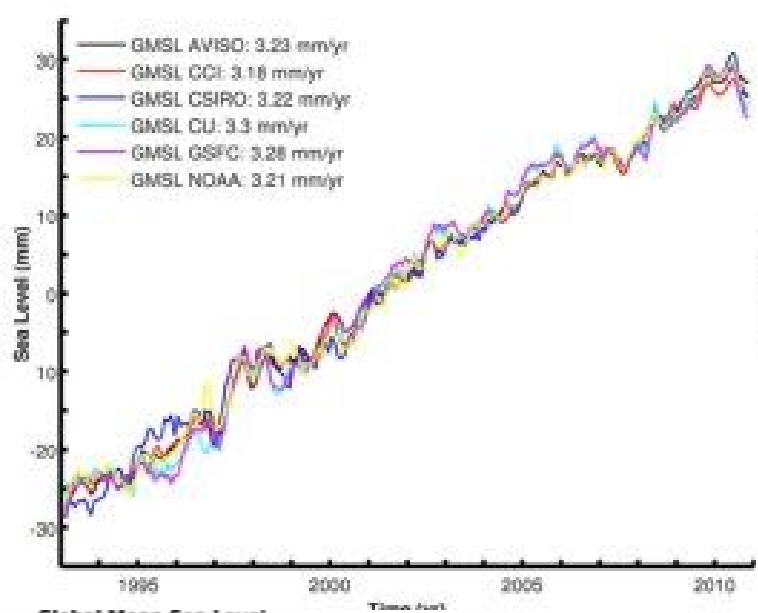
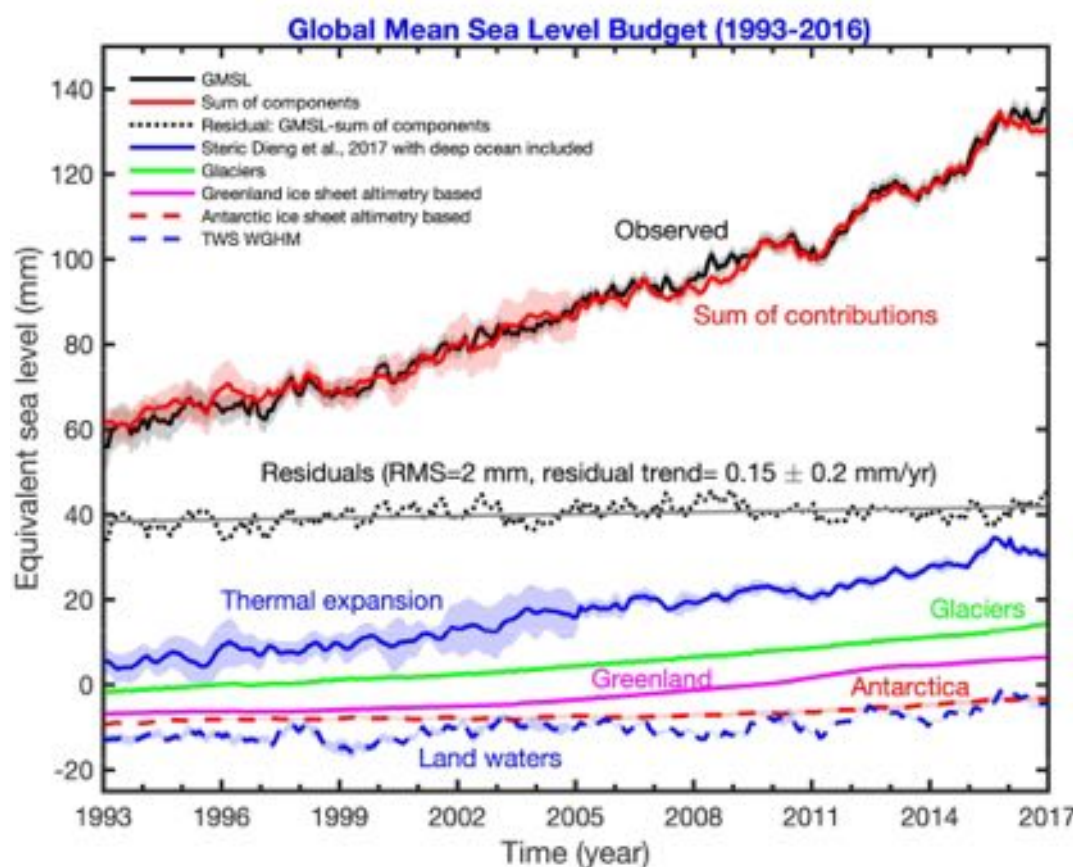
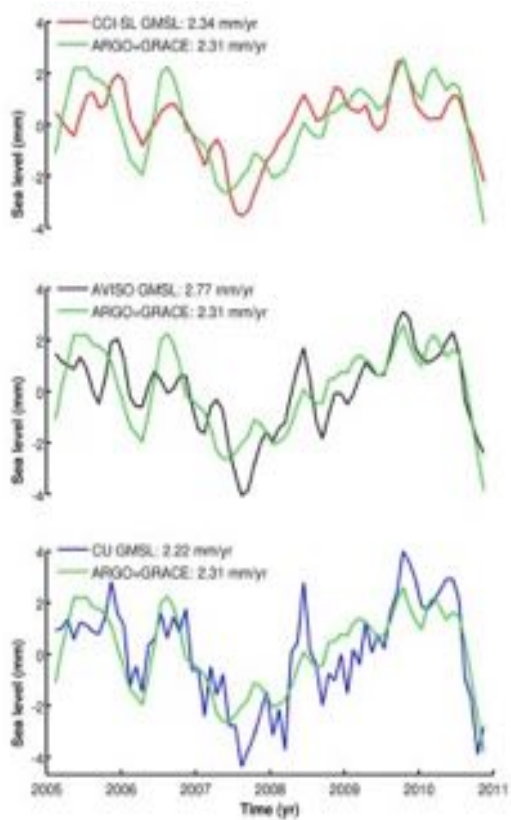


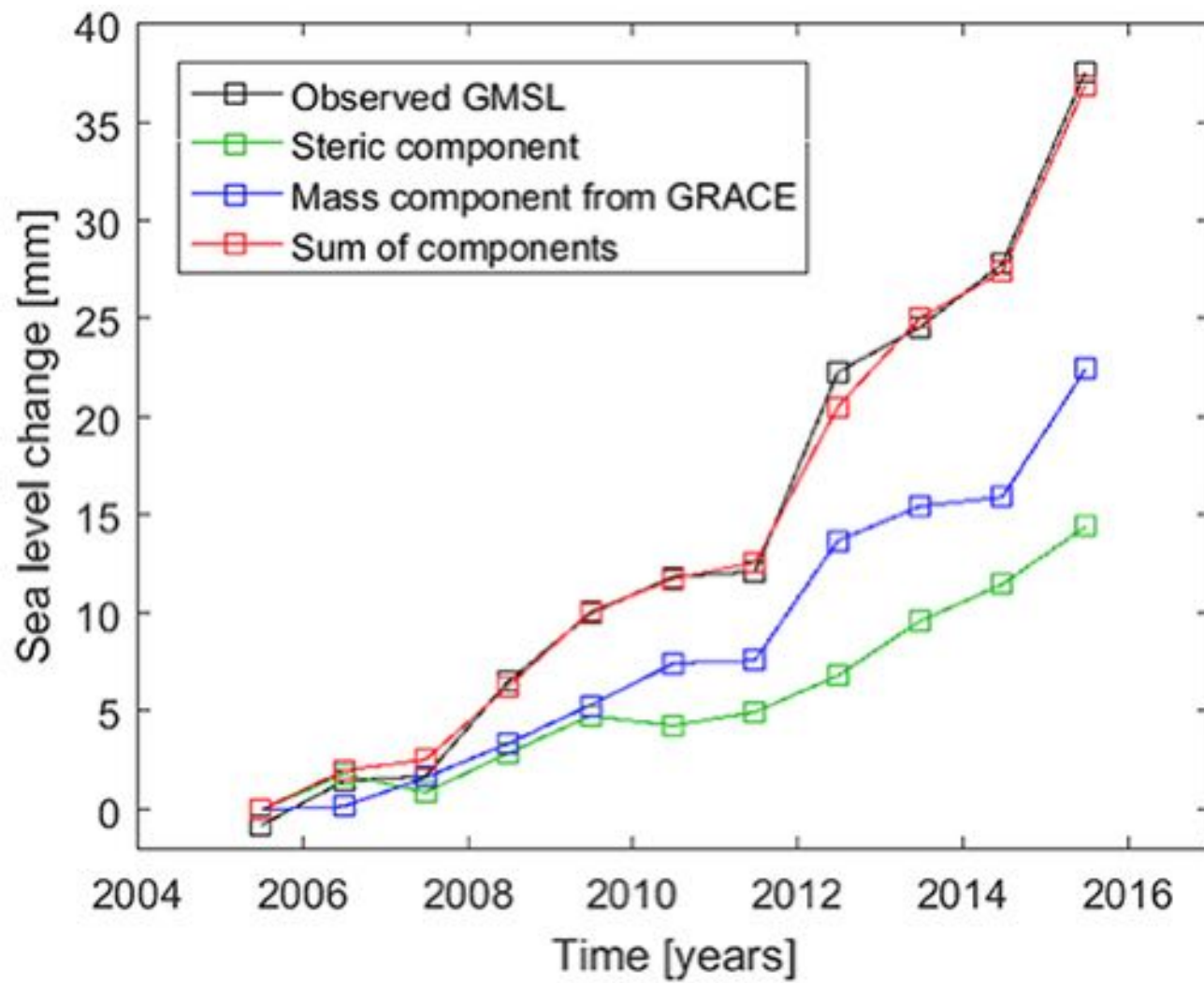
Fig.1. Evolution of the global mean sea level measured by satellite altimetry between January 1993 and April 2020 (source: LEGOS).

https://youtu.be/m5PPURqEONI?list=PLfwaHdOcxQyxWr4CXMLpvvPsdA33_y1gU



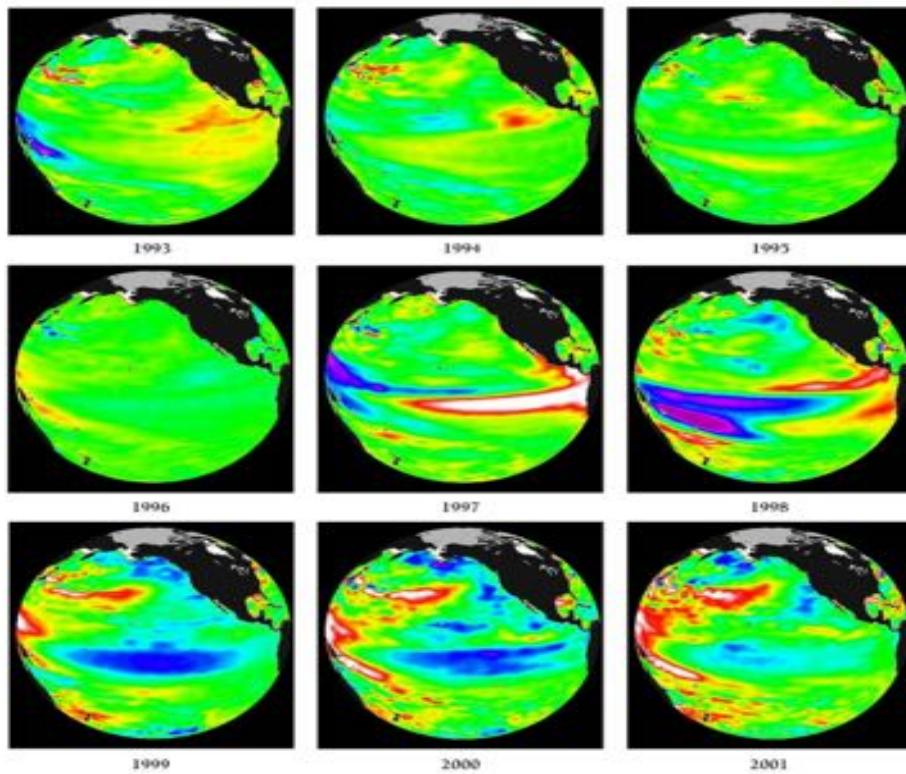
Spatial scales	Temporal scales	Altimetry errors	User requirements
Global MSL	Long-term evolution (> 10 years)	< 0.5 mm year ⁻¹	0.3 mm year ⁻¹
	Interannual signals (< 5 years)	< 2 mm over 1 year	0.5 mm over 1 year
Regional MSL	Annual signals	< 1 mm	Not defined
	Long-term evolution (> 10 years)	< 3 mm year ⁻¹	1 mm year ⁻¹
	Annual signals	< 1 cm	Not defined

Component	Trends (mm yr ⁻¹) 1993-present	Component	Trend (mm yr ⁻¹) 2005-present
1. GMSL (TOPEX-A drift corrected)	3.07 ± 0.37	1. GMSL	3.5 ± 0.2
2. Thermosteric sea level (full depth)	1.3 ± 0.4	2. Thermosteric sea level (full depth)	1.3 ± 0.4
3. Glaciers	0.65 ± 0.15	3. Glaciers	0.74 ± 0.1
4. Greenland	0.48 ± 0.10	4. Greenland	0.76 ± 0.1
5. Antarctica	0.25 ± 0.10	5. Antarctica	0.42 ± 0.1
6. TWS	/	6. TWS from GRACE (mean of Reager et al., 2016 and Scanlon et al., 2018)	-0.27 ± 0.15
7. Sum of components (without TWS → 2.+3.+4.+5.+)	2.7 ± 0.23	7. Sum of components (2.+3.+4.+5.+6.)	2.95 ± 0.21
8. GMSL minus sum of components (without TWS)	0.37 ± 0.3	8. Sum of components (thermosteric full depth + GRACE-based ocean mass)	3.6 ± 0.4
		9. GMSL minus sum of components (including GRACE-based TWS → 2.+3.+4.+5.+6.)	0.55 ± 0.3
		10. GMSL minus sum of components (without GRACE-based TWS → 2.+3.+4.+5.)	0.28 ± 0.2
		11. GMSL minus sum of components (thermosteric full depth + GRACE-based ocean mass)	-0.1 ± 0.3





National Aeronautics and
Space Administration
Jet Propulsion Laboratory
California Institute of Technology
Pasadena, California



-180 -160 -140 -100 -60 -20 20 60 100 140
Sea Level Relative to Average, millimeters

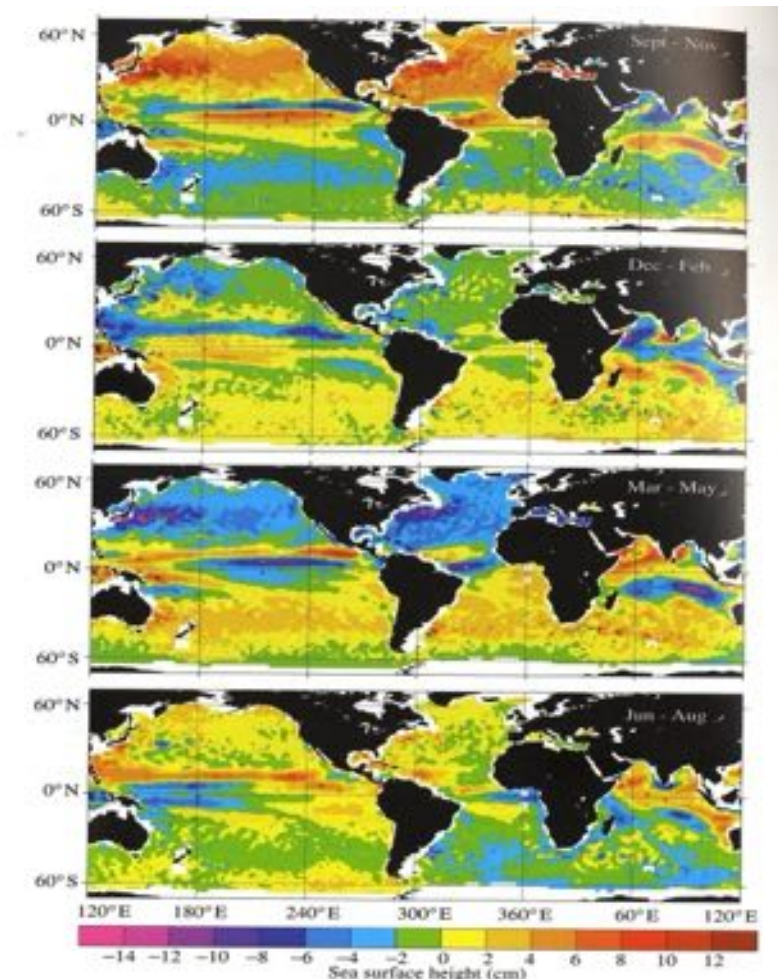
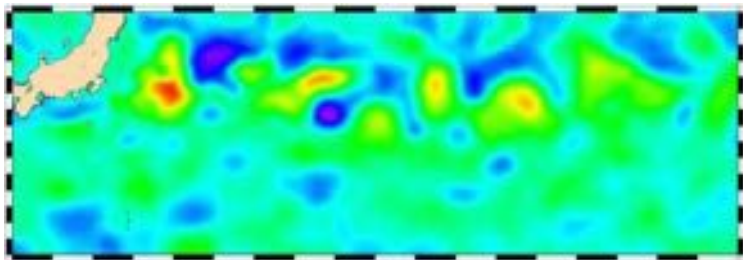


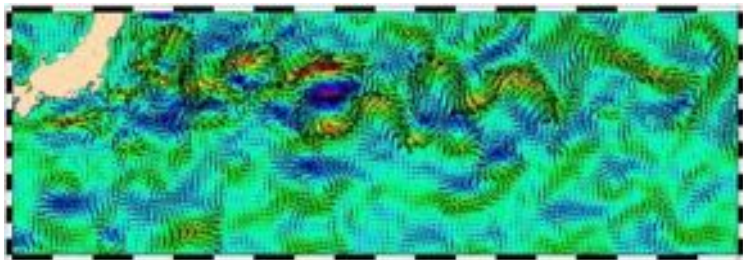
Plate 18. Seasonal mean anomalies of the TOPEX sea surface heights relative to the 9-year mean field. Top image is September–November 1992–2000; second is December 1992–2000 through February 1993–2001, third is March–May 1993–2001; fourth is June–August 1993–2001. Contour interval is 2 cm (Courtesy Detlef Stammer, used with permission).

Sea surface height: applications

Oceanic eddies



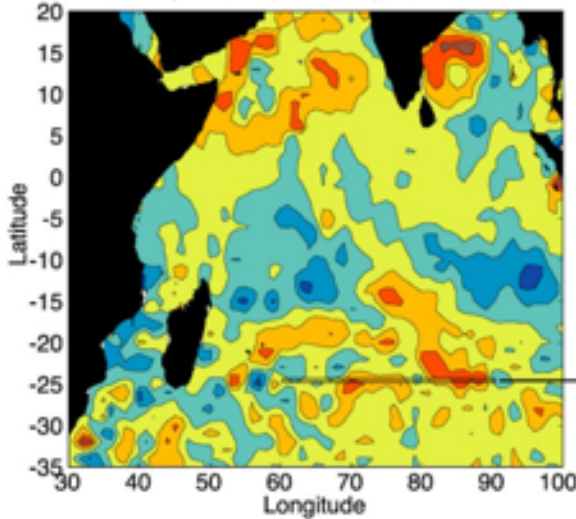
From SSH anomalies to geostrophic current



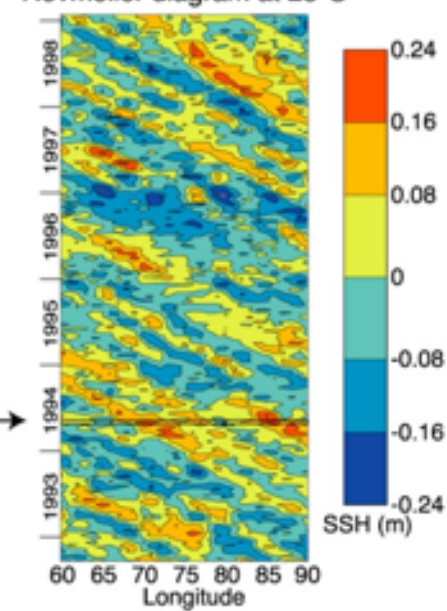
<http://earth.esa.int>

Kelvin and Rossby waves

Sea Surface Height from TOPEX/POSEIDON
cycle 60 (1-11 May 1994)



Hovmöller diagram at 25°S



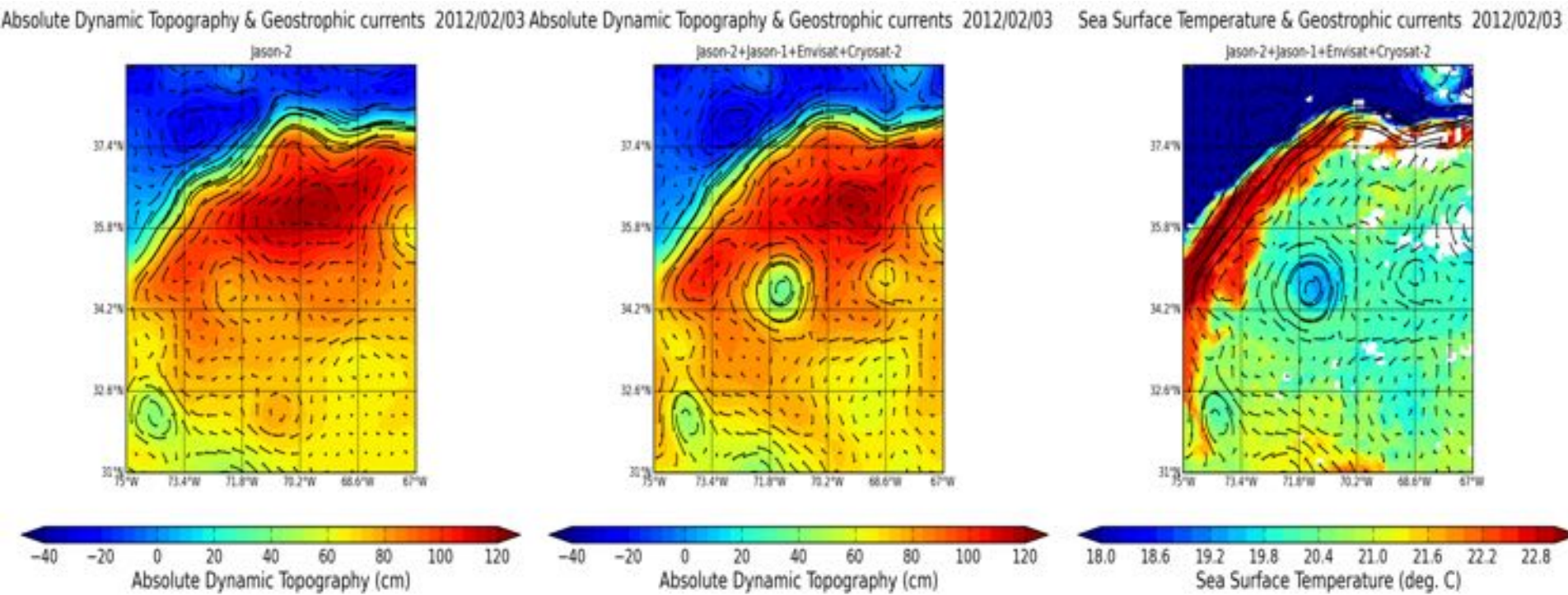
Cipollini et al., 2005

Radar altimetry provides information on:

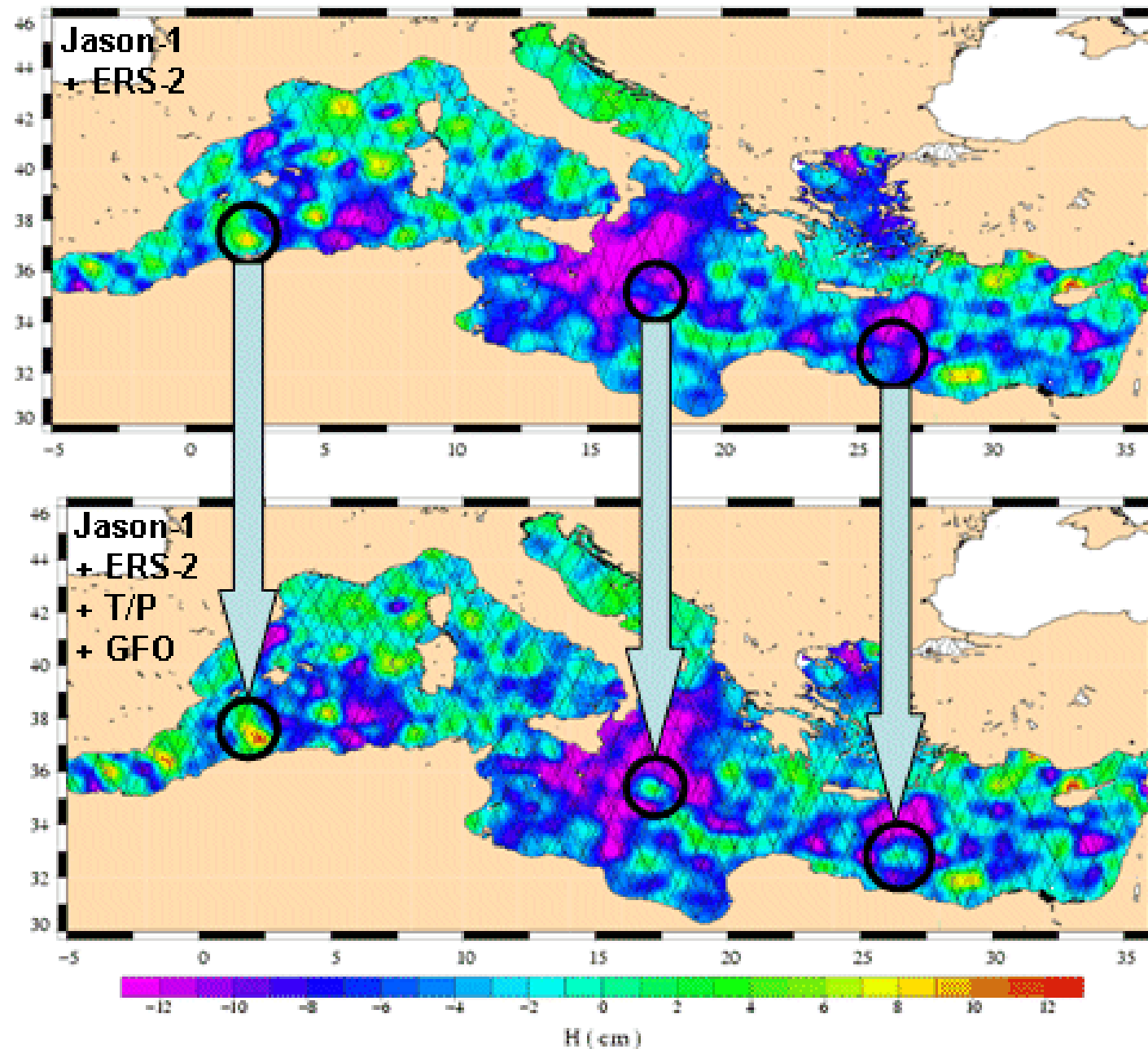
Waves height, velocity of wind

Bathymetry

Thickness of sea ice and topography of glaciers



Carte de topographie dynamique absolue (en m) superposée aux vecteurs de courants géostrophiques absolus dans l'océan Atlantique le 03/02/2012, réalisées à partir des données de *Jason-2* seul (à gauche) et de la combinaison de *Jason-1+Envisat+Jason-2+Cryosat-2* (au milieu). Carte de température de surface (*SST* en °C, à droite) superposée aux vecteurs de courants géostrophiques.



Cartes d'anomalies de hauteur de mer en Méditerranée le 11 juin 2003 obtenues avec *Jason-1 + ERS-2* (haut) et *Jason-1+ERS-2+T/P+GFO* (bas)

Content

- 101 Remote Sensing
- How to observe the ocean from space?
- Sea-surface temperature
- Sea surface height
- **Ocean Color Radiometry**
- Vertical profiles of the upper ocean

Basic principles

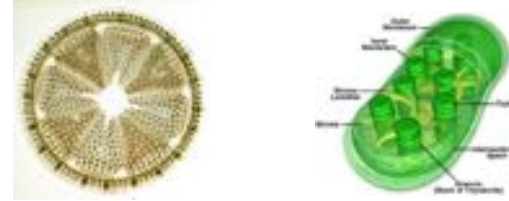
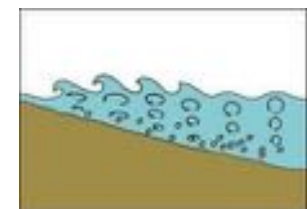
How to interpret ocean color images?



The surface ocean color is regulated by the optical properties of the pure water and of those of the different particulate and dissolved matters that are in the surface layer

Basic principles

The factors influencing the ocean color are:

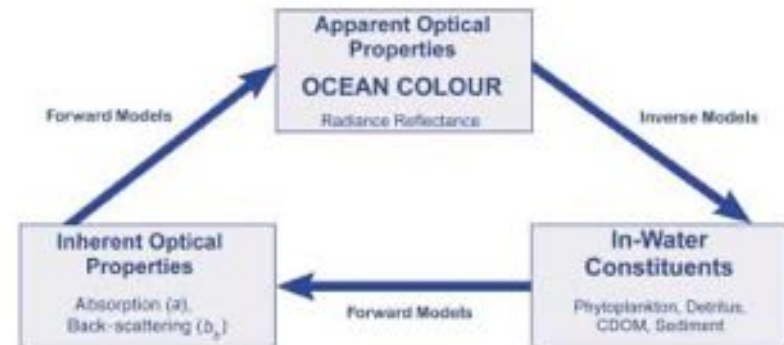
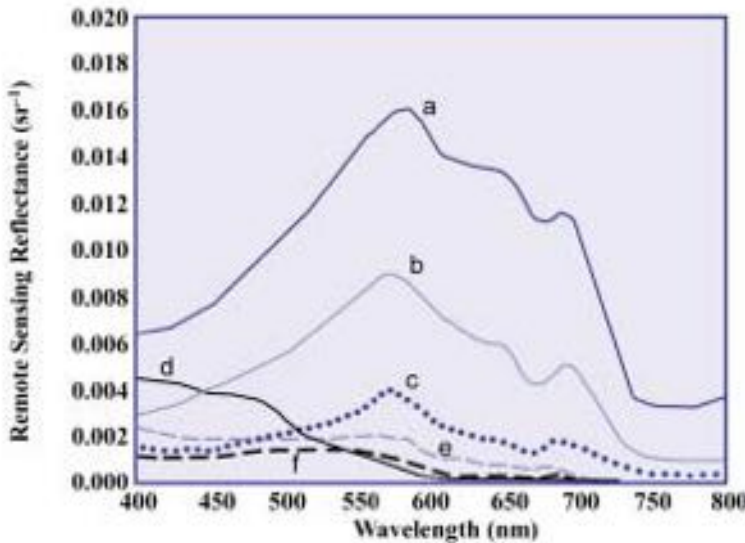
- Pure water
- Phytoplankton and its pigments (chlorophyll)
- The dissolved organic matter
 - “Colored Dissolved Organic Matter” (CDOM, or yellow substances or *gelbstoff*) from the degradation of the vegetal matter from marines or land ecosystems.
- Suspended particulate matter
 - The organic particles including the material from the degradation of phytoplankton or zooplankton (+ bacteria etc)
 - The inorganic particles (sand, dust) from terrestrial erosion and that are brought to the oceans via
 - Rivers discharges
 - Wind
 - Re-suspension from hydrodynamics

Basic principles



- The most clearest seawaters absorb the red light and transmit and scatter the light at the shortest wavelengths (blue waters)
- Phytoplankton contains pigments such as chlorophyll (and other accessories pigments) that absorb at other wavelengths and that contribute to the green color of the oceans
- In the coastal waters, the inorganic suspended matter backscatters the light contributing to the green, yellow and brown of the ocean color

Basic principles



The remote-sensing reflectance $\text{Rrs}(\lambda)$ is a Apparent Optical Properties (AOP) and is a function of the back-scattering and absorption coefficient of the different optical active agents in the seawaters:

$$\text{Rrs}(\lambda) = G \cdot b_b(\lambda) / a(\lambda)$$

with G a parameter dependent of the incoming irradiance and a and b_b are the Inherent Optical Properties (IOPs)

→ The remote-sensing reflectance Rrs is not the final product but its accuracy impacts the quality of the ocean color products

Why studying IOPs?

- They control the propagation of the light in the water (primary production, visibility, impact of UV, relationship with predation, vertical migrations, etc)
- They modify the thermal balance of the water column (impact on the deposition of heat in the water column et so on the mixing layers)
- Proxies of biogeochemical parameters (Chl, CDOM, POC, PIC, size, detritus, minéral/organic, phyto species, etc)
- Can be measured at high frequencies and continuously
- Can be estimated from space (access to large spatial and temporal scales → Global studies over a long period of time)

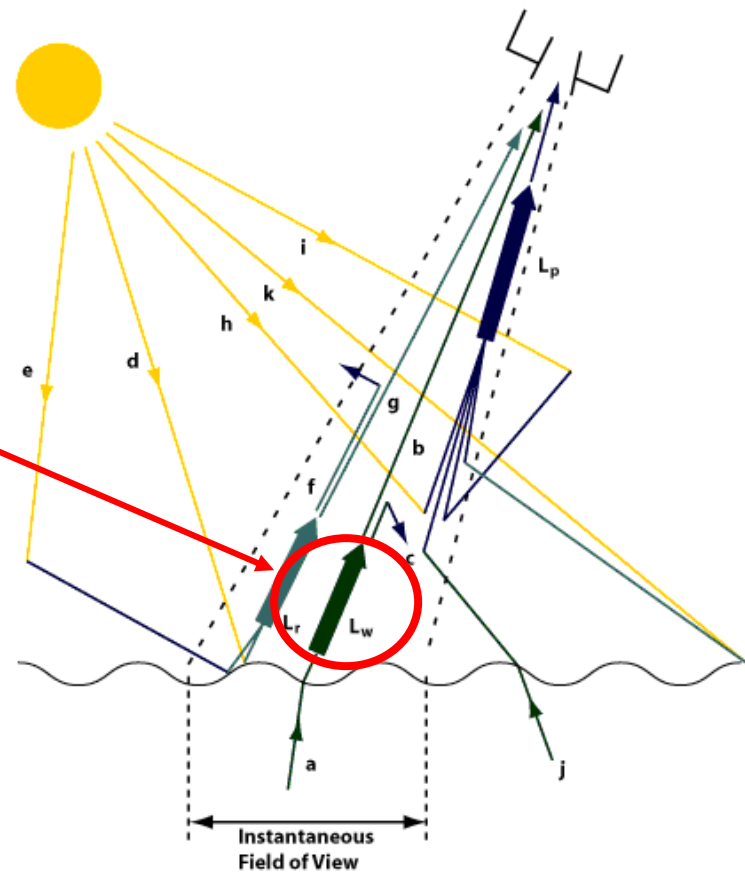


Ocean Color Radiometry (OCR)

Goal: To provide quantitative data of bio-optical properties of the global ocean (IOPs, Chl, POC, CDM, species, ...)

How: Remote sensing of the water leaving radiance, L_w , in the visible part of the spectrum

Main issue:
Atmospheric correction



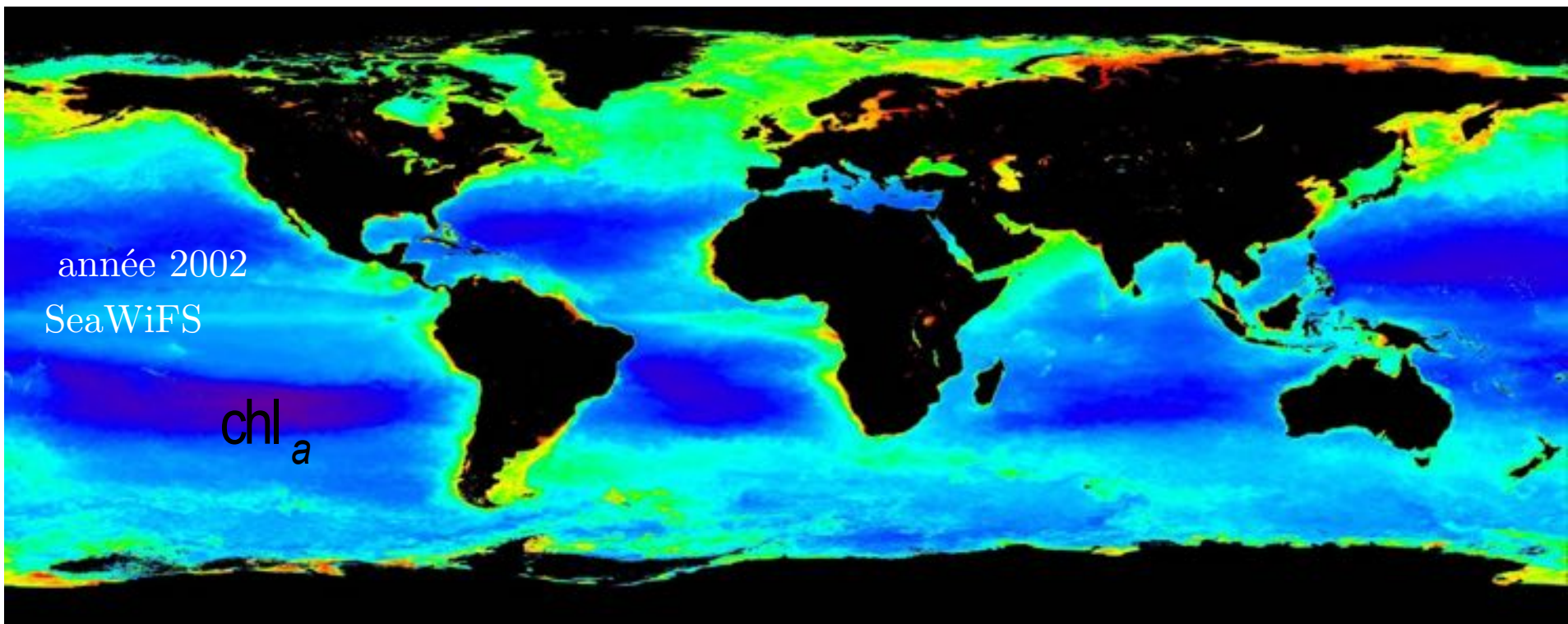
Remote Sensing of Ocean Color

Space-borne observations of ocean color are the only tools to monitor at high spatial and temporal resolutions the bio-optical and biogeochemical parameters of the ocean

année 2002

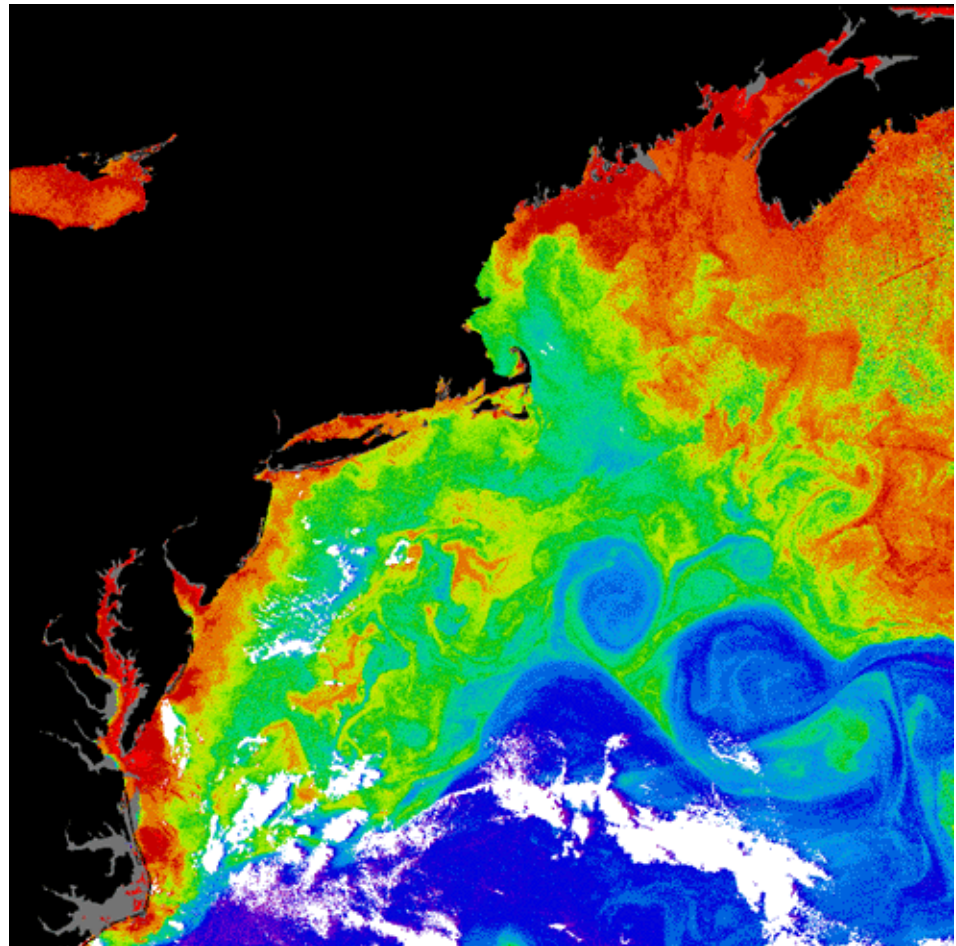
SeaWiFS

chl_a

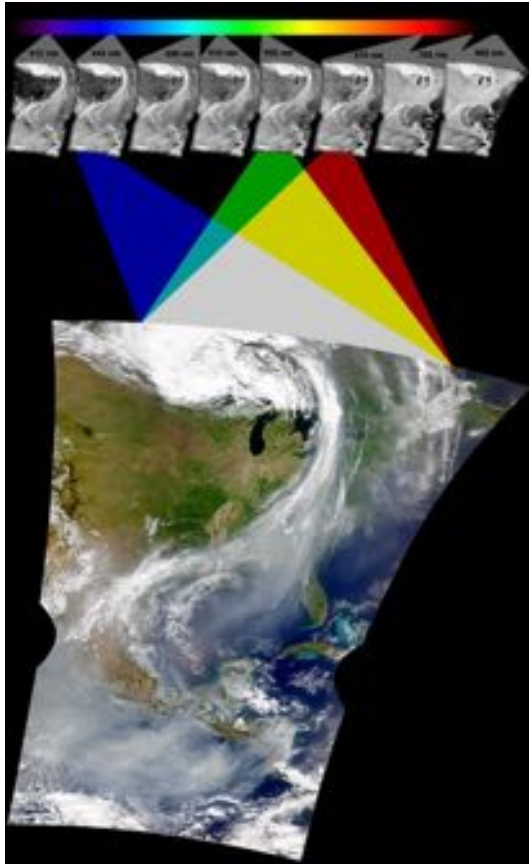


Ocean color remote sensors

- First sensor:
CZCS (1978-1986)
- Successors:
PoDER 1 (1996-1997)
PoDER 2 (2003)
SeaWiFS (1997-2010)
- Followers:
MODIS (2002-)
MERIS (2002-2012)
- New generation
GOCI (2010-)
VIIRS (2011-)
OLCI (2016-)



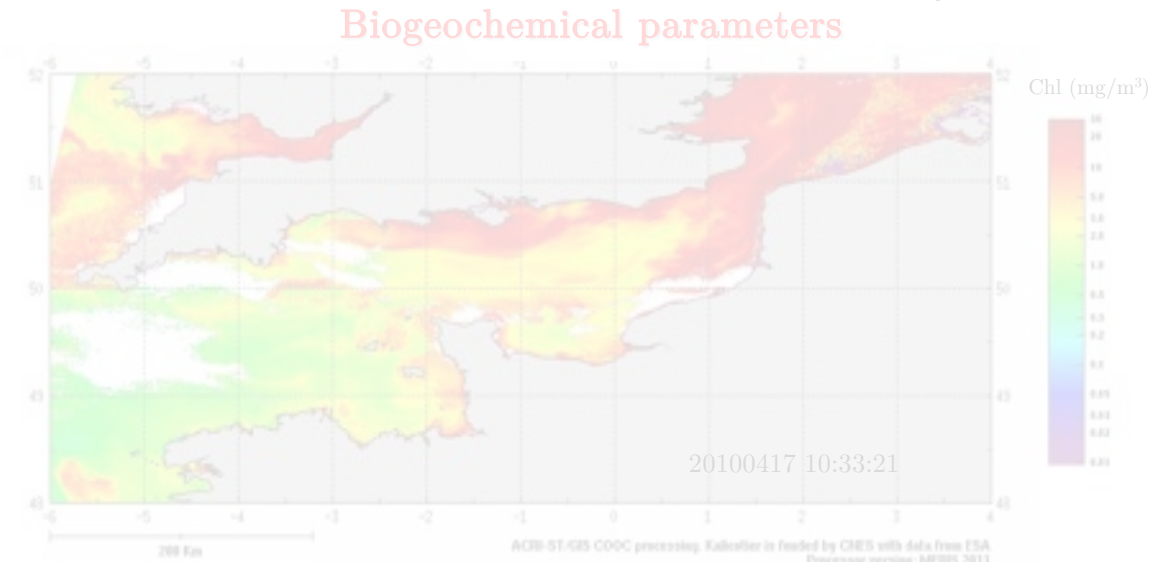
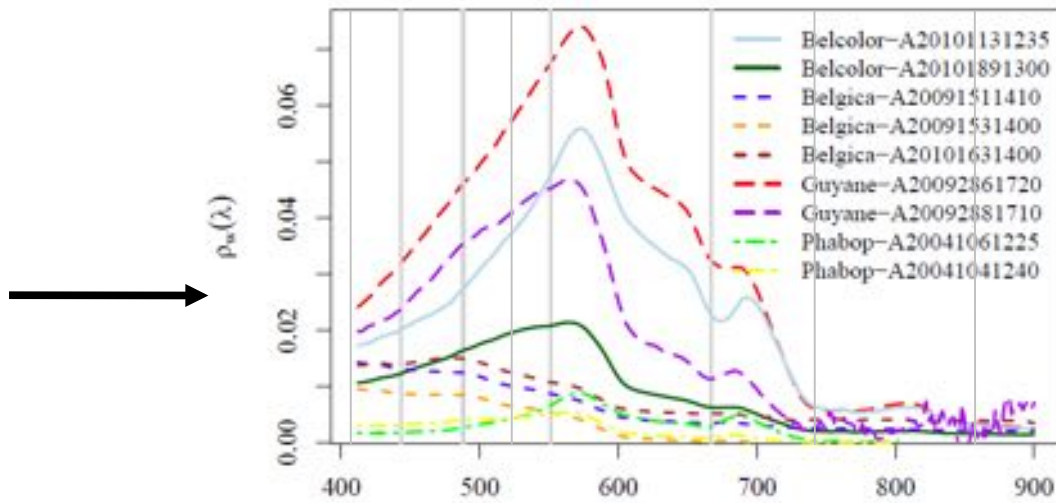
From satellite to biogeochemical parameters... A challenging task



<http://oceancolor.gsfc.nasa.gov/>

$\rho_t(\lambda)$ = top of atmosphere reflectance

$\rho_w(\lambda)$ = water-leaving reflectance (ocean color)



<http://kalicotier.gis-cooc.org/>

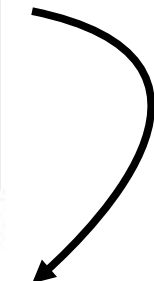
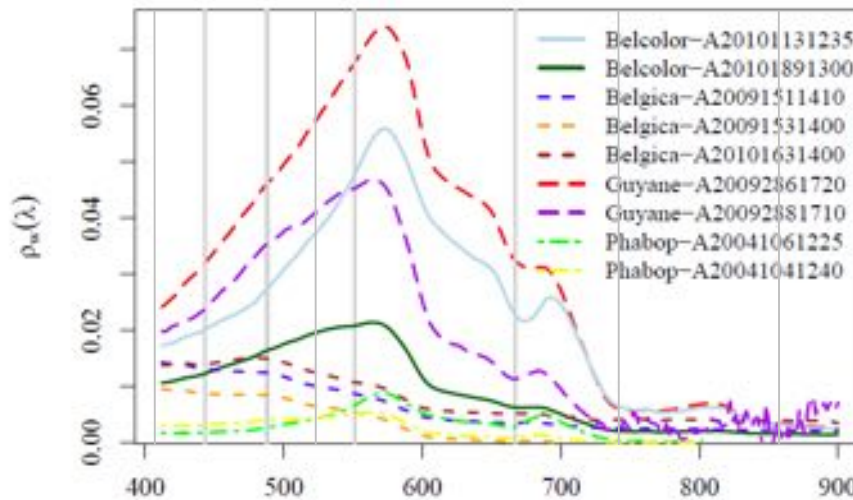
From satellite to biogeochemical parameters... A challenging task



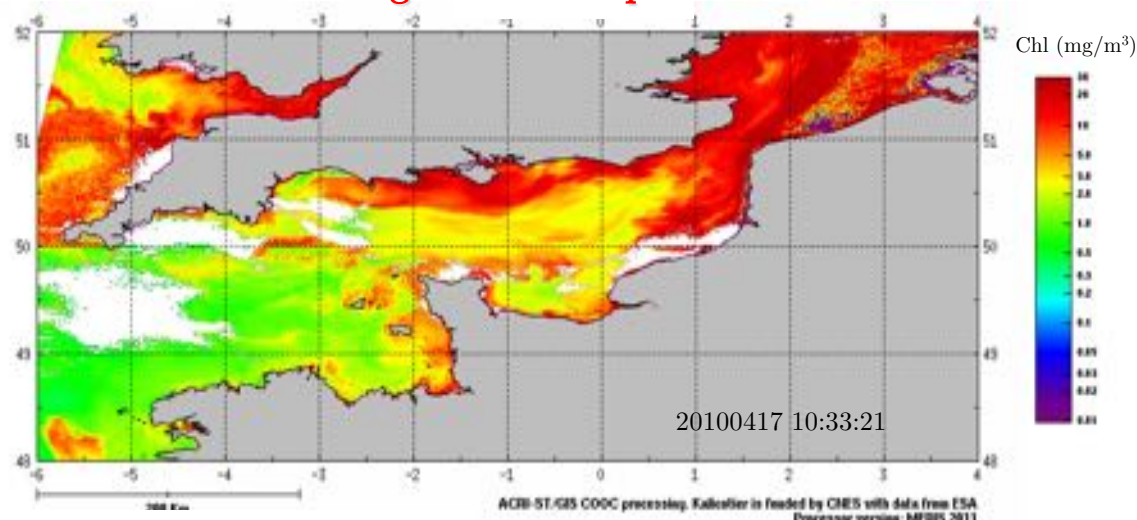
<http://oceancolor.gsfc.nasa.gov/>

$\rho_t(\lambda)$ = top of atmosphere reflectance

$\rho_w(\lambda)$ = water-leaving reflectance (ocean color)



Biogeochemical parameters



<http://kalicotier.gis-cooc.org/>

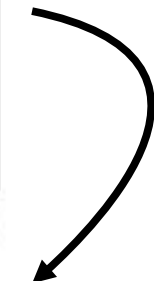
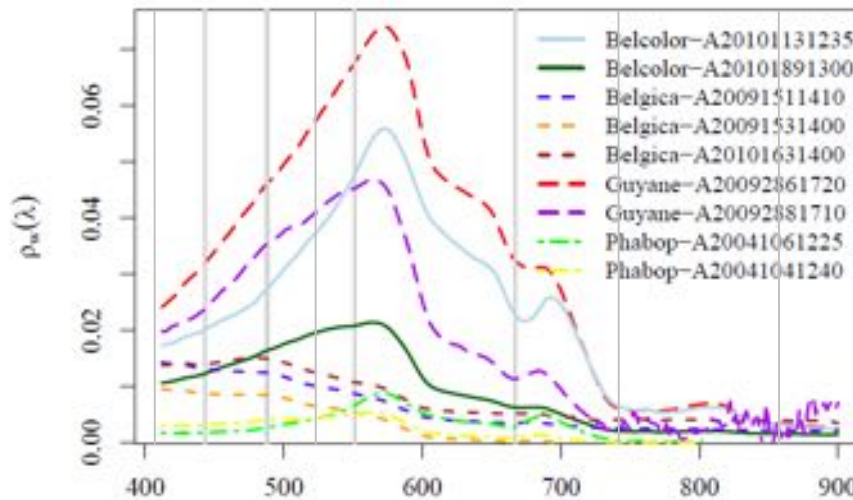
From satellite to biogeochemical parameters... A challenging task



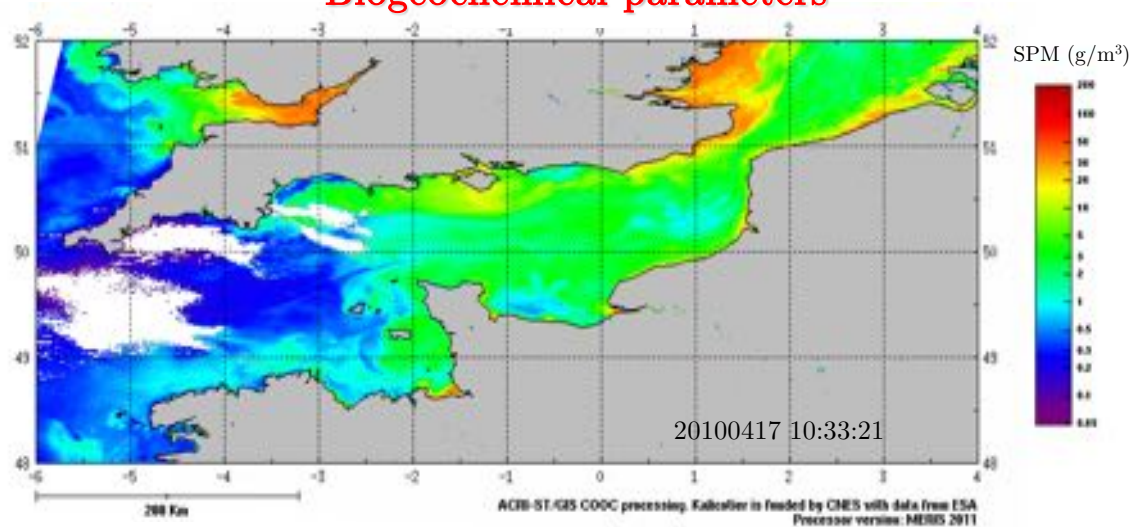
<http://oceancolor.gsfc.nasa.gov/>

$\rho_t(\lambda)$ = top of atmosphere reflectance

$\rho_w(\lambda)$ = water-leaving reflectance (ocean color)

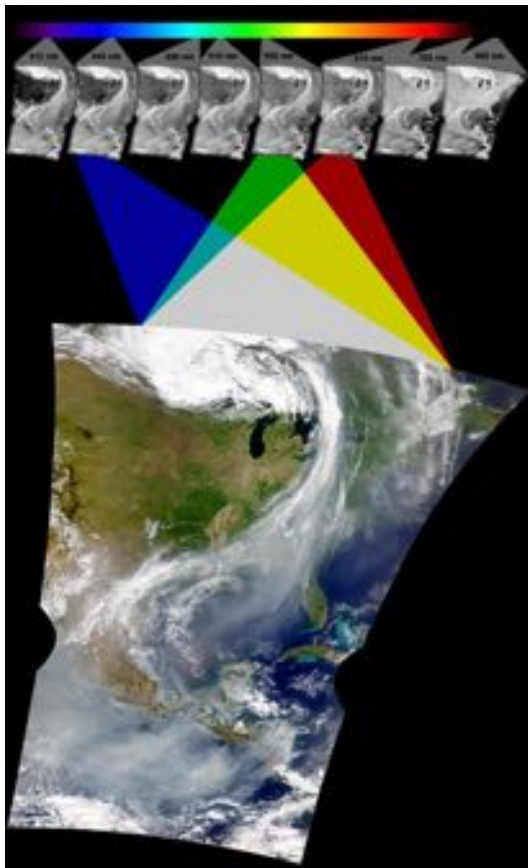


Biogeochemical parameters



<http://kalicotier.gis-cooc.org/>

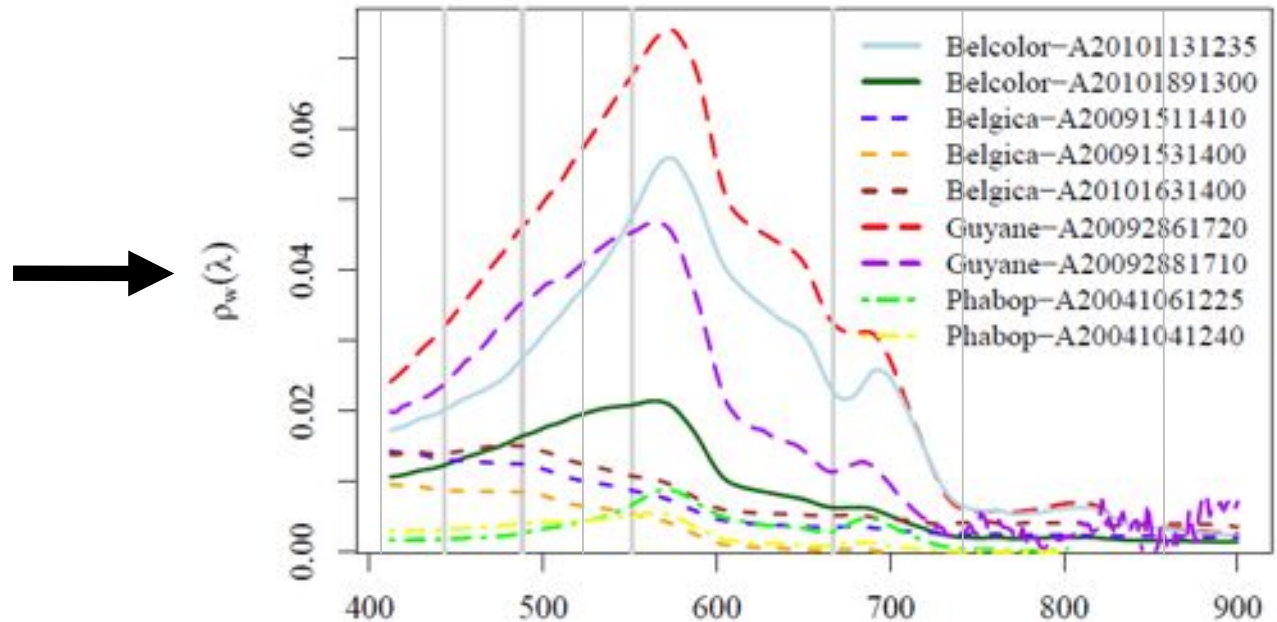
From satellite to biogeochemical parameters... A challenging task



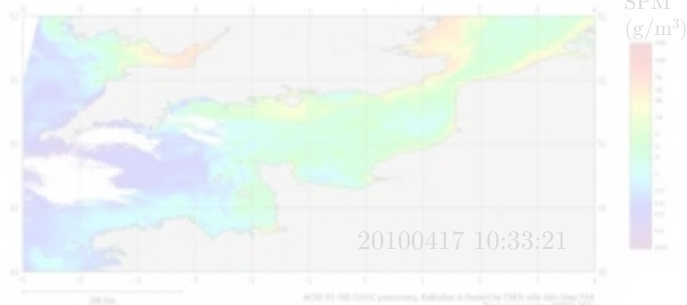
<http://oceancolor.gsfc.nasa.gov/>

$\rho_t(\lambda)$ = top of atmosphere reflectance

$\rho_w(\lambda)$ = water-leaving reflectance (ocean color)



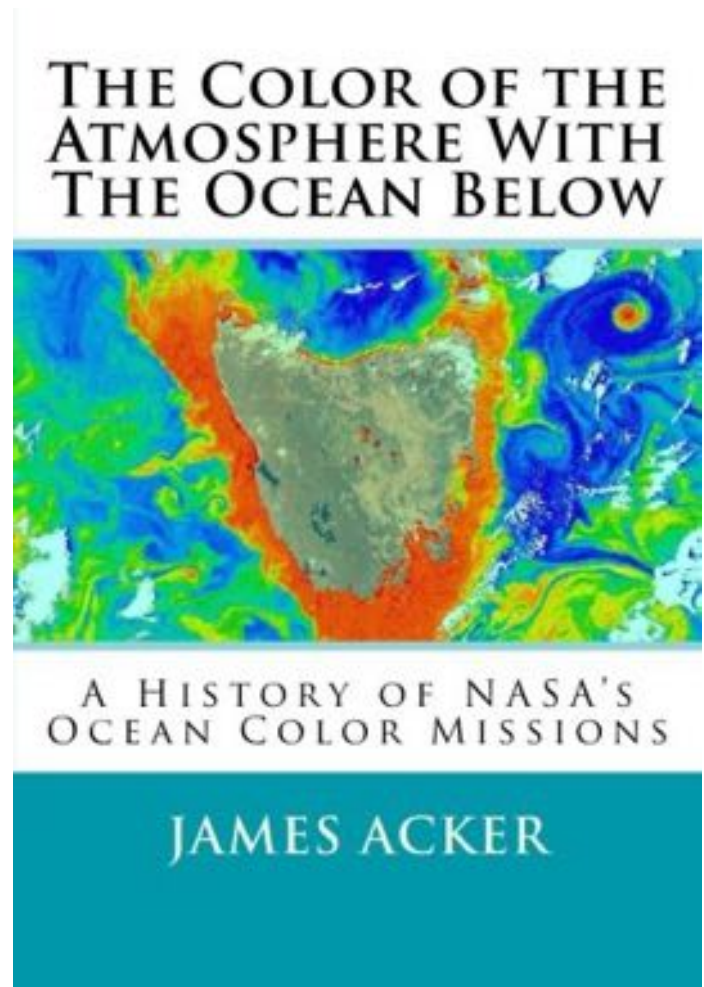
Biogeochemical parameters



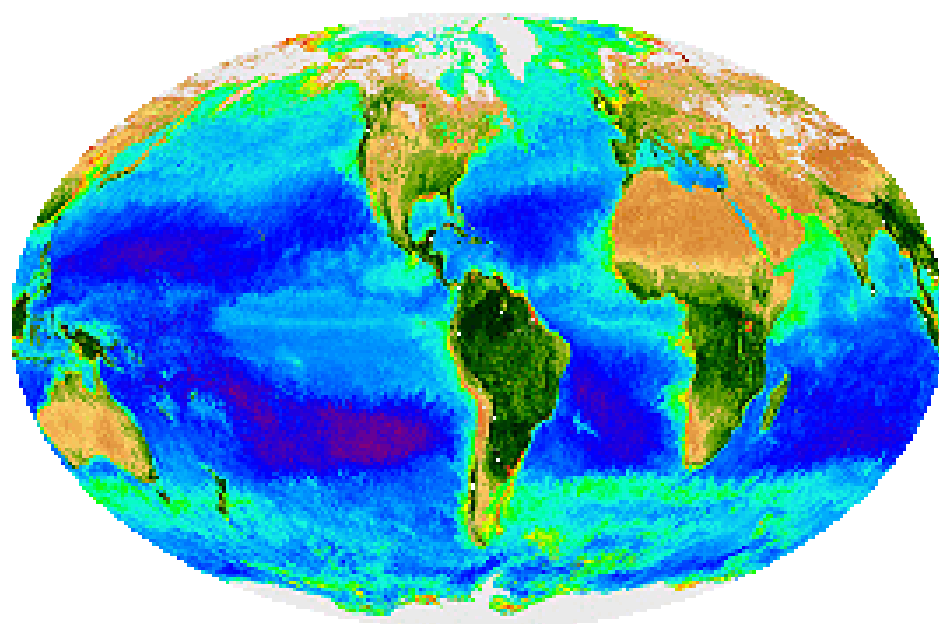
<http://kalicotier.gis-cooc.org/>

History of atmospheric correction

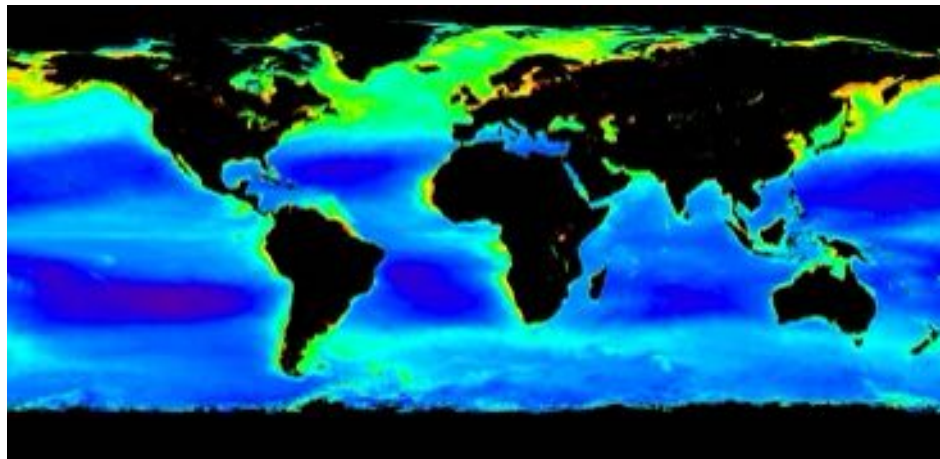
- Color photographs obtained by spacecraft
- Clarke et al. (1970): measurements of radiance spectra from aircraft → Detection of chl-a + atmos. effects
- Gordon (1978; 1980): single-scattering AC for CZCS
- Gordon and Wang (1994): multiple-scattering AC for SeaWiFS
- Coastal waters + absorbing aerosols



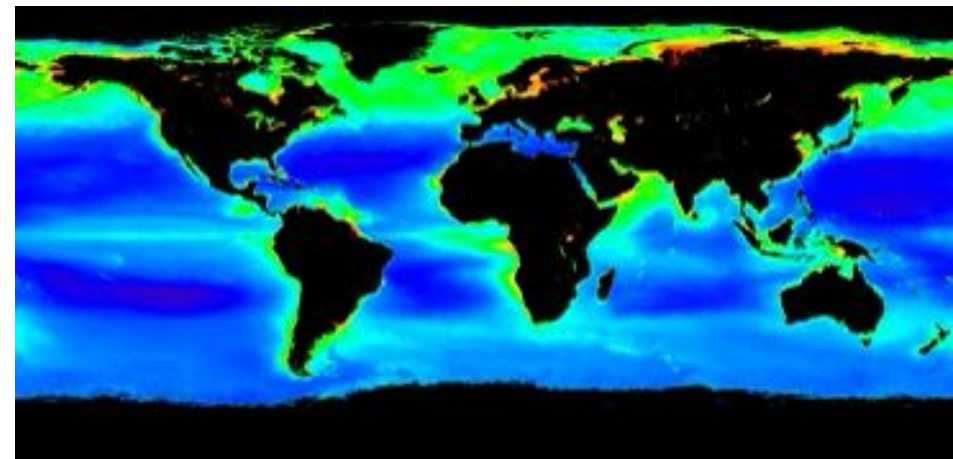
Chlorophyll-a concentration: Historical product of remote sensing of ocean color



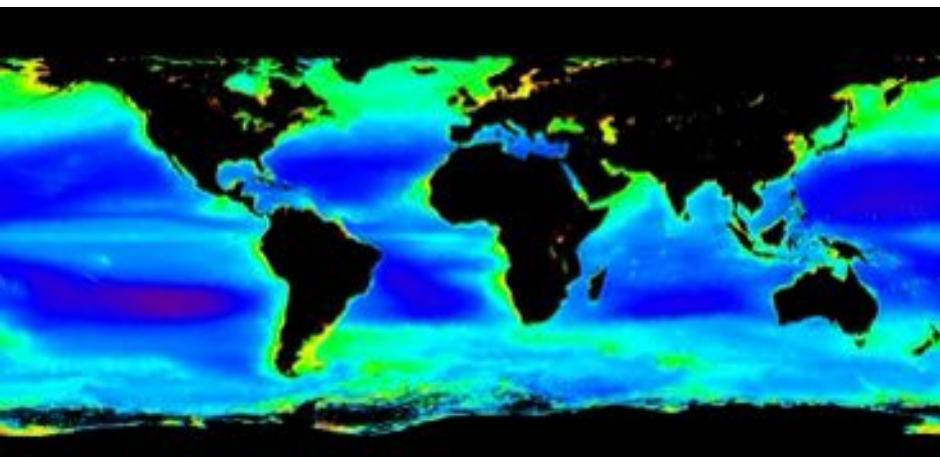
Source :<http://oceancolor.gsfc.nasa.gov/>



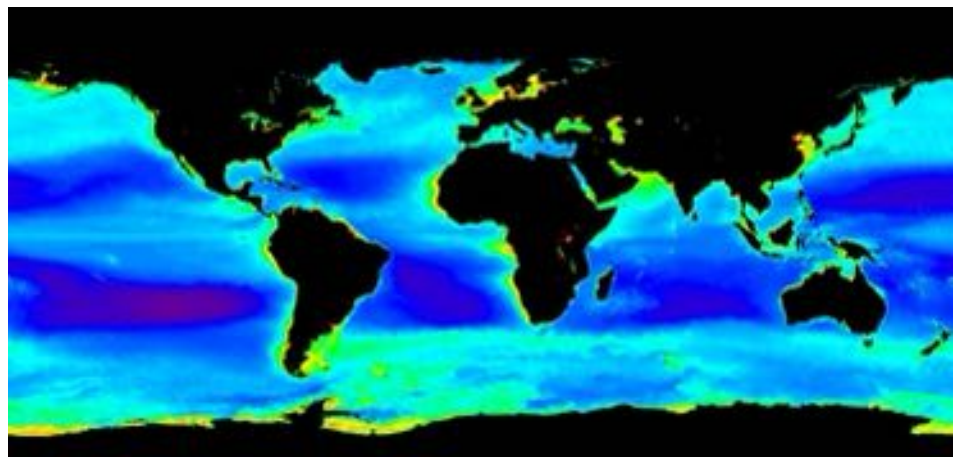
Spring



Summer



Fall



Winter

Seasonal mean of the chlorophyll-a concentration between 1997 and 2006 from SeaWiFS

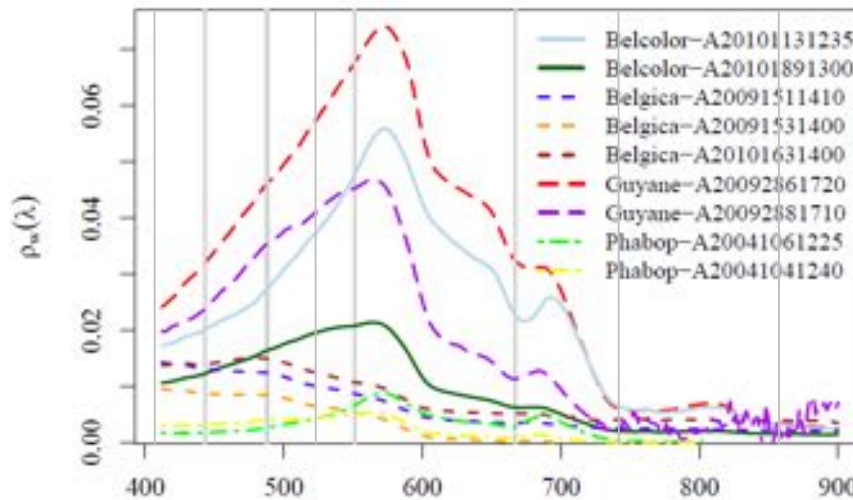
From satellite to biogeochemical parameters... A challenging task



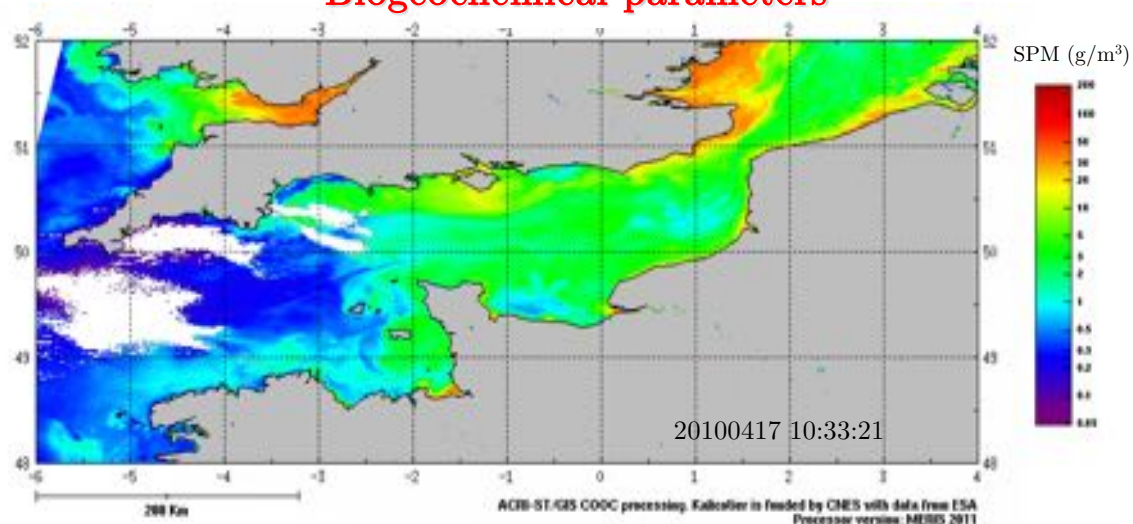
<http://oceancolor.gsfc.nasa.gov/>

$\rho_t(\lambda)$ = top of atmosphere reflectance

$\rho_w(\lambda)$ = water-leaving reflectance (ocean color)



Biogeochemical parameters



<http://kalicotier.gis-cooc.org/>

New bio-optical algorithms are developed and validated

- Inherent Optical Properties
 - *Loisel et al. (2014a); Loisel et al. (2018), Jorge et al. (2021)*
- Vertical attenuation coefficient, K_d
 - *Jamet et al. (2012)*
- Dissolved Organic Carbon, DOC
 - *Vantrepotte et al. (2015)*
- Suspended Particulate Matter, SPM
 - *Loisel et al. (2014b); Han et al. (2015)*
- Chlorophyll-a concentration, Chl
 - *Loisel et al., 2017*
- Particulate Organic Carbon, POC
 - *Tran et al., 2019*

New bio-optical algorithms are developed and validated

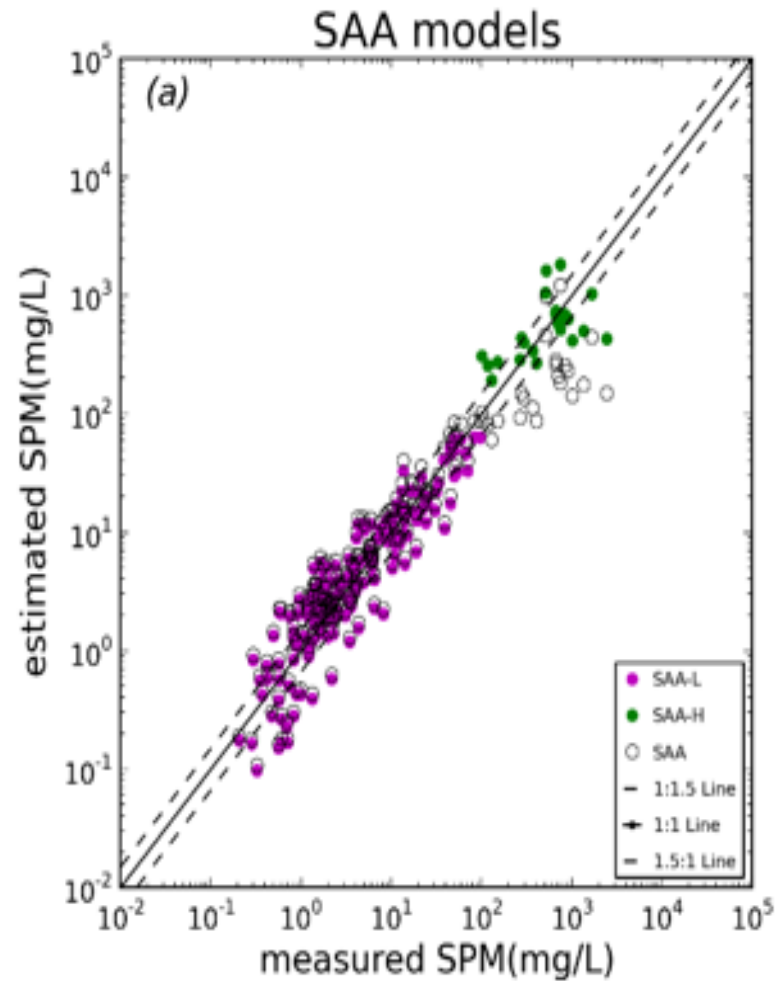
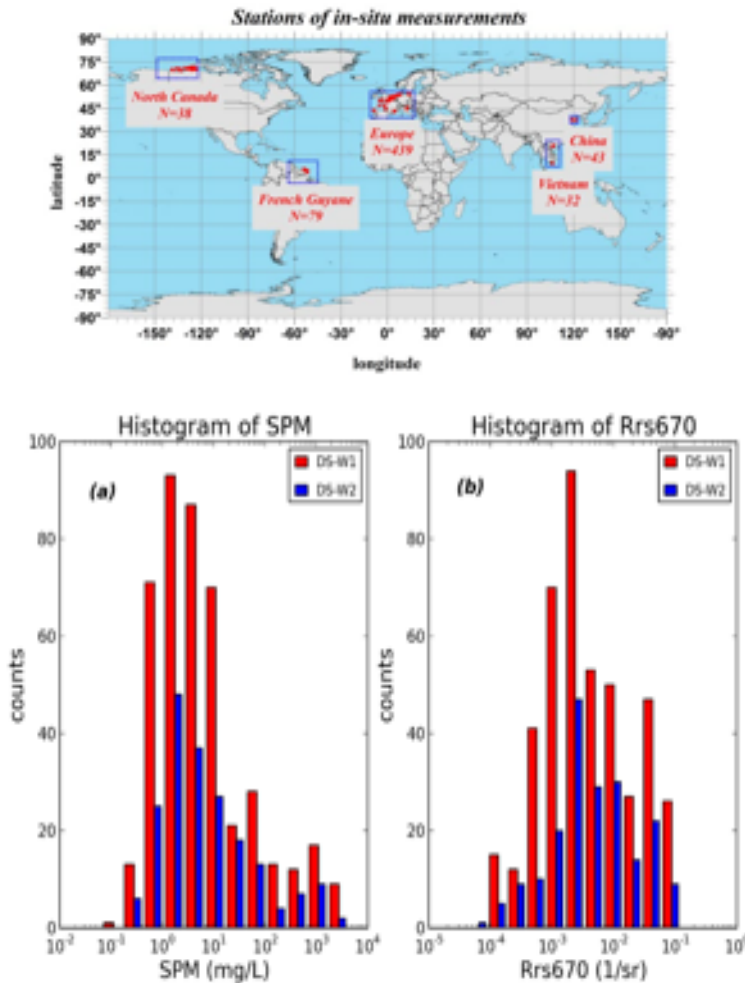
- Inherent Optical Properties
 - *Loisel et al. (2014a); Loisel et al. (2018), Jorge et al. (2021)*
- Vertical attenuation coefficient, K_d
 - *Jamet et al. (2012)*
- Dissolved Organic Carbon, DOC
 - *Vantrepotte et al. (2015)*
- **Suspended Particulate Matter, SPM**
 - *Loisel et al. (2014b); Han et al. (2015)*
- Chlorophyll-a concentration, Chl
 - *Loisel et al., 2017*
- Particulate Organic Carbon, POC
 - *Tran et al., 2019*

The analysis of the spatio-temporal variability of these different parameters at global scale requires a specific methodology which has first been tested for SPM.

The SPM monitoring is essential for many reasons:

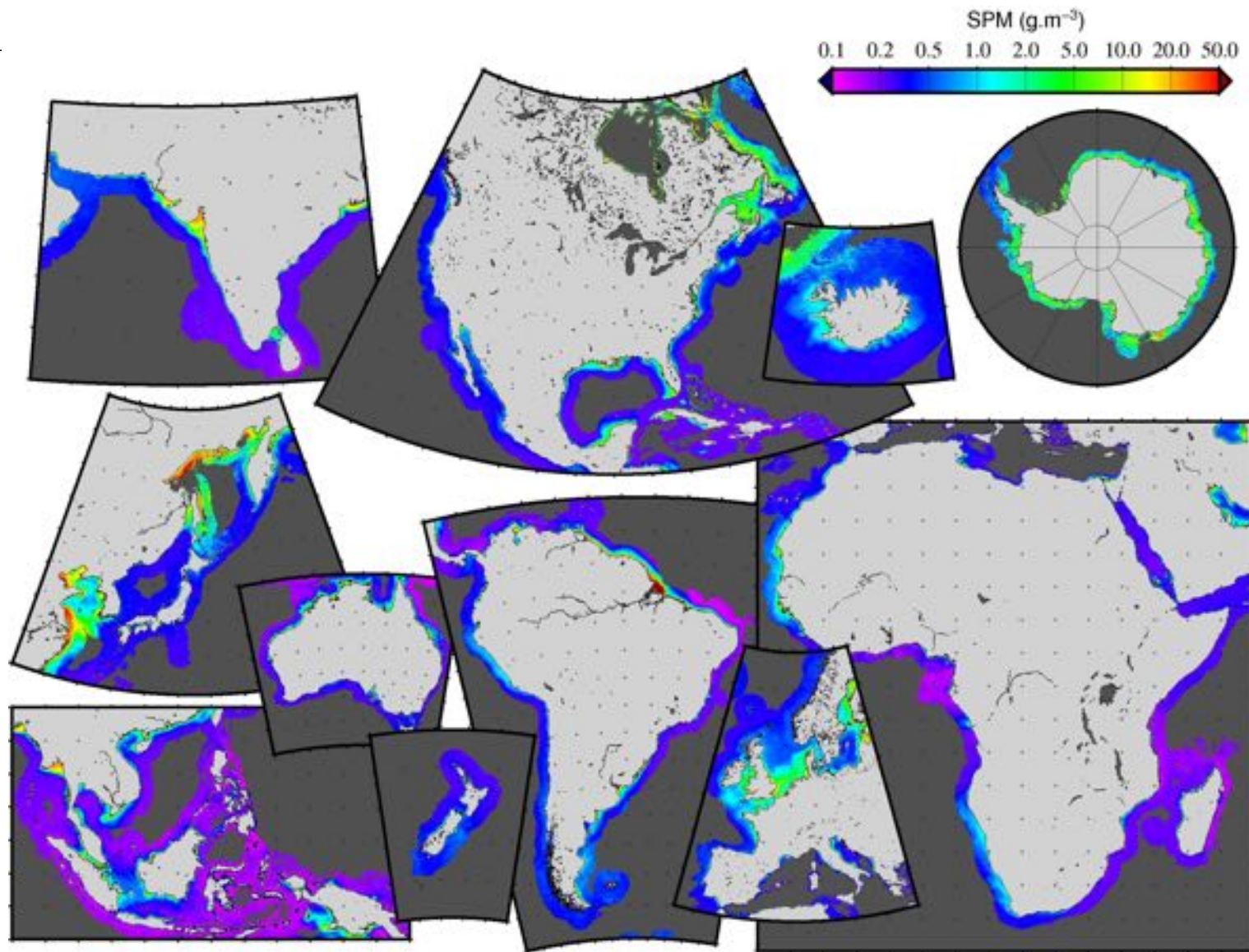
- SPM modifies the availability of light in the water column
- SPM from rivers and land washing is a source of new nutrients for coastal waters
 - Directly impact primary production and the recruitment of fishes
- SPM is tightly related to coastal erosion and accretion processes
 - Direct impacts on the modification of the coastline, as well as on the mangroves evolution

SPM is retrieved by a new semi-analytical algorithm which allows SPM to be assessed over 4 orders of magnitude (thanks to a switching approach) from $R_{rs}(665)$.

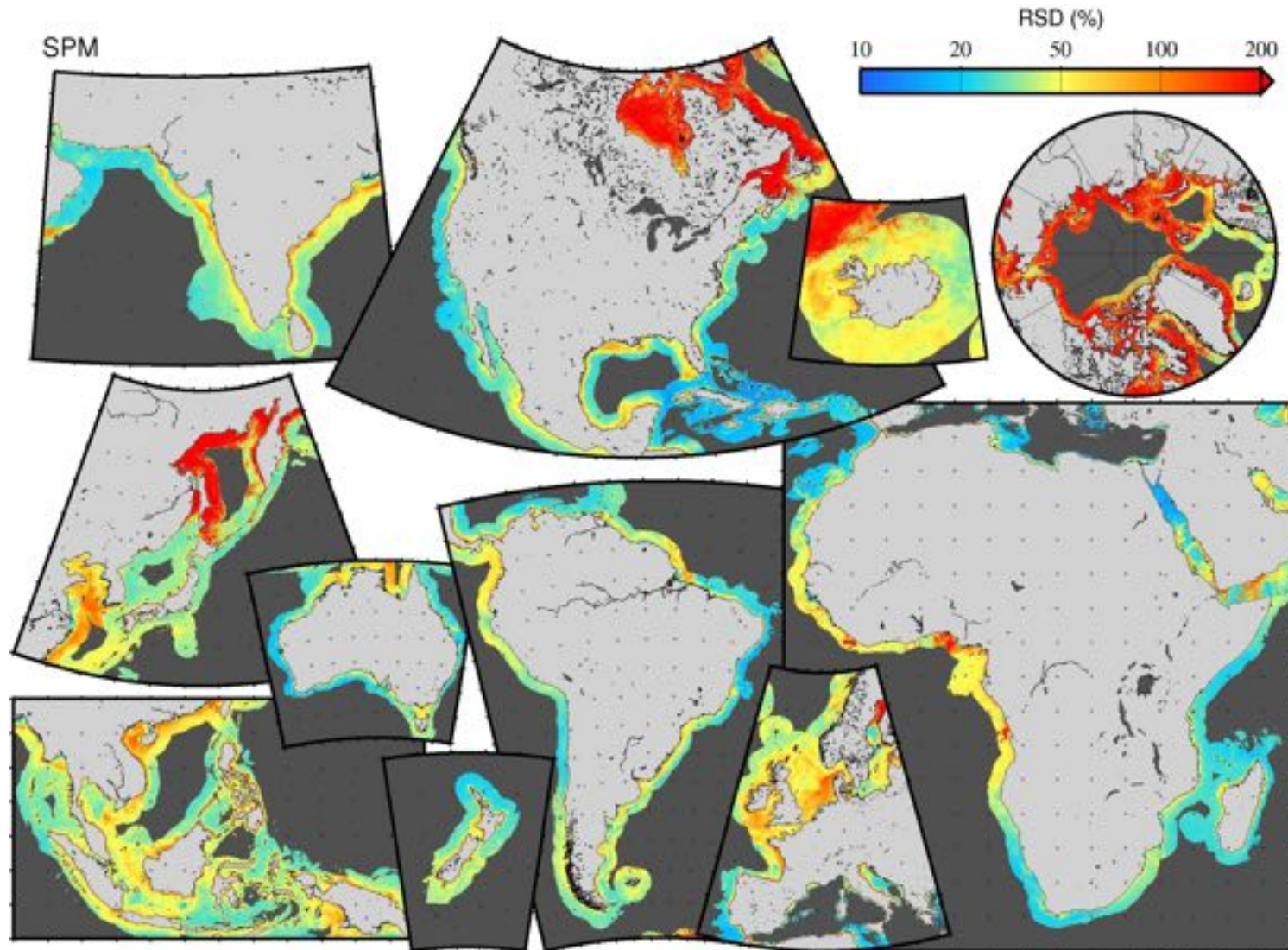


A global climatology has then been developed using the 10 years of the MERIS data.

March



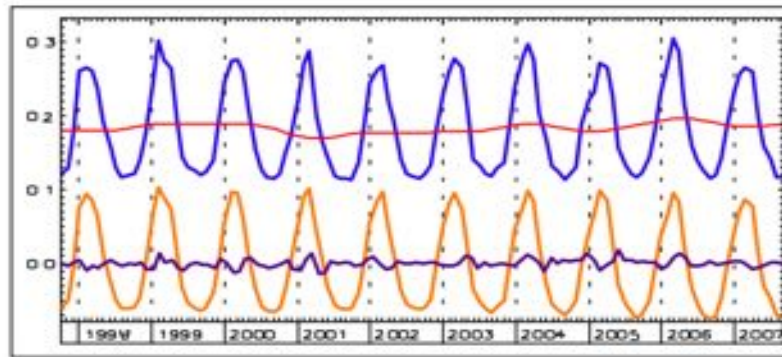
The variation coefficient calculated over the whole archive (monthly) is a simple indicator to quickly identify areas of contrasted temporal variability.



The temporal series have been decomposed using appropriated statistical tools.

Census X-11: iterative bandpass filtering method

(Vantrepotte and Mélin, 2011; Vantrepotte et al., 2011, Pezzoli et al., 2005)



$$X(t) = S(t) + T(t) + I(t)$$

$X(t)$ original series

$T(t)$ Trend-cycle term

$S(t)$ Seasonal term

$I(t)$ Irregular term

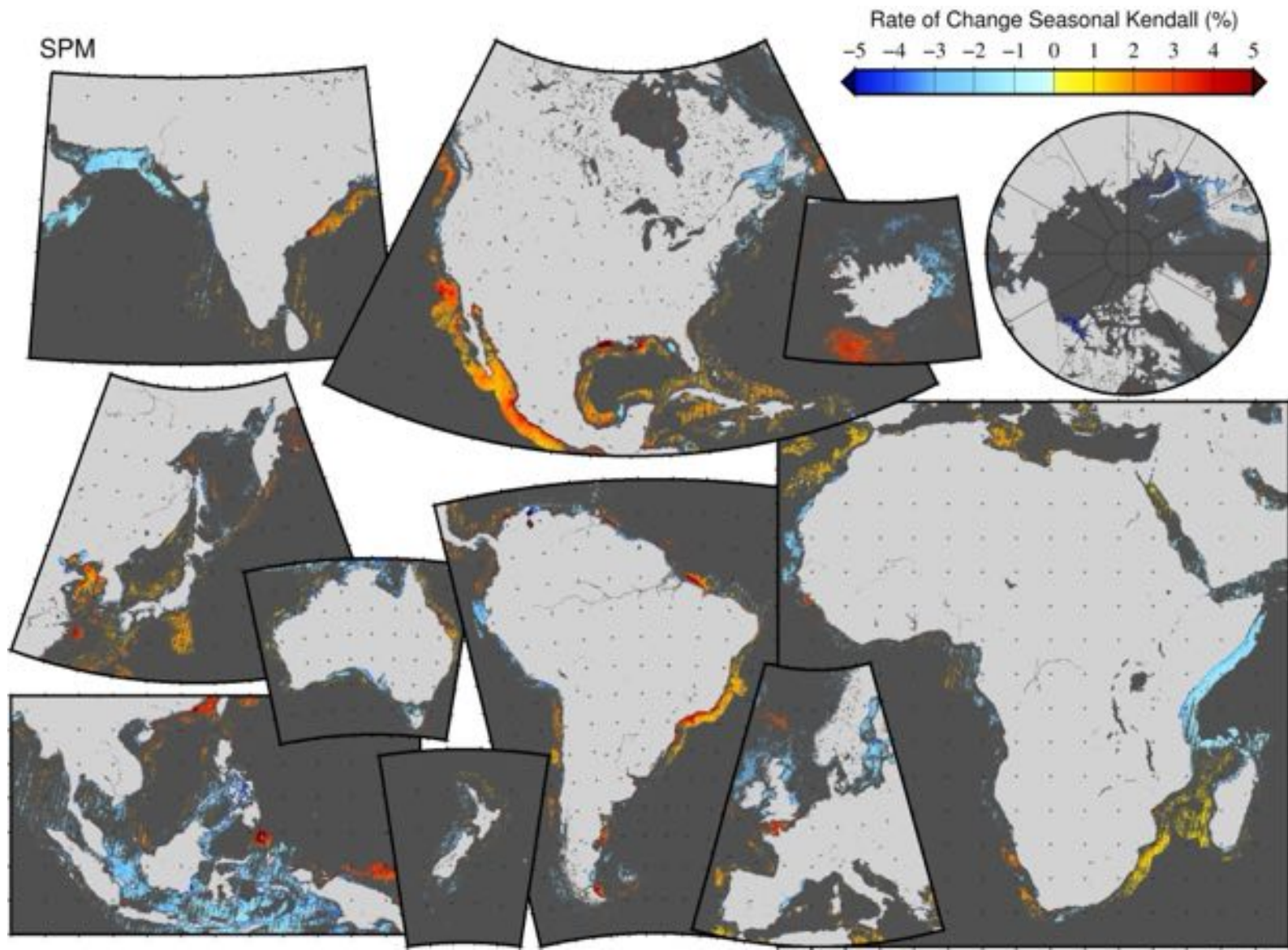
Contribution of each component to the total variance of the series (%)

- $S(t)$ Stability of the seasonal cycle (pseudo-periodical)
- $T(t)$ Nature of the observed trends (and identification of exceptional non-linear trend patterns)
- $I(t)$ Irregular variations -Sub-annual variations

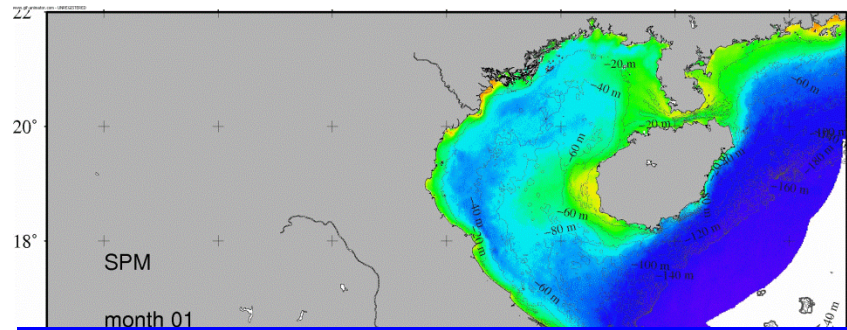
X-11

Trend detection: seasonal Kendal test and
Ken's slope estimator (%/year)

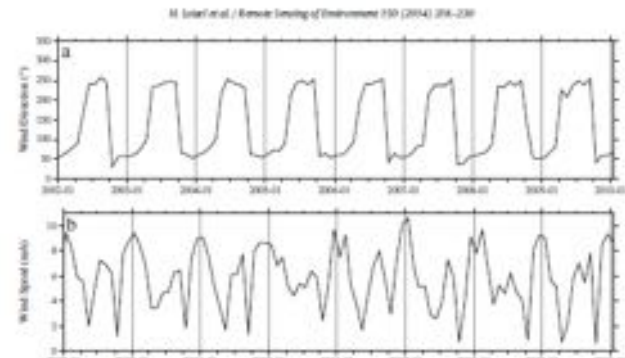
A global vision of the variation of the products (here SPM) is now available showing changes up to 50% in given areas (scale in % per year over ten years)



The combination of SPM products with forcing parameters provides relevant information on the origin of the observed patterns: example for the Mekong delta evolution

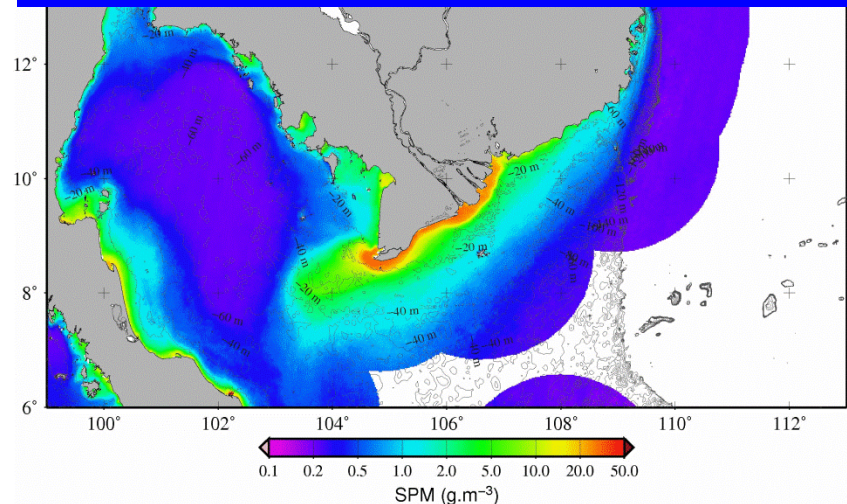


Wind direction

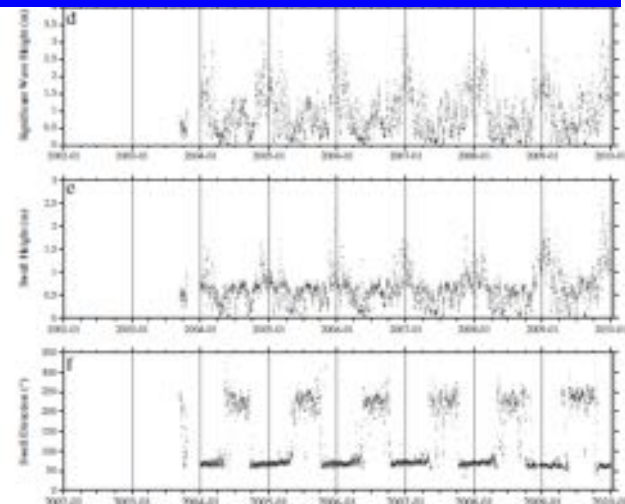


Wind speed

This SPM decreasing rate in the Mekong delta can not be explained by the oceanographic physical forcing parameters



Wave + Swell Height



Swell Height

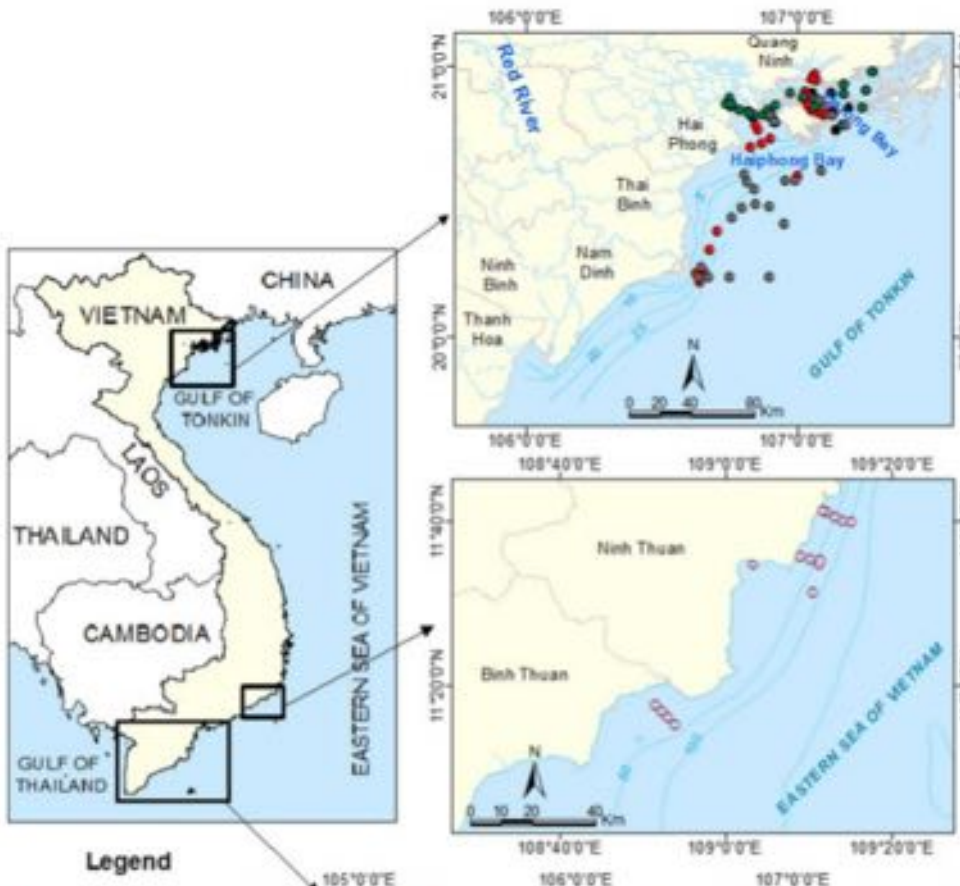
Swell Direction

New bio-optical algorithms are developed and validated

- Inherent Optical Properties
 - *Loisel et al. (2014a); Loisel et al. (2018), Jorge et al. (2021)*
- Vertical attenuation coefficient, K_d
 - *Jamet et al. (2012)*
- Dissolved Organic Carbon, DOC
 - *Vantrepotte et al. (2015)*
- Suspended Particulate Matter, SPM
 - *Loisel et al. (2014b); Han et al. (2015)*
- **Chlorophyll-a concentration, Chl**
 - *Loisel et al., 2017*
- Particulate Organic Carbon, POC
 - *Tran et al., 2019*

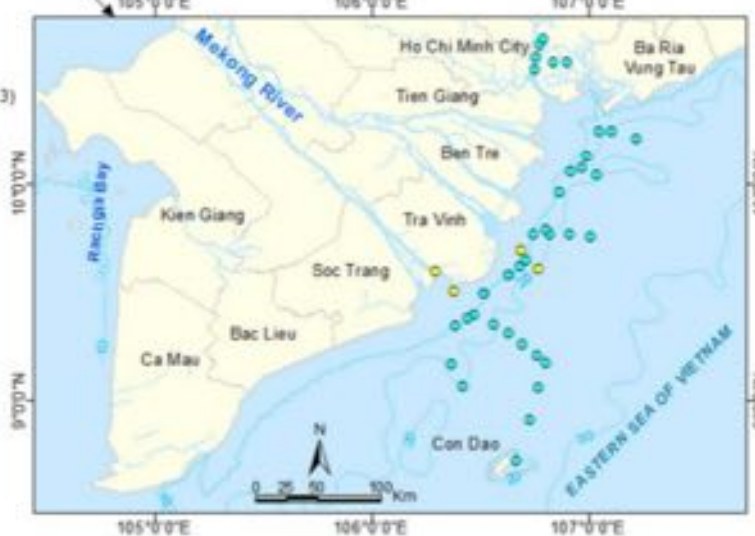
Evaluation of chlorophyll-a algorithms in Vietnamese coastal waters

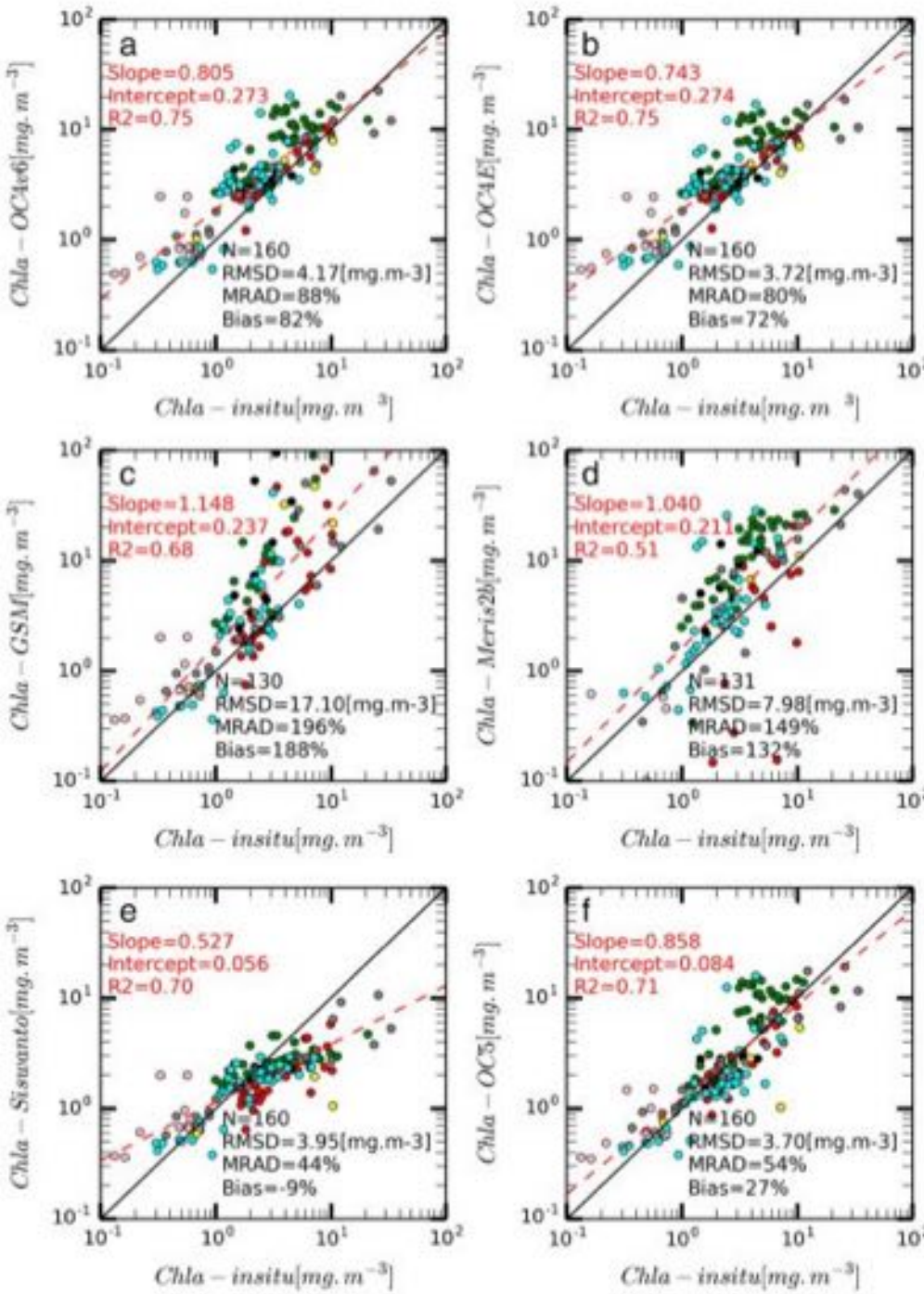
- 5 chl-a algorithms
- In-situ measurements in Vietnamese waters
- Collaboration with STI/VAST (Hanoï), IMER (Haiphong), Institute of Oceanography/VAST (Nha Trang)



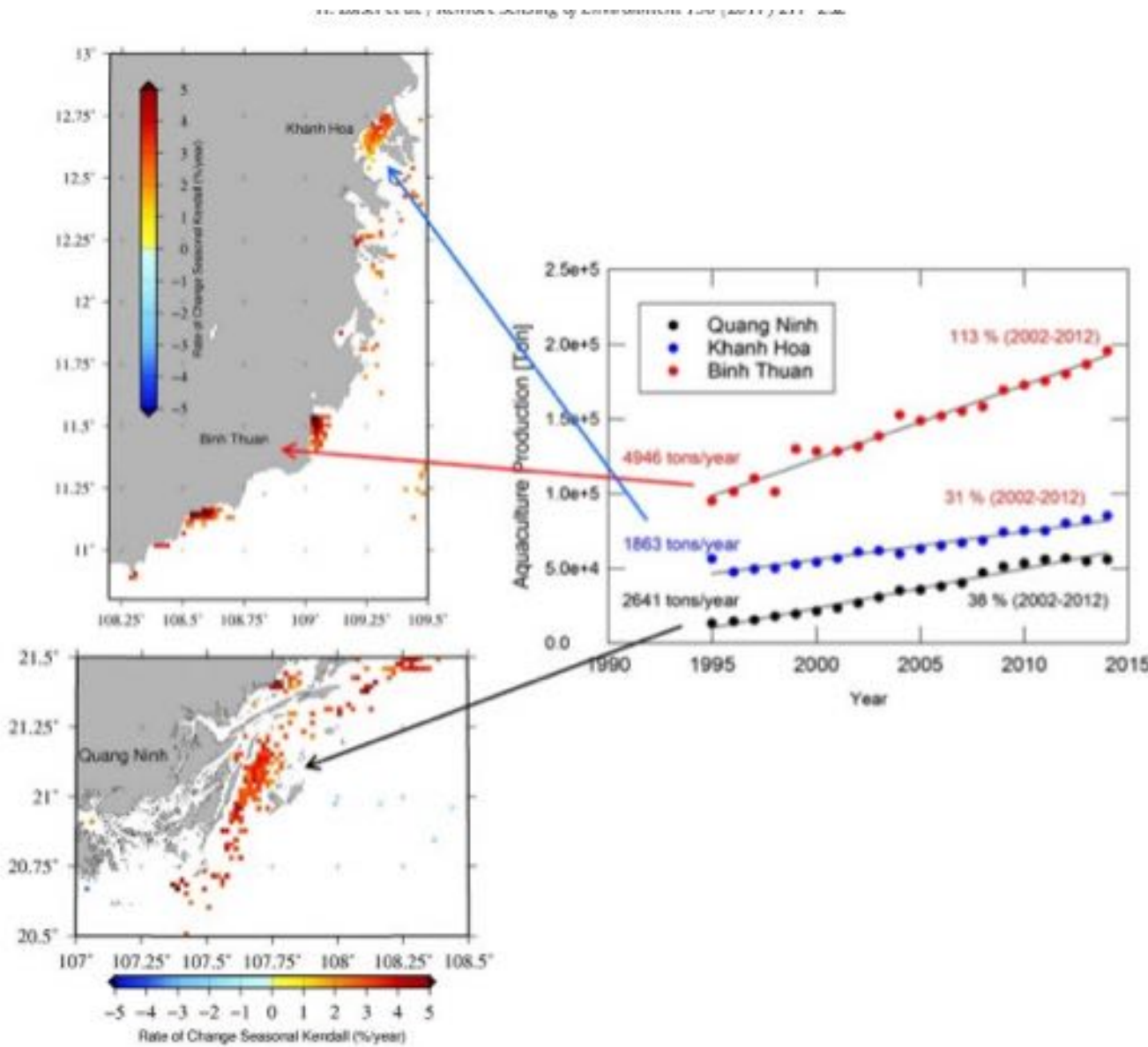
Legend

- HBHE (11/2011)
- HBHE (10/2012)
- HBHE (05-07/2013)
- HBHE (07/2014)
- NT (04/2015)
- MD (03/2012)
- MD (06/2014)





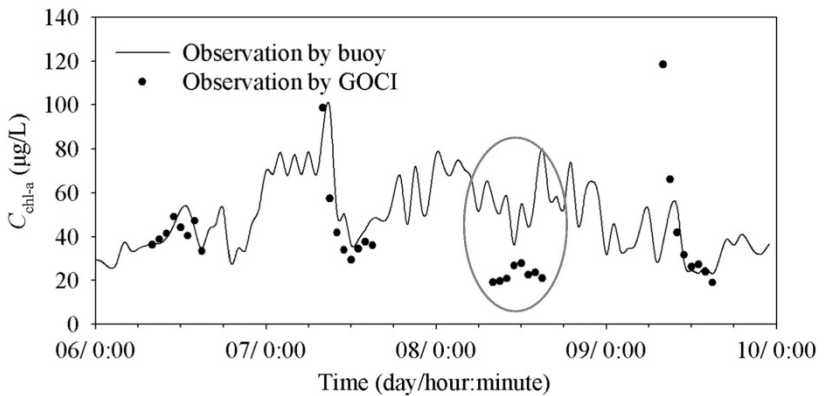
Impact of aquaculture



Monitoring [Chl-a] with geostationnary GOCI

- GOCI:

- South-Korea
- Spectral bandes similar as SeaWiFS
- 1 image / hour (8/day)



Estimation of the turbidity and suspended particulate matter from geostationary sensor SEVIRI on METEOSAT Second Generation (MSG)

- SEVIRI:

- Limited spectral resolution
- Enough bands for SPM
- 1 image every 15 min

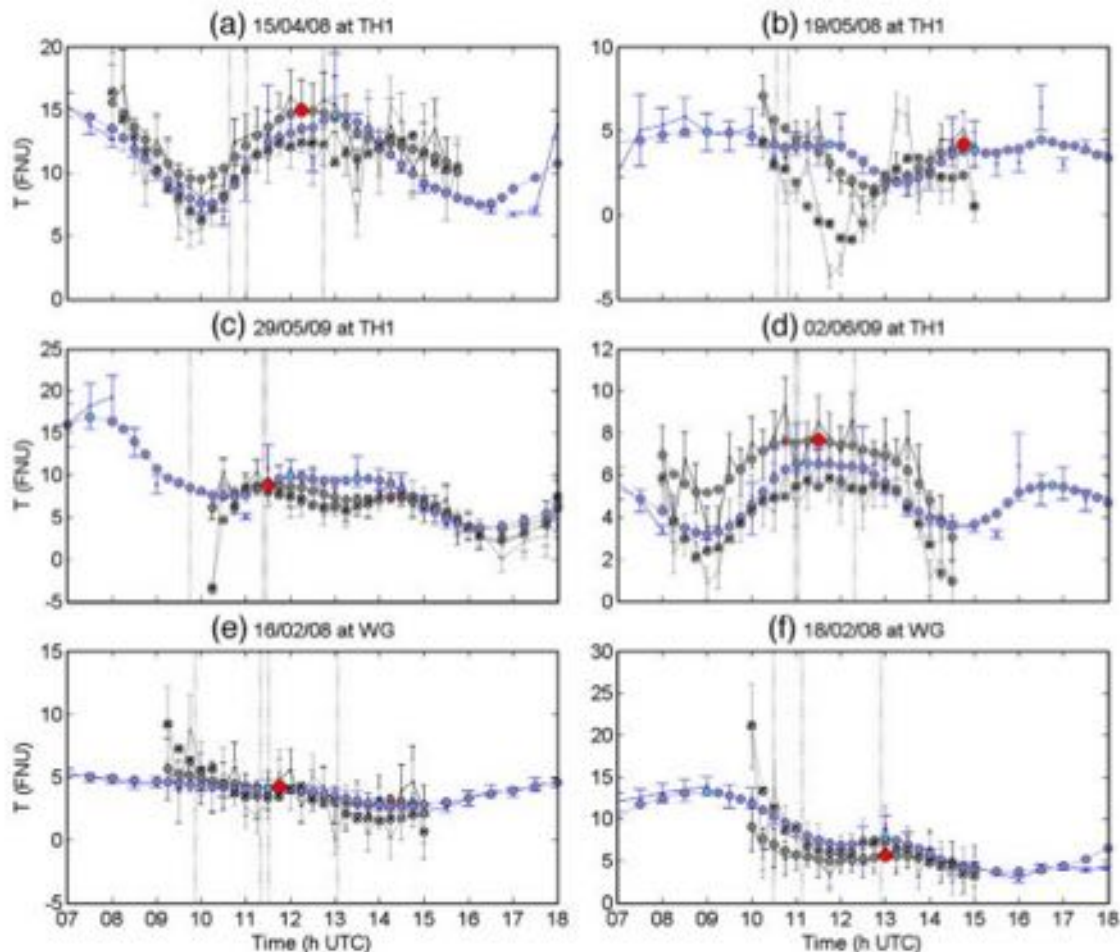
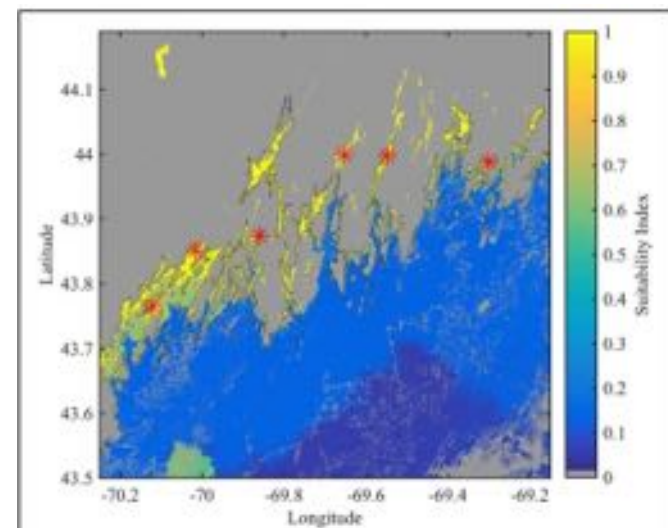
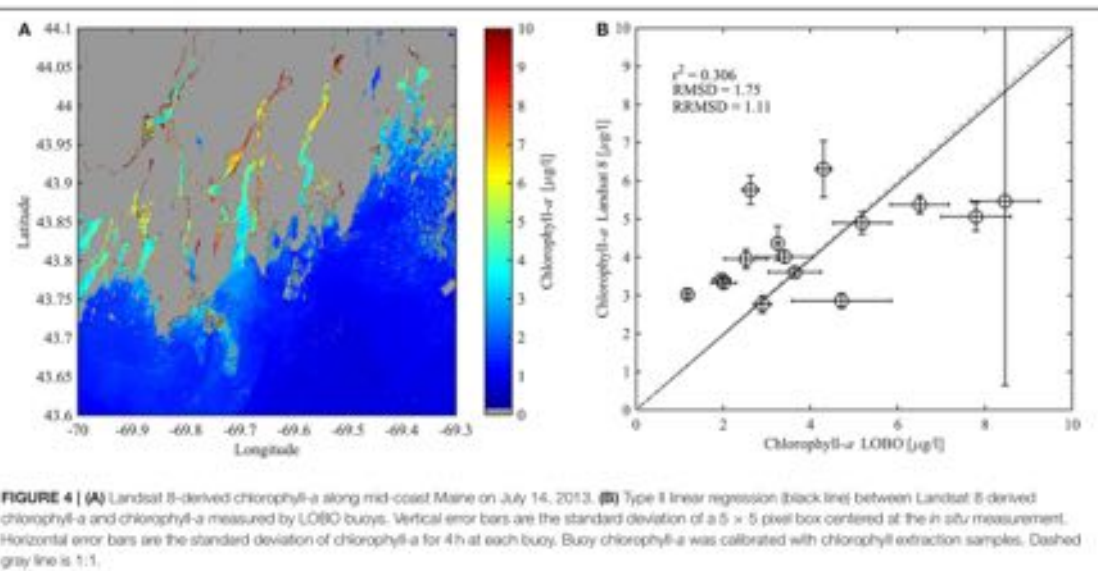
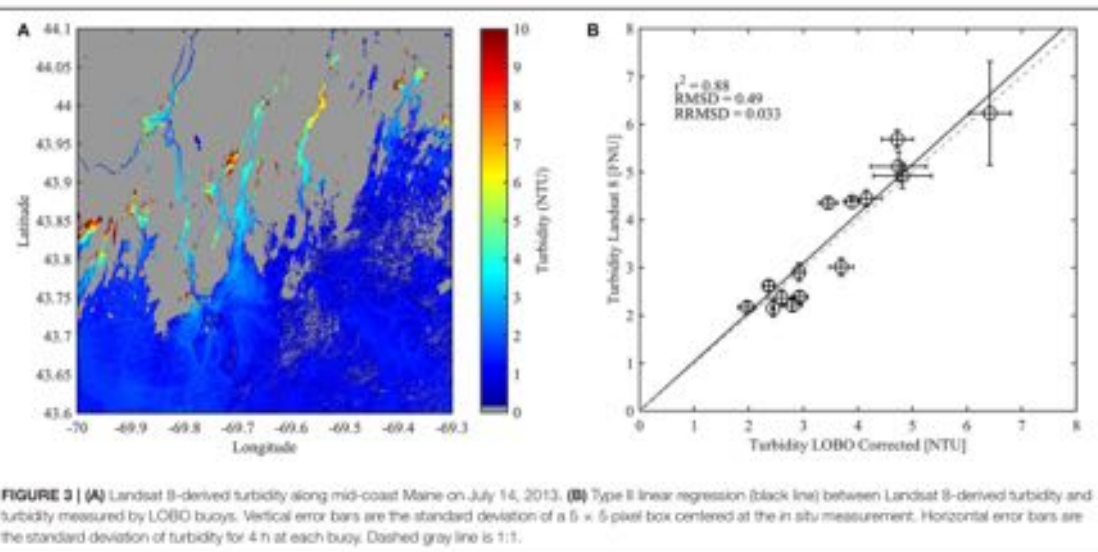
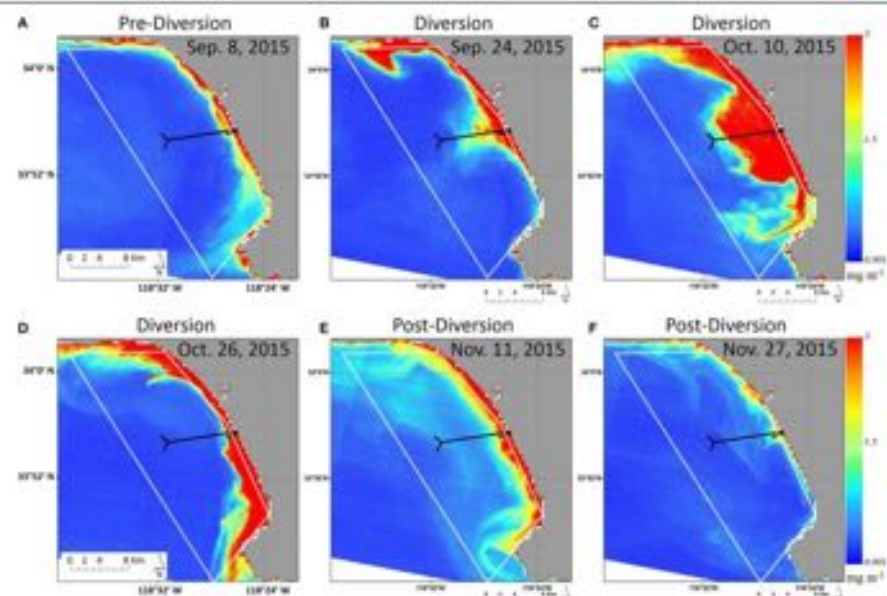
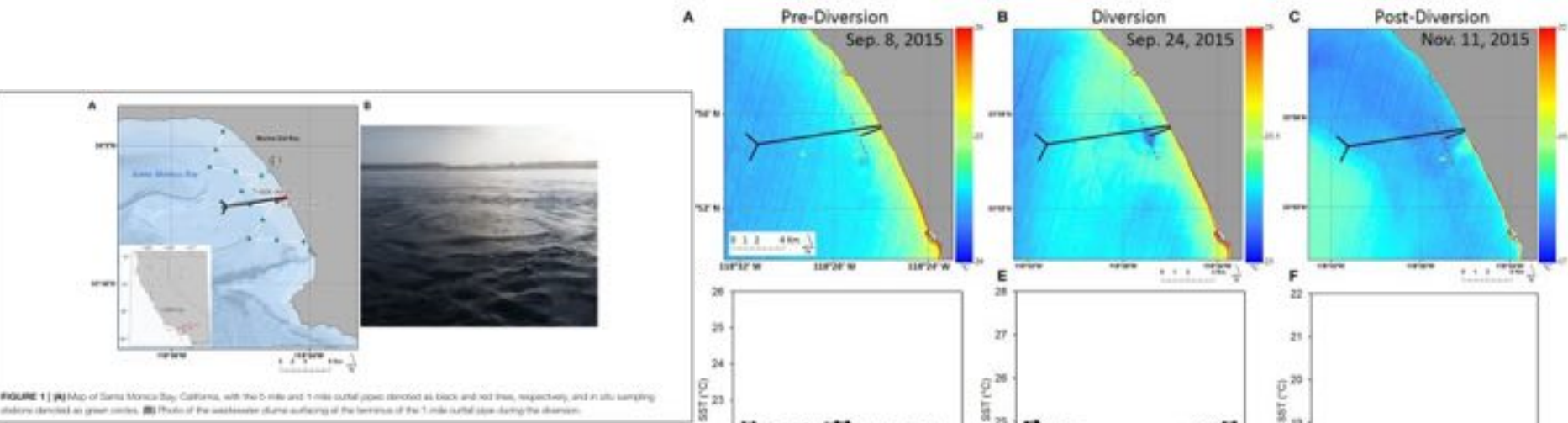


Fig. 8. Randomly selected original and smoothed time series of T obtained from SEVIRI and SmartBuoys. SEVIRI T data from the VIS06 and HRV bands with their uncertainty (see Eq. (36)) are shown by the black and grey error bars, respectively. Temporally smoothed data series for VIS06 (\circ) and HRV (\otimes) T products are shown in grey, with global (big red dot) and local (small red dots) maxima. SmartBuoy T and its uncertainty is shown by the blue error bars, while the temporally smoothed data series is shown by blue circles with local maxima highlighted in cyan. Grey vertical dotted lines represent data availability from MODIS Aqua/Terra and MERIS ENVISAT.

Oyster Aquaculture Site Selection Using Landsat 8-Derived Sea Surface Temperature, Turbidity, and Chlorophyll a



Application of Landsat 8 for Monitoring Impacts of Wastewater Discharge on Coastal Water Quality



Landsat 8 TIRS-derived SST in Santa Monica Bay with the 5-mile and 1-mile outfall pipes shown as black lines and a 4 km alongshore transect at 1-mile outfall pipe denoted by red dashed lines. (A–F) SSTs across the 4 km alongshore transect, from north to south. (A,D) SST on 8 September 2015. (B,E) SST on 24 September 2015, during the diversion; (C,F) SST on 11 November 2015, after the diversion. Cooler SSTs were detected at the 1-mile outfall pipe during the diversion, due to entrainment of cold bottom water as the wastewater plume surfaced. Pre- and post-diversion, no SST increased at the terminus of the 1-mile outfall pipe. The warm signature of an oil tanker to the southwest of the 1-mile outfall pipe is clearly visible, released from September to November due to seasonal cooling, therefore each image is shown on different temperature scales.

Content

- 101 Remote Sensing
- How to observe the ocean from space?
- Sea-surface temperature
- Sea surface height
- Ocean Color Radiometry
- **Vertical profiles of the upper ocean**

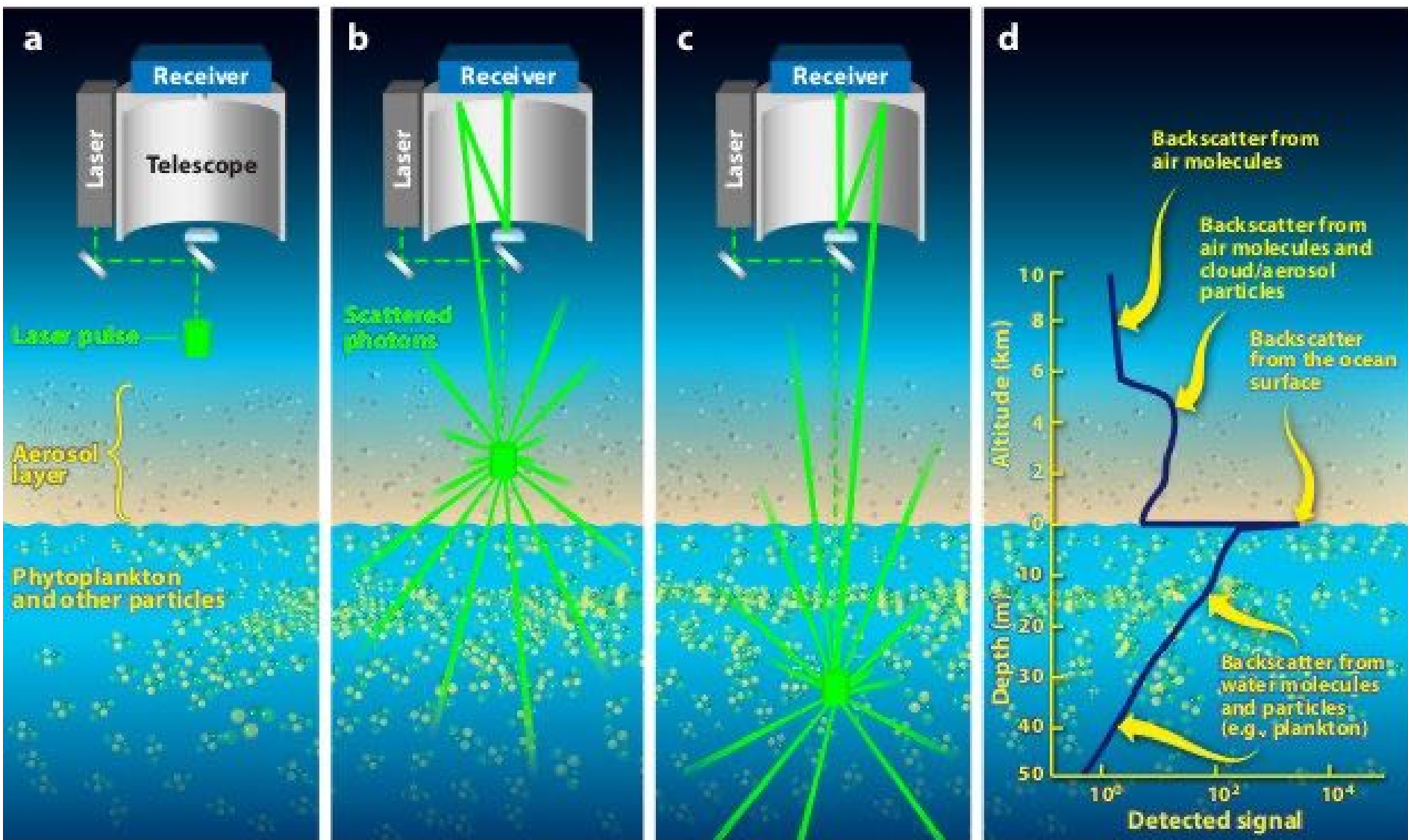
Limitations of ocean color images

- No night-time observations
- No observations over clouds and absorbing aerosols
- No observations for high solar angles $> 70^\circ$ (high latitudes)
- Vertically-weighted values over the water column
- No polarization

→ LIDAR

Lidar 101

- Lidar: LIght Detection And Ranging
- Active technique based on interaction of laser light with matter
- Most common lidar at 532 nm (Q-switched, frequency-doubled Nd:YAG laser)



Lidar 101

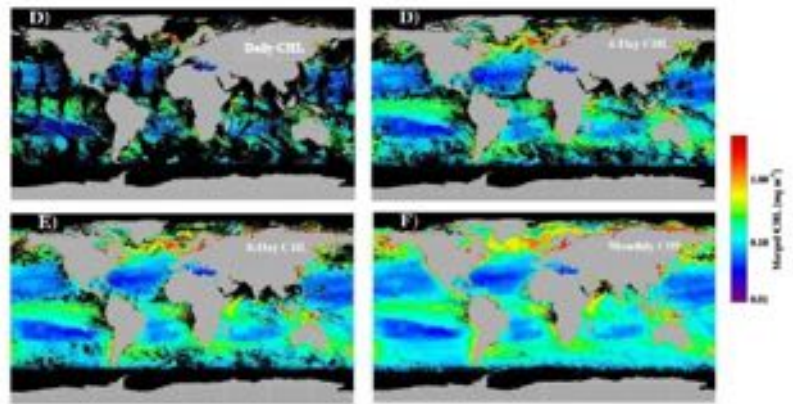
- Active technique based on interaction of laser light with matter
- Most common lidar at 532 nm (Q-switched, frequency-doubled Nd:YAG laser)
- **Lidar equation:**
$$S(z) = \frac{EAO(z)T_0 T_s^2 \eta n \nu}{2(nH + z)^2} \beta(\pi, z) \exp \left[-2 \int_0^z \alpha(z') dz' \right] + S_B$$

With

- Fraction corresponds to the instrument characteristics
- β is the volume scattering coefficient at a scattering angle of π radians
- α is the lidar attenuation coefficient
- S_B is the photocurrent due to background light.

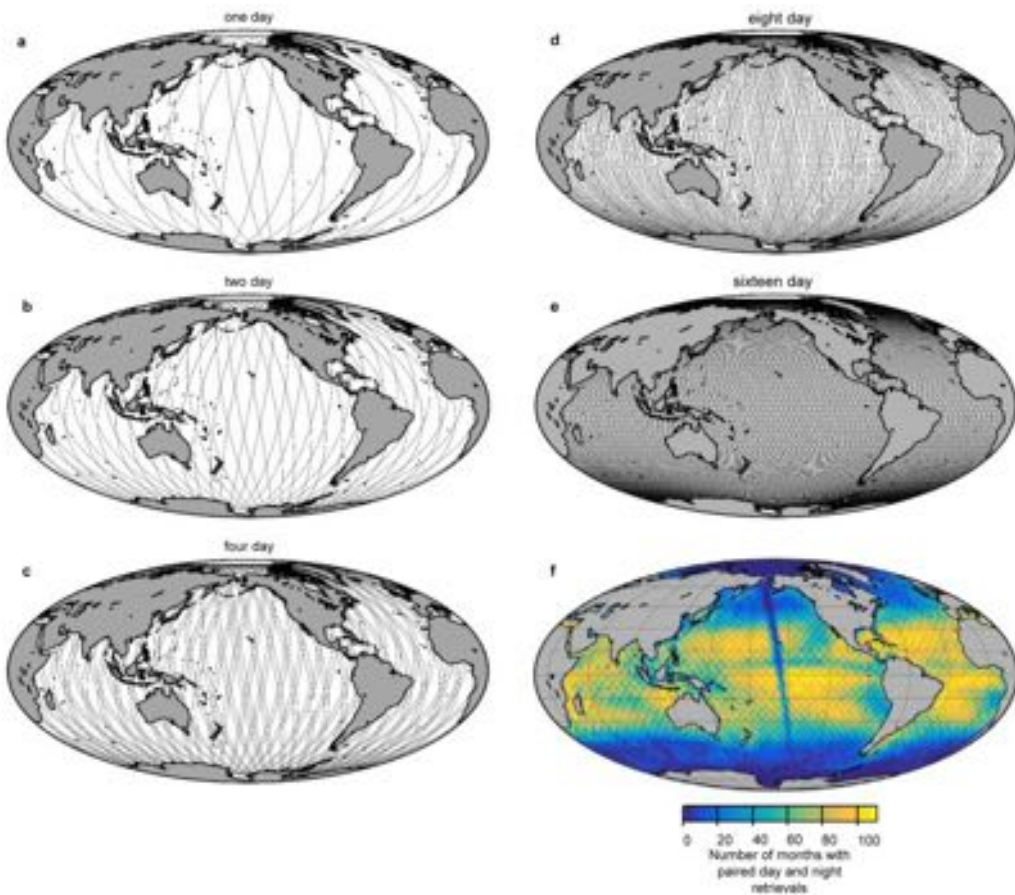
Limitations of oceanic lidar

- One (or two) wavelengths: 532 nm (355nm)
- Low spatial coverage (footprint: \sim 10-80 m)
- Low repetitivity: 16 days
(CALIOP/CALIPSO)/91 jours
(ATLAS/IceSat-2)
- Elastic backscatter lidar: One equation/2 unknowns



Average percentage cover of the ocean (standard deviation)

	SeaWiFS	MODIS-AQUA	MERIS	MERGED
Daily	14.58 (1.03)	11.81 (1.03)	7.77 (1.05)	25.22 (1.88)
4-Day	41.62 (4.67)	33.91 (2.97)	25.18 (4.97)	56.98 (6.24)
8-Day	59.06 (6.72)	51.31 (4.52)	40.23 (6.90)	72.50 (7.59)
Monthly	82.95 (9.79)	79.43 (4.75)	73.34 (9.47)	87.69 (8.87)



How to observe with lidar?

- Air-borne
- Ship-borne
- Space-borne

Scientific applications

- Fisheries
- Scattering layer
- Bio-optical properties of the upper ocean
- Vertical structure of the upper ocean
- Air bubbles
- SST
- Bathymetry
- Internal waves

Scientific applications

- **Fisheries**
- Scattering layer
- Bio-optical properties of the upper ocean
- Vertical structure of the upper ocean
- Air bubbles
- SST
- Bathymetry
- Internal waves

Airborne Lidar: Fisheries (1/2)

- Feasibility to detect fish since 1974
- Individual count of fish
- Species detection

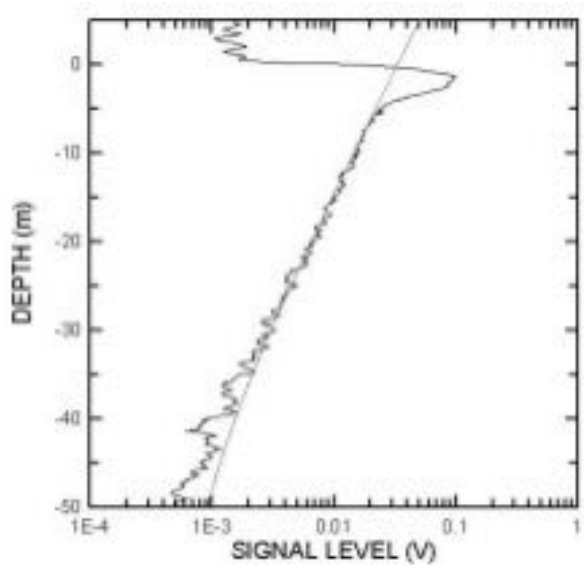


Fig. 7 Typical single-pulse return from clear water with two-point fit.

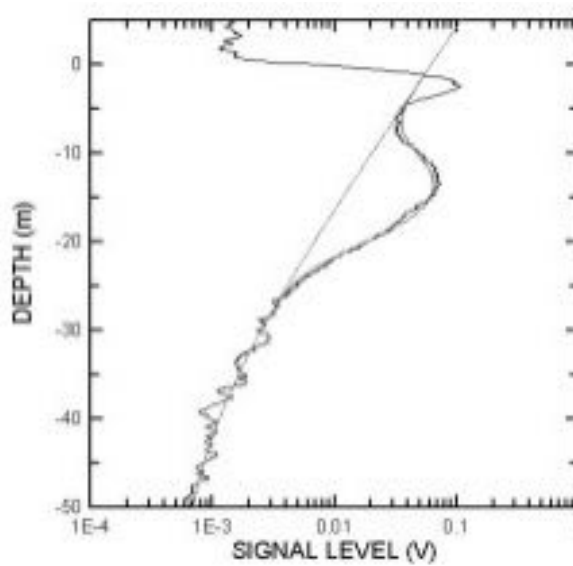
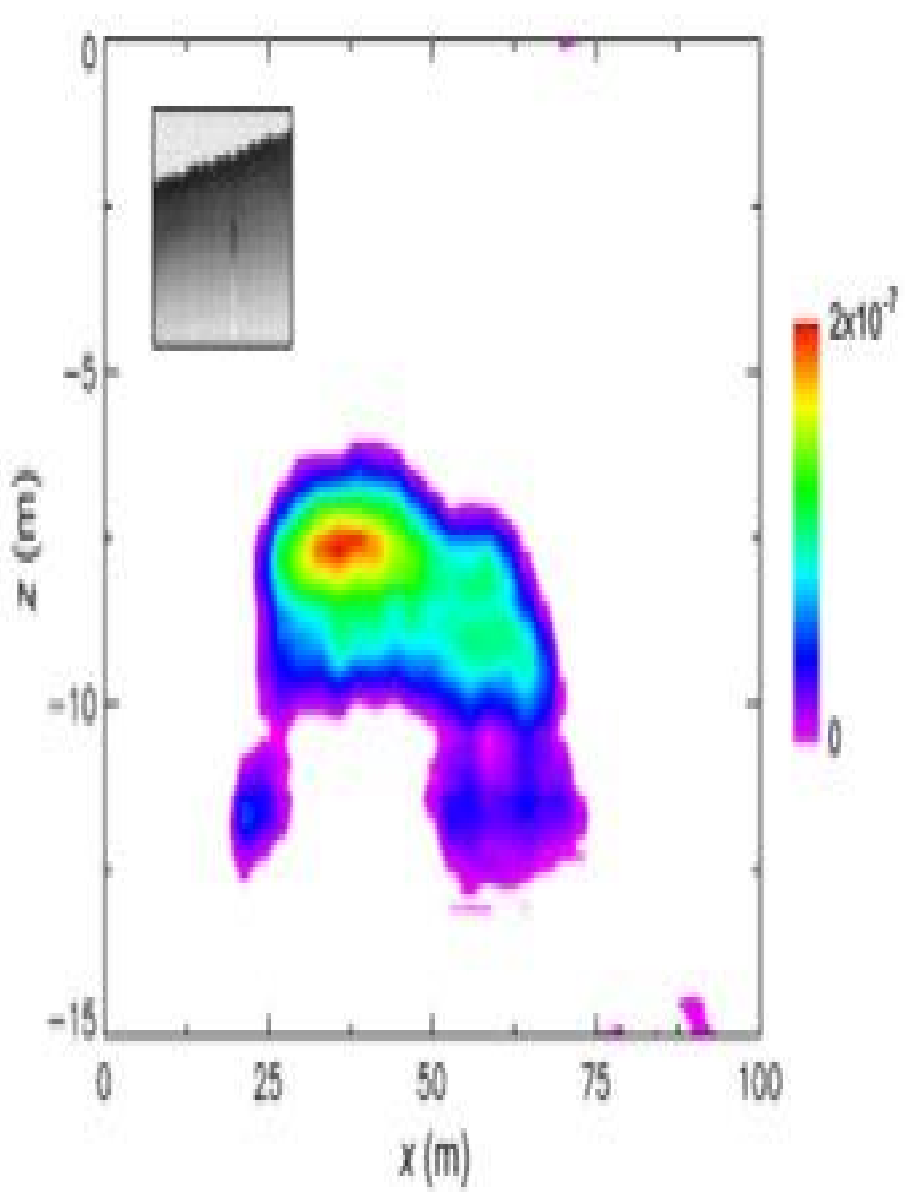
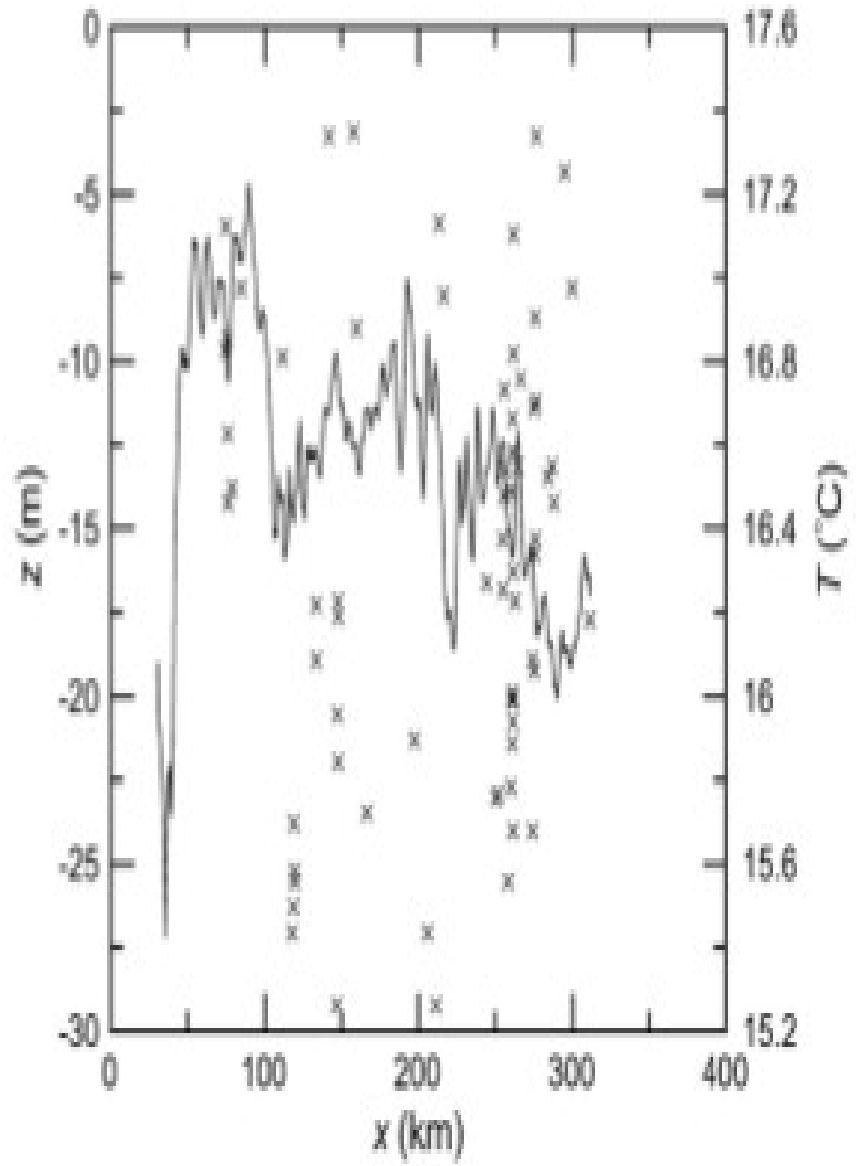


Fig. 8 Typical single-pulse return with fish signal with two-point fit to clear-water return and Gaussian fit to fish return.

Airborne Lidar: Fisheries (2/2)



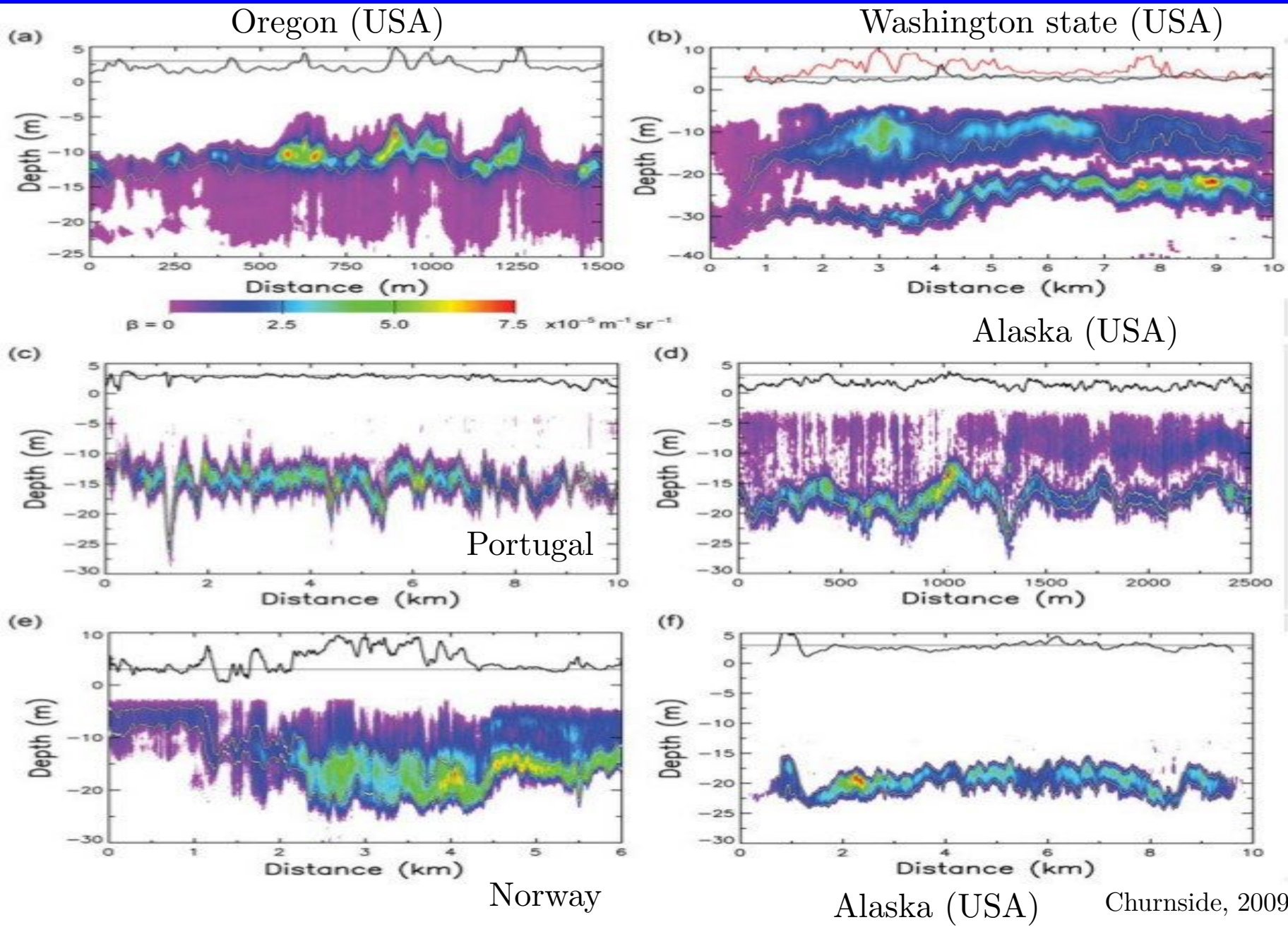
Scientific applications

- Fisheries
- **Scattering layer**
- Bio-optical properties of the upper ocean
- Vertical structure of the upper ocean
- Air bubbles
- SST
- Bathymetry
- Internal waves

Airborne lidar: Scattering layers (1/3)

- Hyp.: vertical mixing processes in the ocean upper layers sufficiently intense to limit the persistence and extend of areas thinner than few meters
- These layers can affect the biogeochemical processus in the upper ocean (primary production, HABs)
- Thin plankton layers: high concentrations of nutrients and phytoplankton found in thin layers often associated with pycnocline

Airborne Lidar : Scattering layers (2/3)

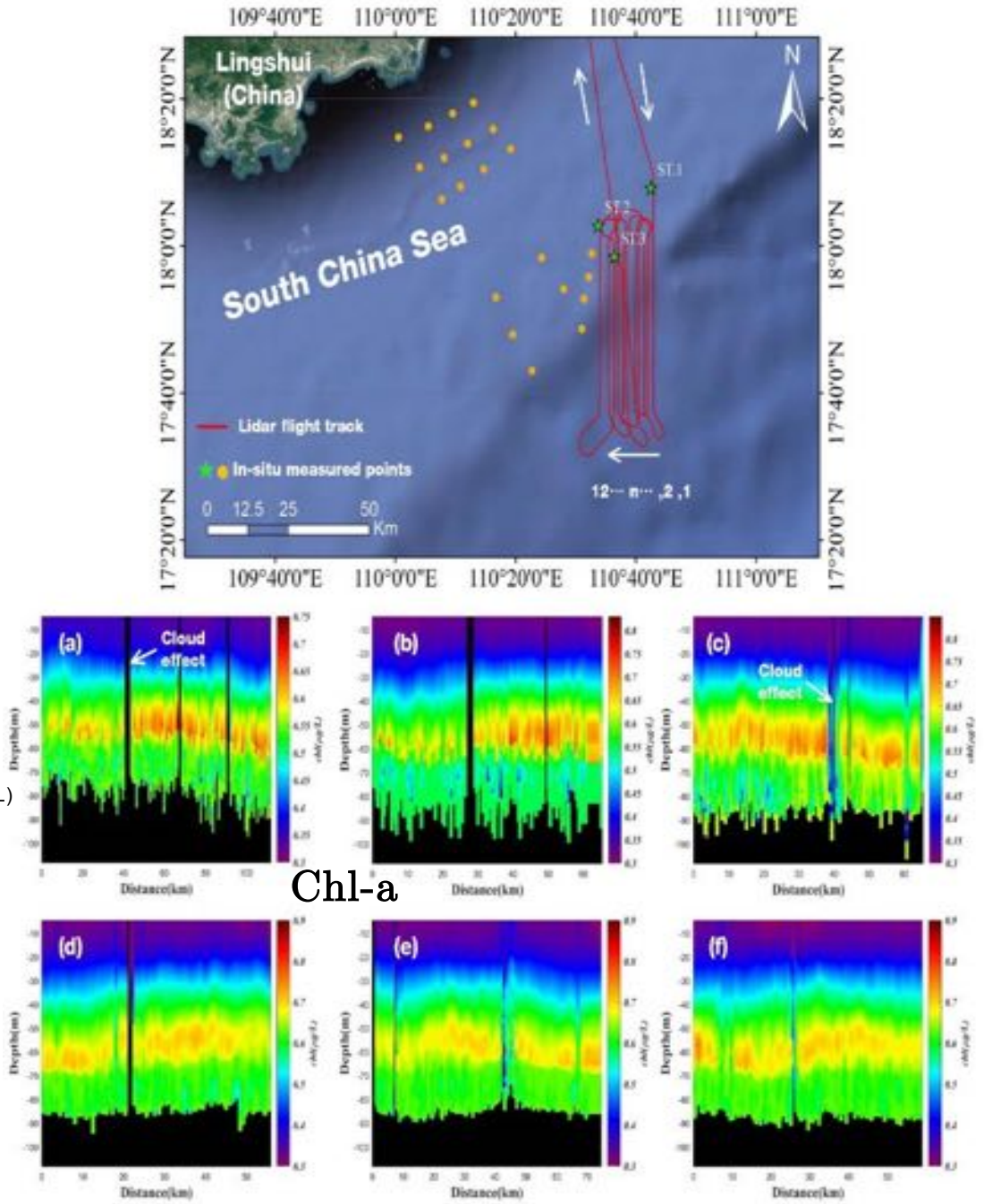
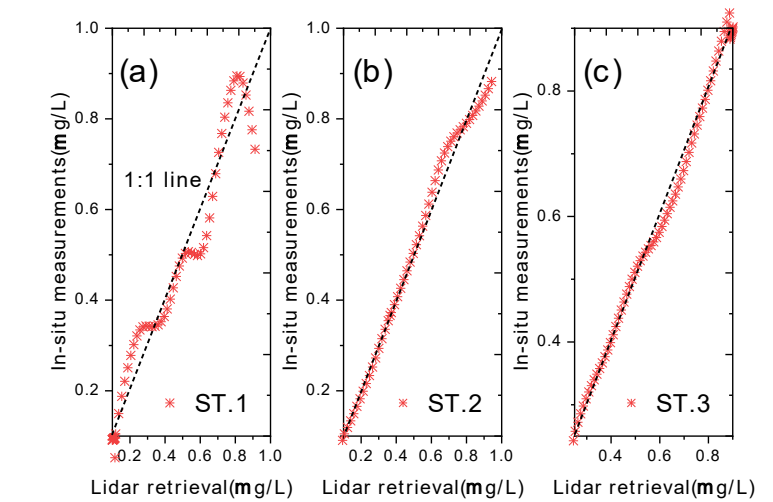
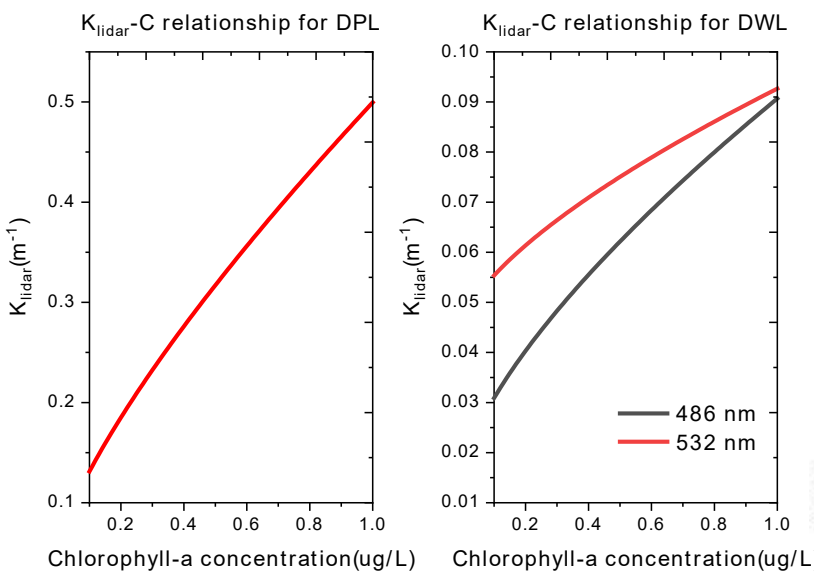


Airborne Lidar: Scattering layers (3/3)

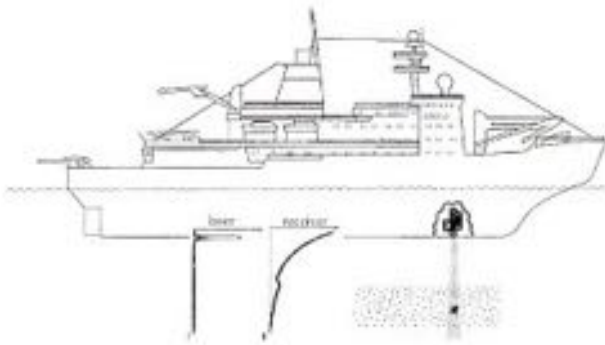
- Occurrence of thin layers and mechanisms of formation:
 - Associated with wind-driven and topographic upwelling, fresh-water influx and warm core eddies

Scientific applications

- Fisheries
- Scattering layer
- **Bio-optical properties of the upper ocean**
- Vertical structure of the upper ocean
- Air bubbles
- SST
- Bathymetry
- Internal waves



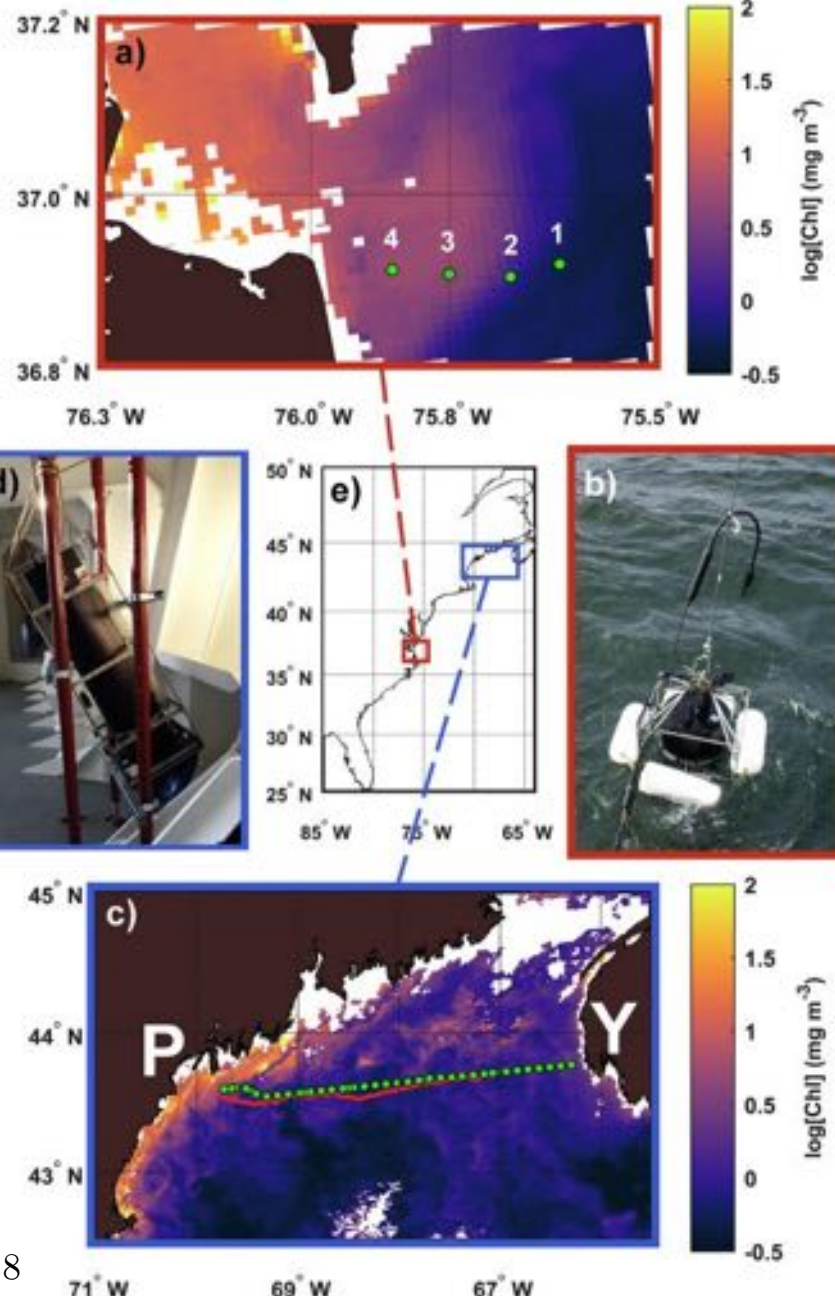
Ship-borne Lidar



Reuter et al., 1995

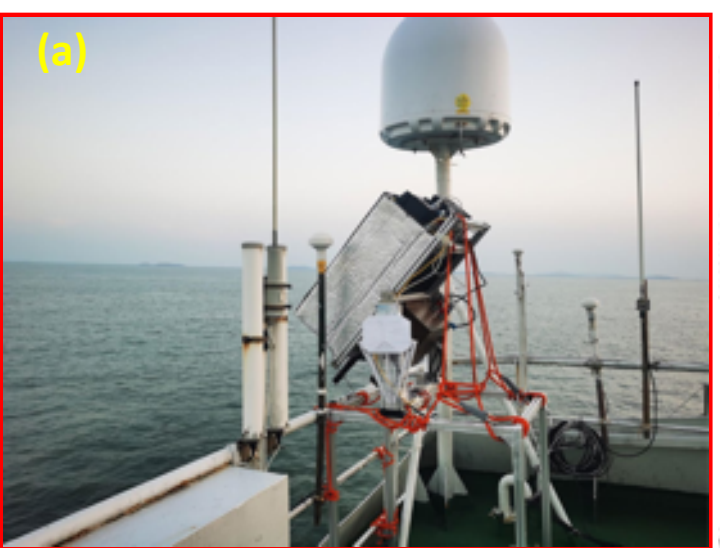


Babichenko et al., 2016

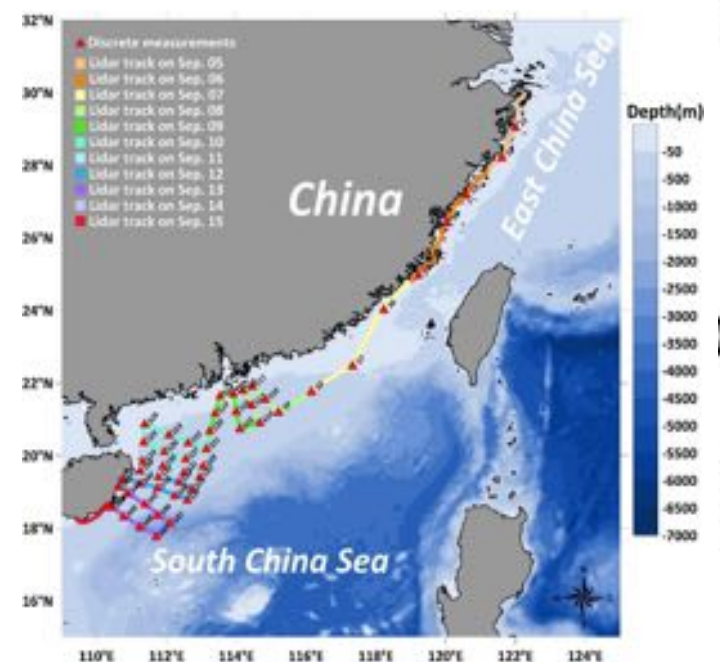


Collister et al., 2018

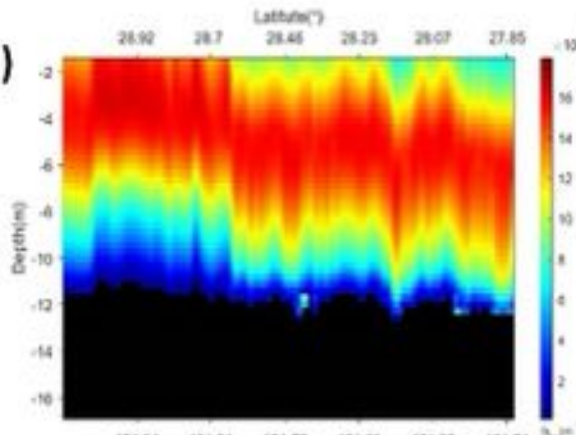
(a)



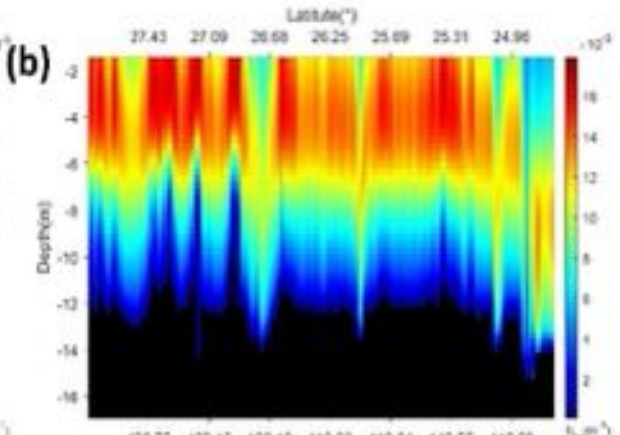
shipboard integrated Mie-Raman-fluorescence lidar



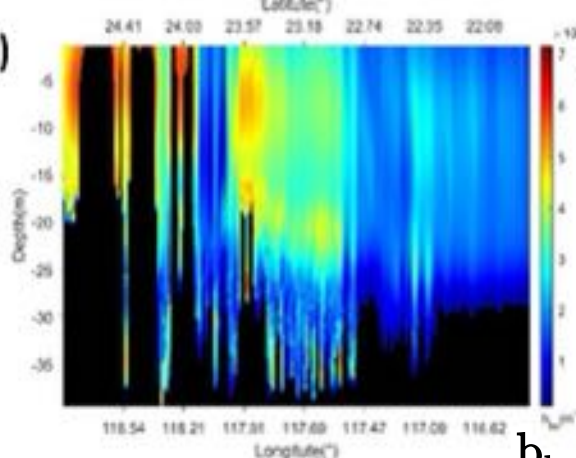
(b)



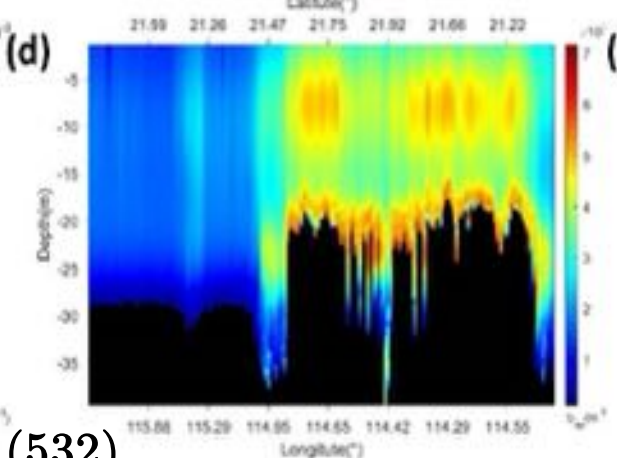
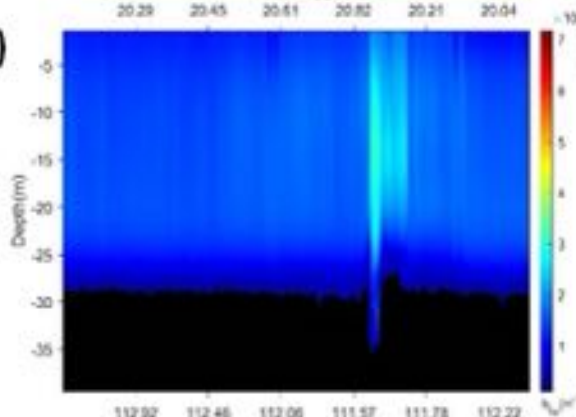
(b)



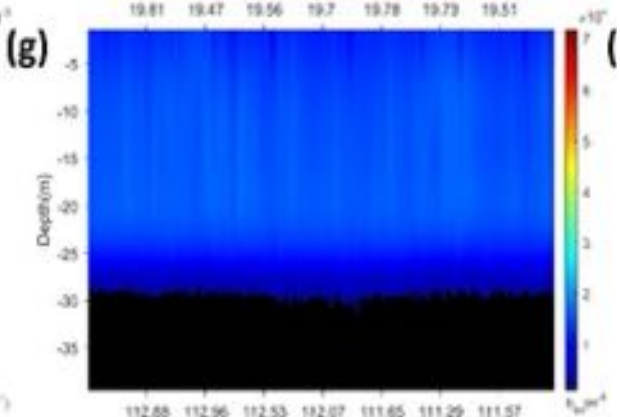
(d)



(d)

 $b_{bp}(532)$ 

(g)



(h)

(i)

(j)

(k)

(l)

(m)

(n)

(o)

(p)

(q)

(r)

(s)

(t)

(u)

(v)

(w)

(x)

(y)

(z)

(aa)

(bb)

(cc)

(dd)

(ee)

(ff)

(gg)

(hh)

(ii)

(jj)

(kk)

(ll)

(mm)

(nn)

(oo)

(pp)

(qq)

(rr)

(ss)

(tt)

(uu)

(vv)

(ww)

(xx)

(yy)

(zz)

(aa)

(bb)

(cc)

(dd)

(ee)

(ff)

(gg)

(hh)

(ii)

(jj)

(kk)

(ll)

(mm)

(nn)

(oo)

(pp)

(qq)

(rr)

(ss)

(tt)

(uu)

(vv)

(ww)

(xx)

(yy)

(zz)

(aa)

(bb)

(cc)

(dd)

(ee)

(ff)

(gg)

(hh)

(ii)

(jj)

(kk)

(ll)

(mm)

(nn)

(oo)

(pp)

(qq)

(rr)

(ss)

(tt)

(uu)

(vv)

(ww)

(xx)

(yy)

(zz)

(aa)

(bb)

(cc)

(dd)

(ee)

(ff)

(gg)

(hh)

(ii)

(jj)

(kk)

(ll)

(mm)

(nn)

(oo)

(pp)

(qq)

(rr)

(ss)

(tt)

(uu)

(vv)

(ww)

(xx)

(yy)

(zz)

(aa)

(bb)

(cc)

(dd)

(ee)

(ff)

(gg)

(hh)

(ii)

(jj)

(kk)

(ll)

(mm)

(nn)

(oo)

(pp)

(qq)

(rr)

(ss)

(tt)

(uu)

(vv)

(ww)

(xx)

(yy)

(zz)

(aa)

(bb)

(cc)

(dd)

(ee)

(ff)

(gg)

(hh)

(ii)

(jj)

(kk)

(ll)

(mm)

(nn)

(oo)

(pp)

(qq)

(rr)

(ss)

(tt)

(uu)

(vv)

(ww)

(xx)

(yy)

(zz)

(aa)

(bb)

(cc)

(dd)

(ee)

(ff)

(gg)

(hh)

(ii)

(jj)

(kk)

(ll)

(mm)

(nn)

(oo)

(pp)

(qq)

(rr)

(ss)

(tt)

(uu)

(vv)

(ww)

(xx)

(yy)

(zz)

(aa)

(bb)

(cc)

(dd)

(ee)

(ff)

(gg)

(hh)

(ii)

(jj)

(kk)

(ll)

(mm)

(nn)

(oo)

(pp)

(qq)

(rr)

(ss)

(tt)

(uu)

(vv)

(ww)

(xx)

(yy)

(zz)

(aa)

(bb)

(cc)

(dd)

(ee)

(ff)

(gg)

(hh)

(ii)

(jj)

(kk)

(ll)

(mm)

(nn)

(oo)

(pp)

(qq)

(rr)

(ss)

(tt)

(uu)

(vv)

(ww)

(xx)

(yy)

(zz)

(aa)

(bb)

(cc)

(dd)

(ee)

(ff)

(gg)

(hh)

(ii)

(jj)

(kk)

(ll)

(mm)

(nn)

(oo)

(pp)

(qq)

(rr)

(ss)

(tt)

(uu)

(vv)

(ww)

(xx)

(yy)

(zz)

(aa)

(bb)

(cc)

(dd)

(ee)

(ff)

(gg)

(hh)

(ii)

(jj)

(kk)

(ll)

(mm)

(nn)

(oo)

(pp)

(qq)

(rr)

(ss)

(tt)

(uu)

(vv)

(ww)

(xx)

(yy)

(zz)

(aa)

(bb)

(cc)

(dd)

(ee)

(ff)

(gg)

(hh)

(ii)

(jj)

(kk)

(ll)

(mm)

(nn)

(oo)

(pp)

(qq)

(rr)

(ss)

(tt)

(uu)

(vv)

(ww)

(xx)

(yy)

(zz)

(aa)

(bb)

(cc)

(dd)

(ee)

(ff)

(gg)

(hh)

(ii)

(jj)

(kk)

(ll)

(mm)

(nn)

(oo)

(pp)

(qq)

(rr)

(ss)

(tt)

(uu)

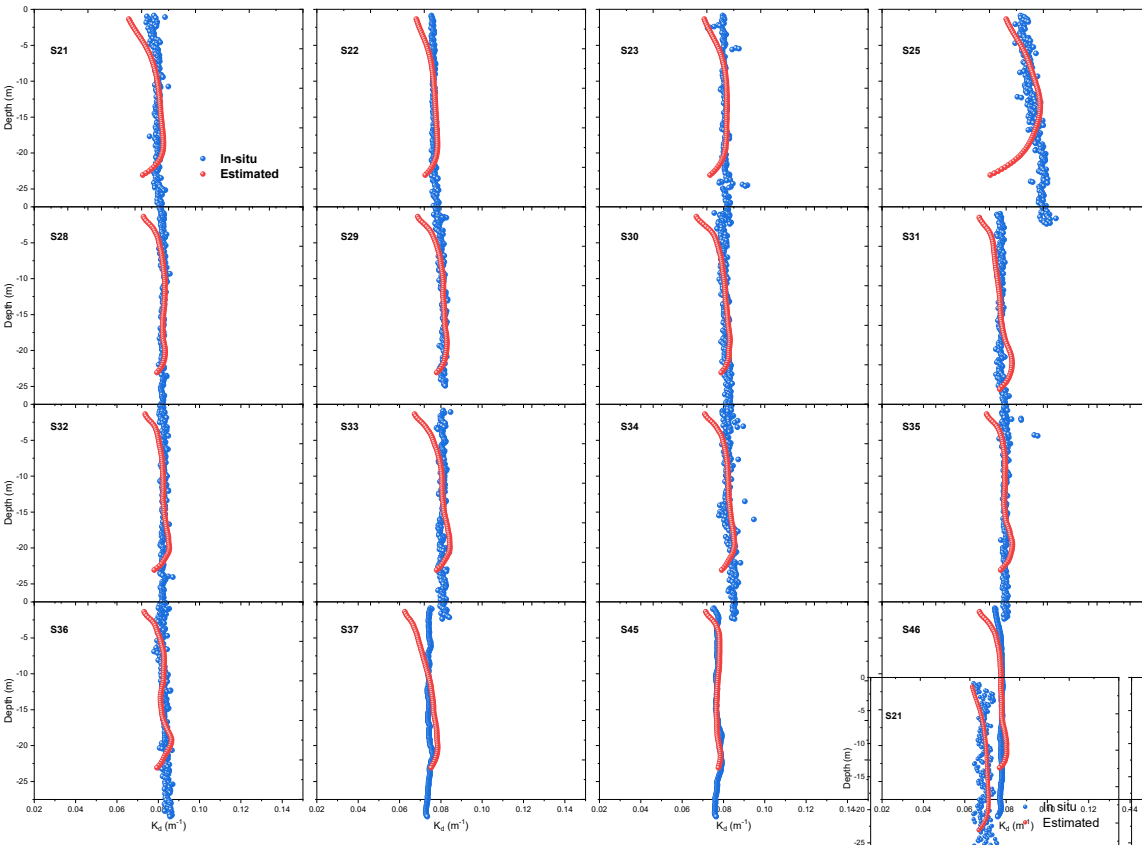
(vv)

(ww)

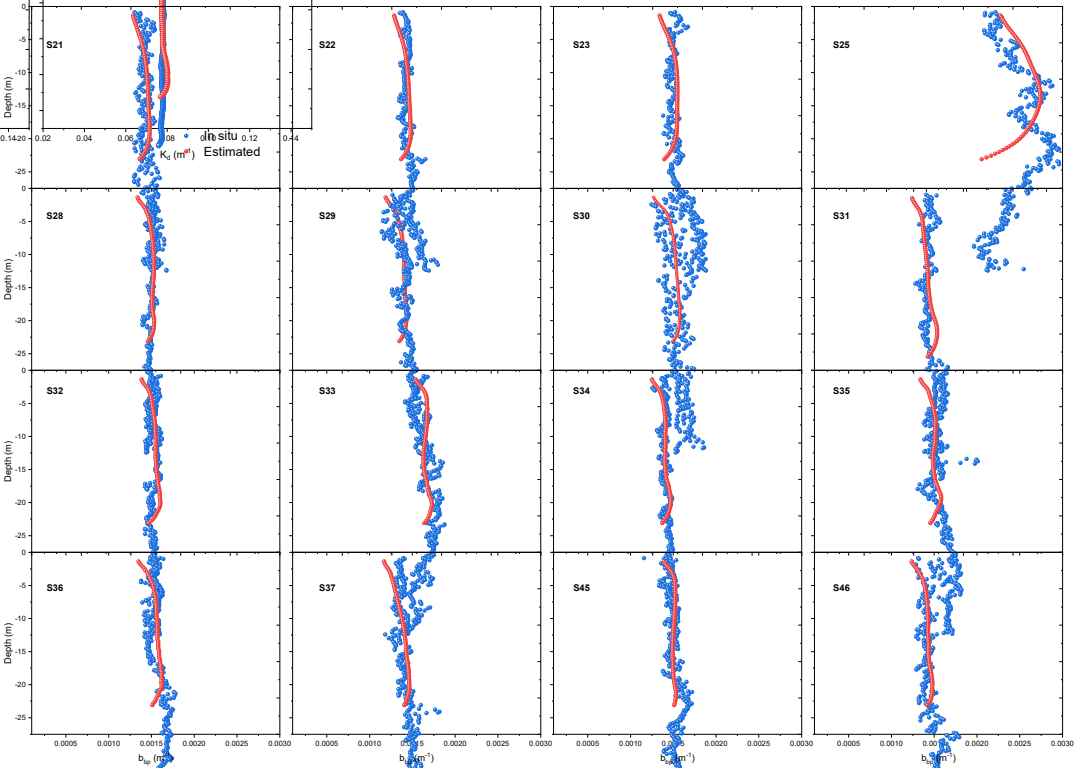
(xx)

(yy)

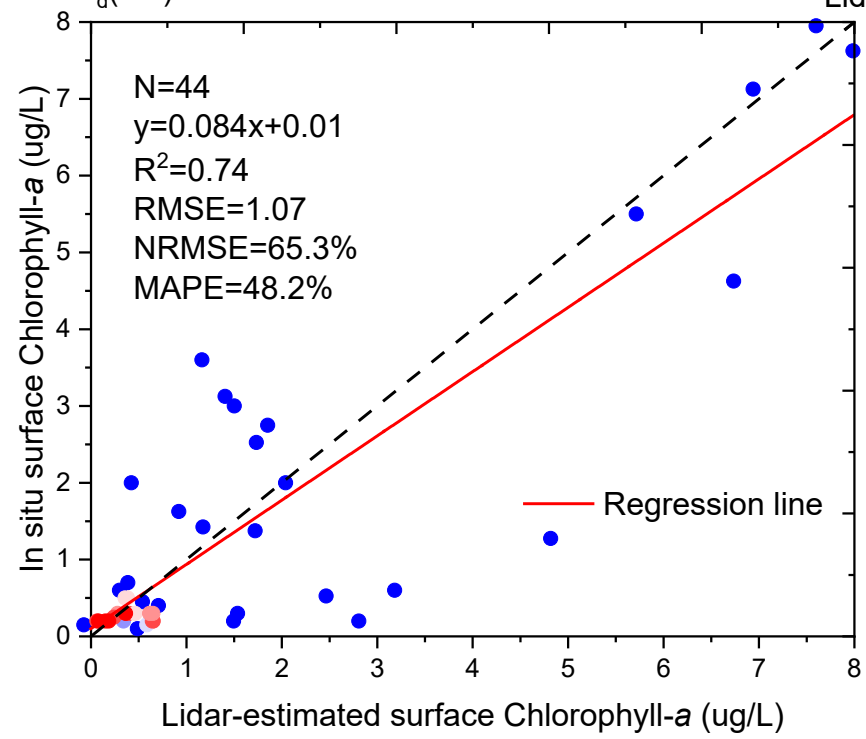
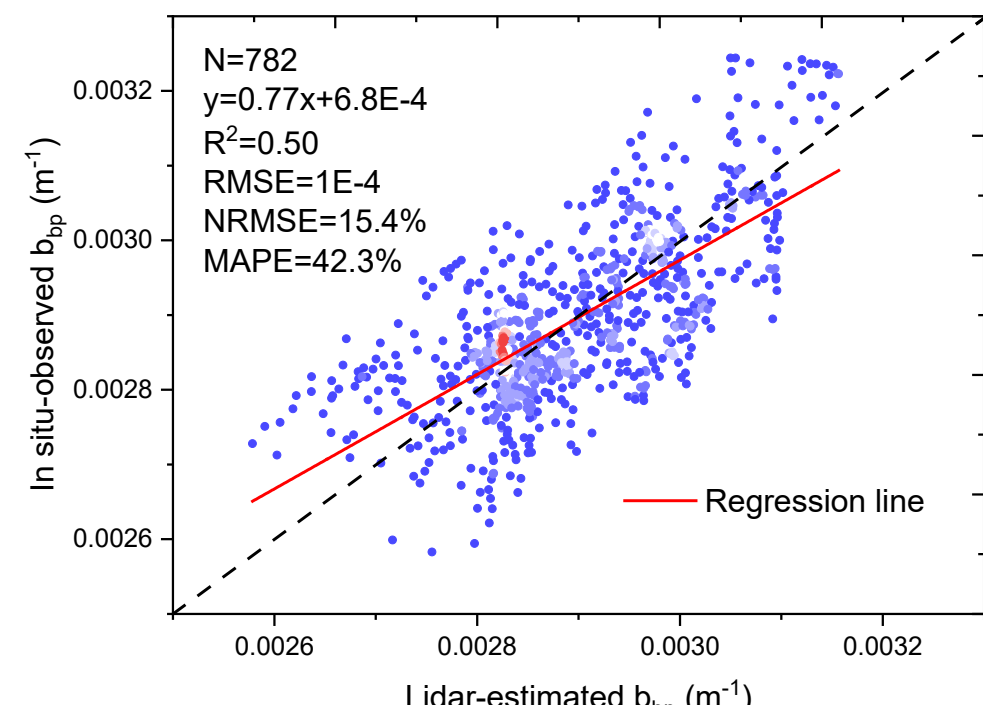
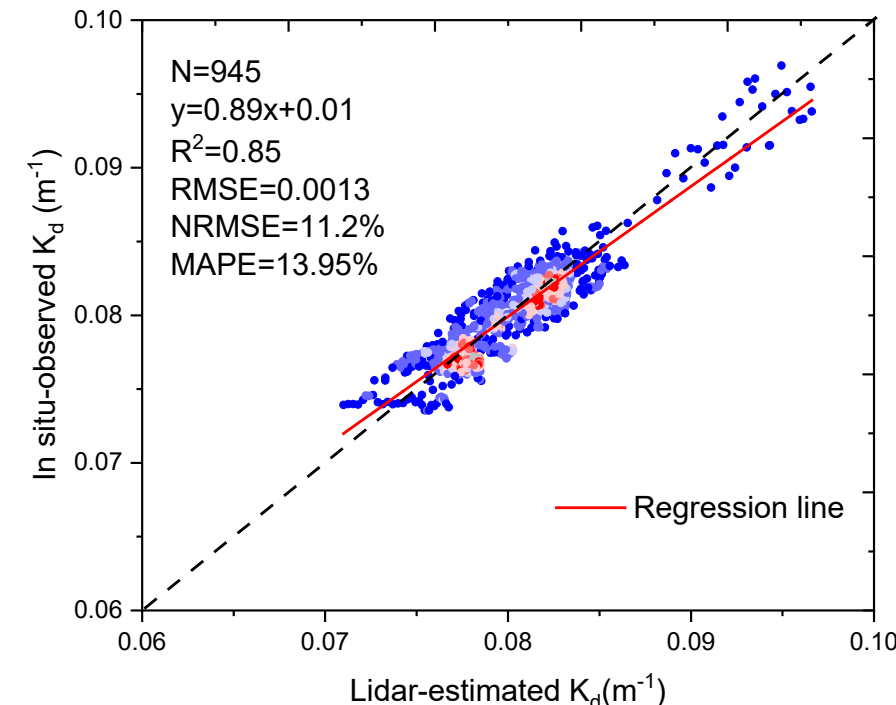
(zz)

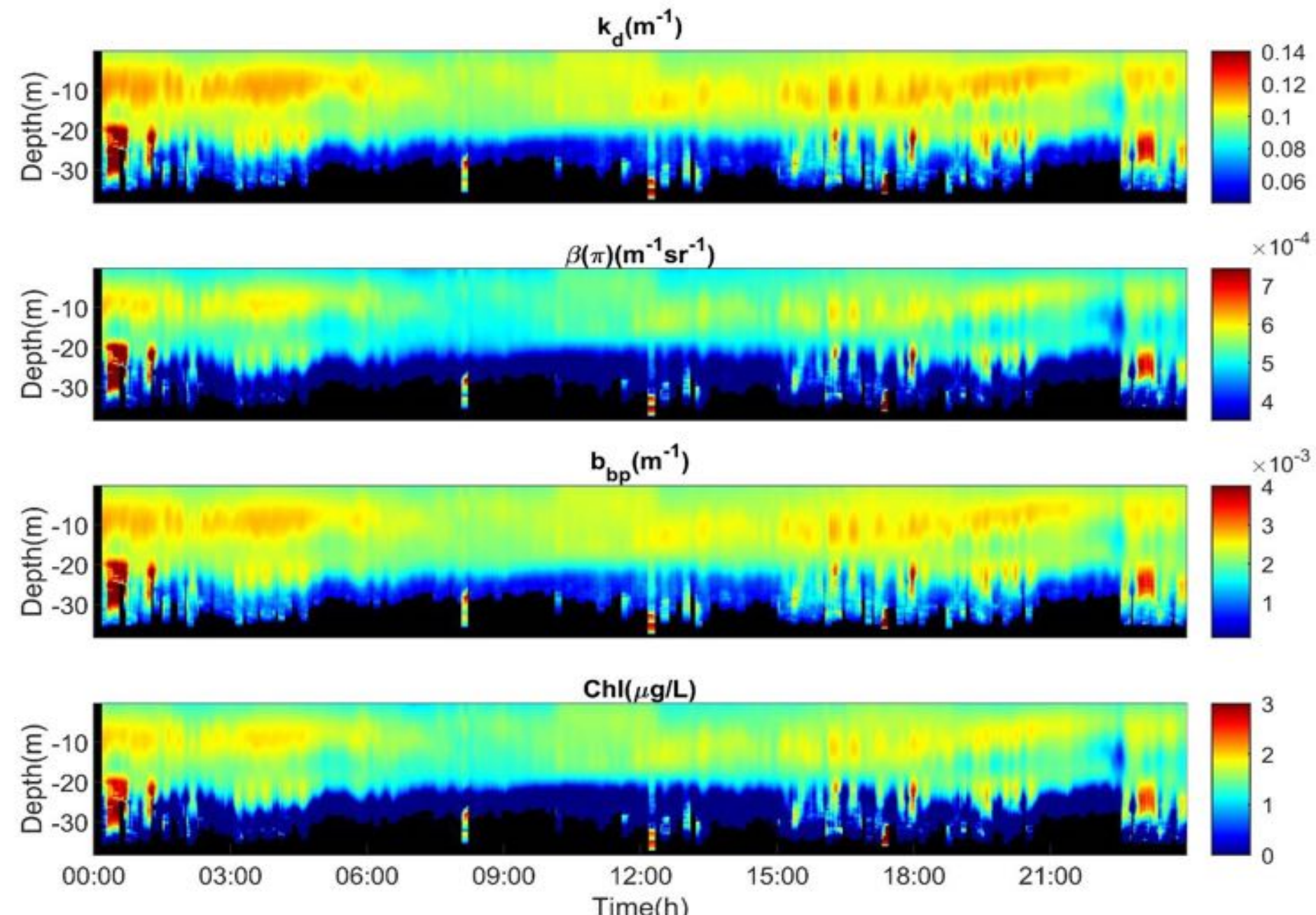


K_d



b_{bp}





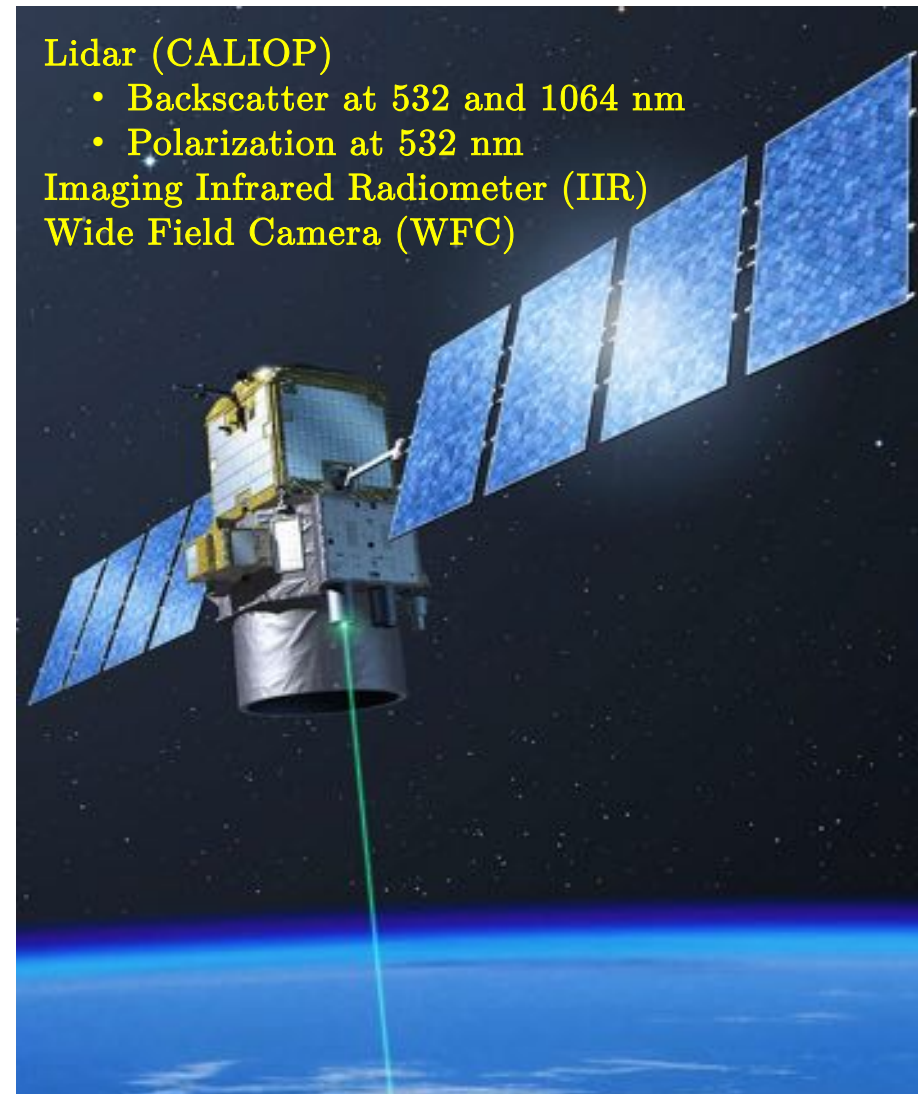
Vertical distributions of IOPs and chlorophyll-a obtained by lidar throughout the whole daytime at the fixed station (110.4434°E, 18.6024°N) on September 14, 2020. The panels from the top to the bottom are K_d , $\beta(\pi)$, b_{bp} , and chlorophyll-a, respectively.

Space-borne lidar

→ Lidar techniques can overcome these issues (Churnside, 2014; Hostetler et al., 2018; Jamet et al., 2019)

Cloud-Aerosol Lidar and Infrared Pathfinder Satellite Observations (CALIPSO)

- Instruments
 - Lidar
 - Imaging Infrared Radiometer (CNES)
 - Wide Field Camera
- Objective global profiling of cloud and aerosols for radiation budget applications
- 14 years of operations in the A-train constellation!
 - Proved the lidar could be capable of high reliability and long lifetime in space



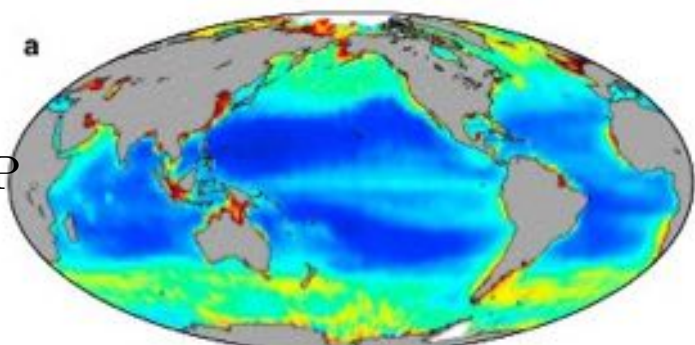
Space-borne lidar

→ Lidar techniques can overcome these issues (Churnside, 2014; Hostetler et al., 2018; Jamet et al., 2019)

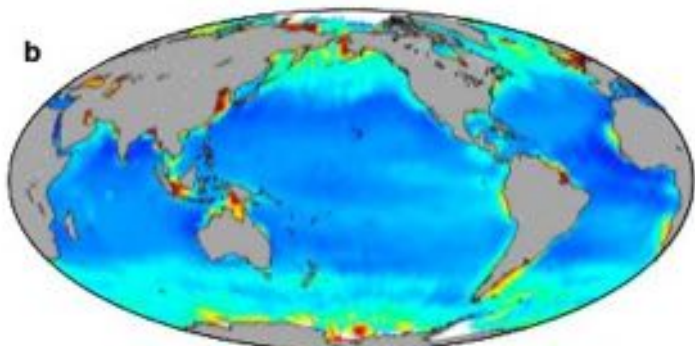
- CALIPSO:
 - Launched in 2006 and still in operation
 - Laser at 532 and 1064 nm
 - Dedicated to aerosol and clouds studies
 - Studies showed that it could be used of ocean color (Behrenfeld et al., 2013, 2016, 2019; Dionisi et al., 2020; Lu et al., 2014)
 - Coarse vertical resolution (22 meters) preventing to get profiles

Ocean color: back-scattering coefficient

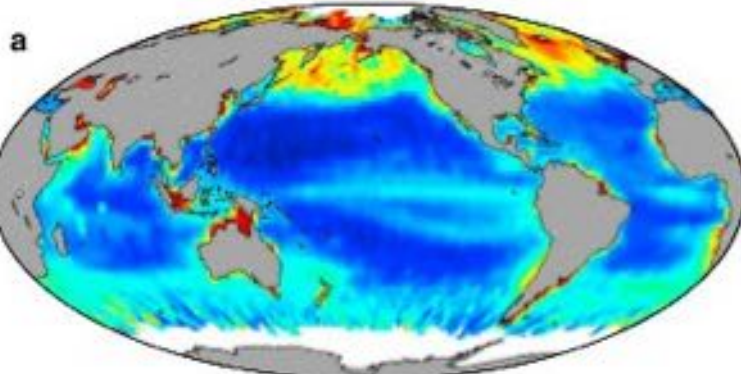
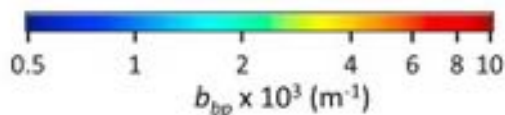
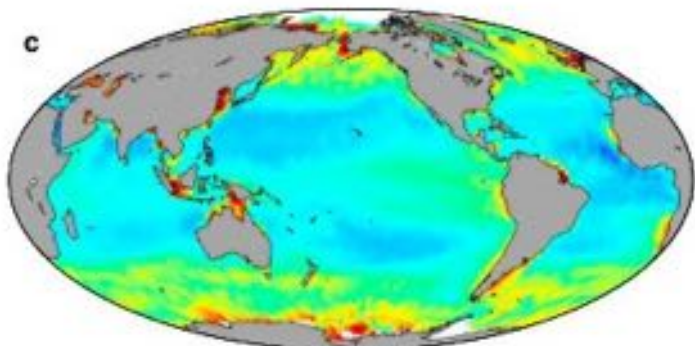
CALIOP



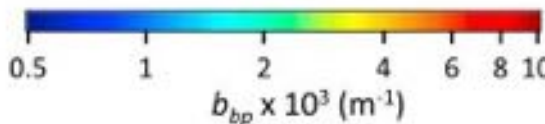
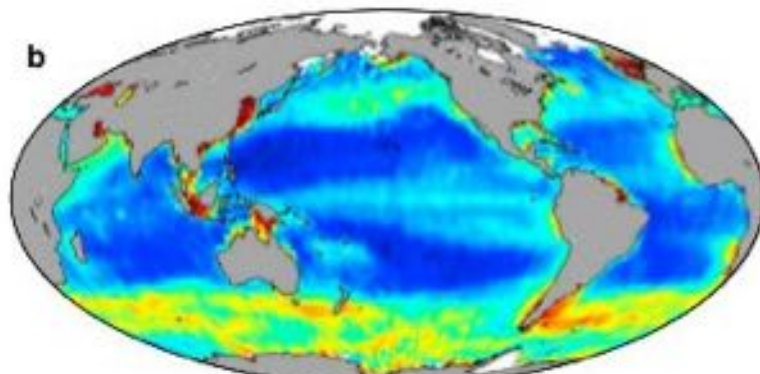
b



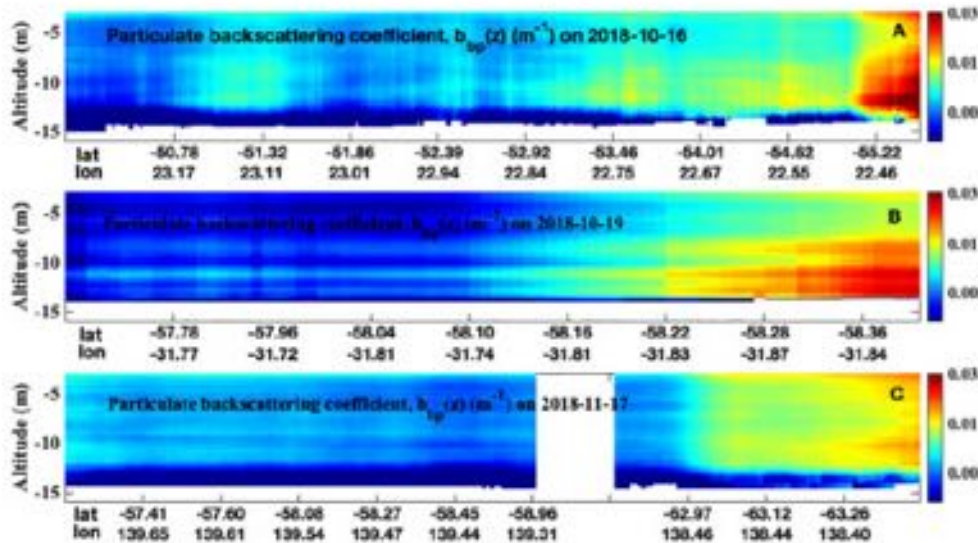
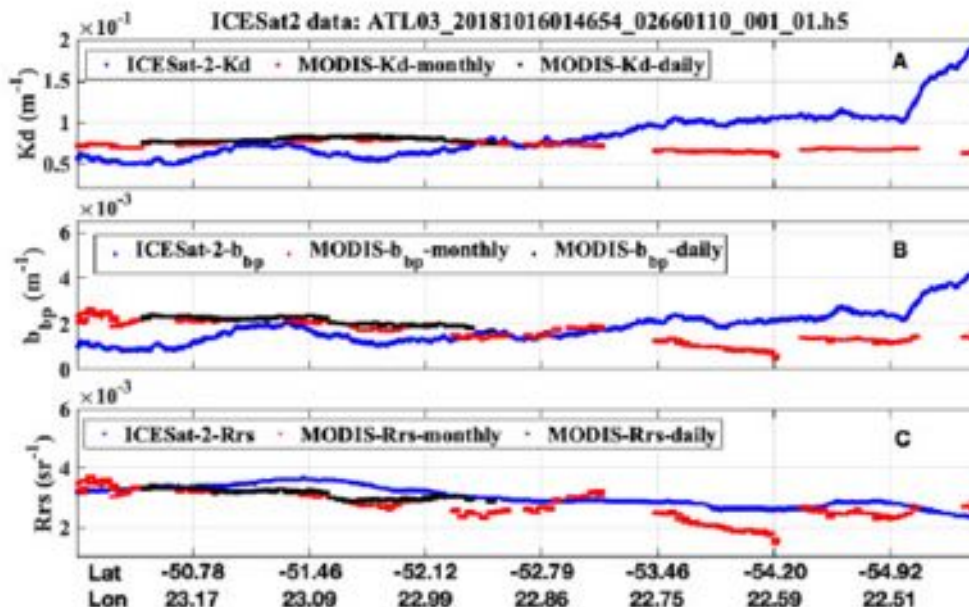
c



b



IceSat-2: Profiles of b_{bp}



Study of the polar areas

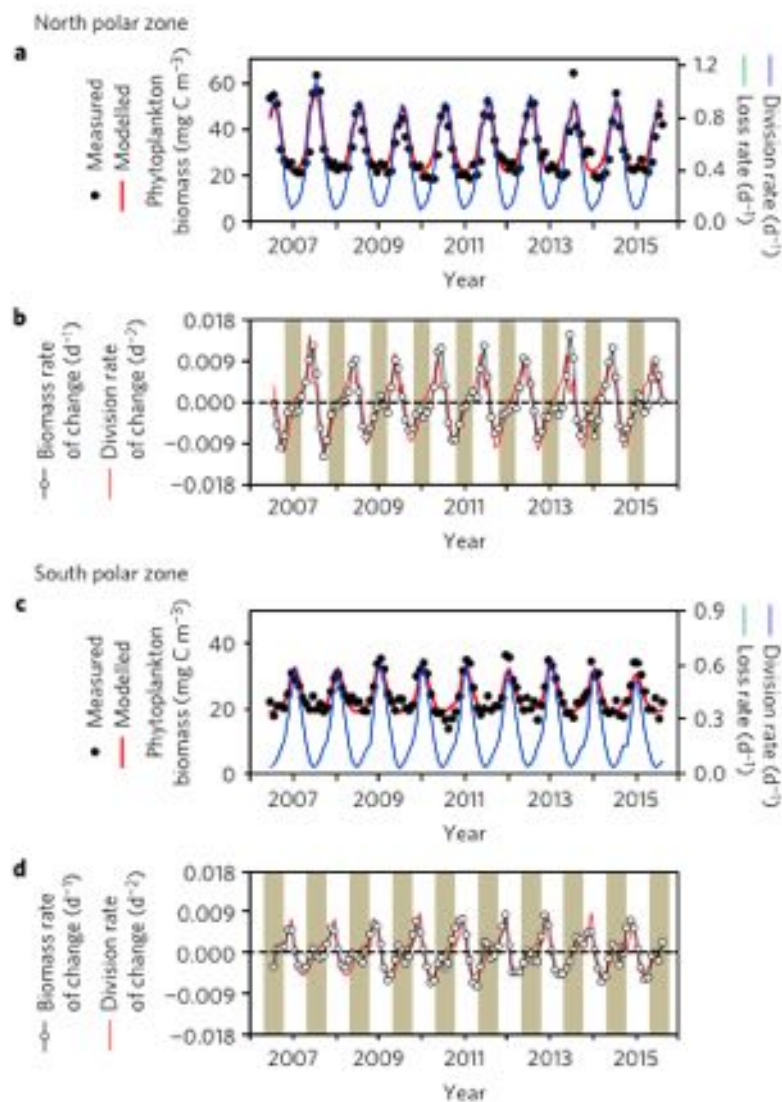
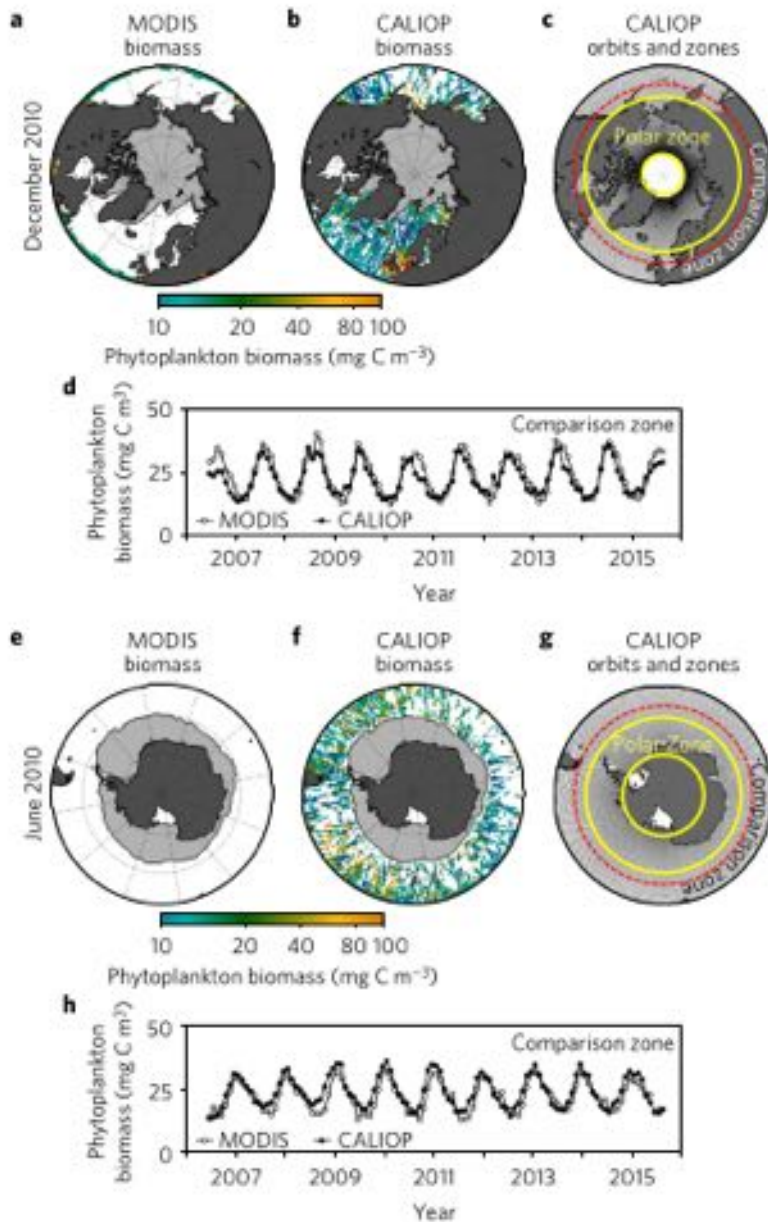
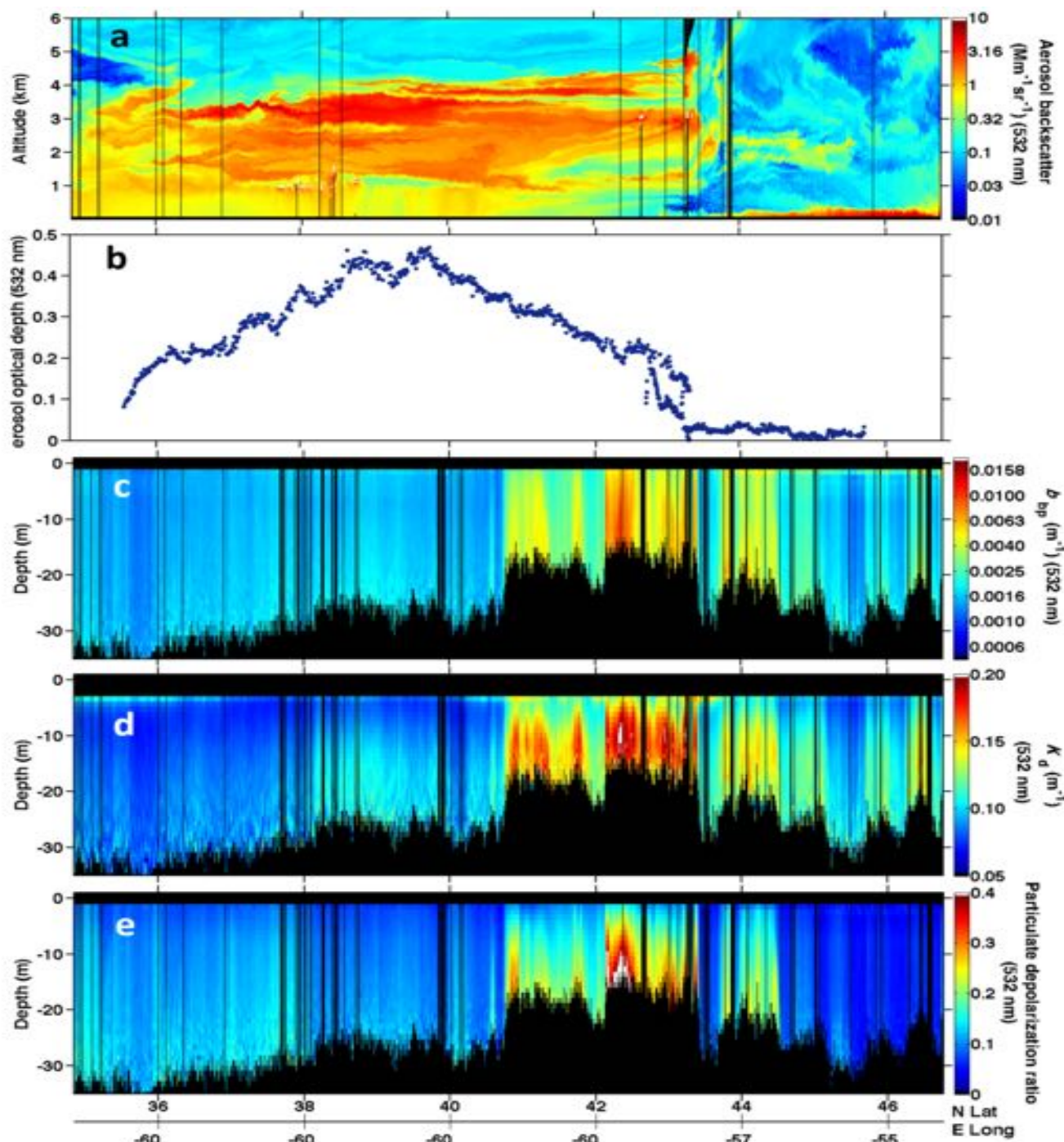
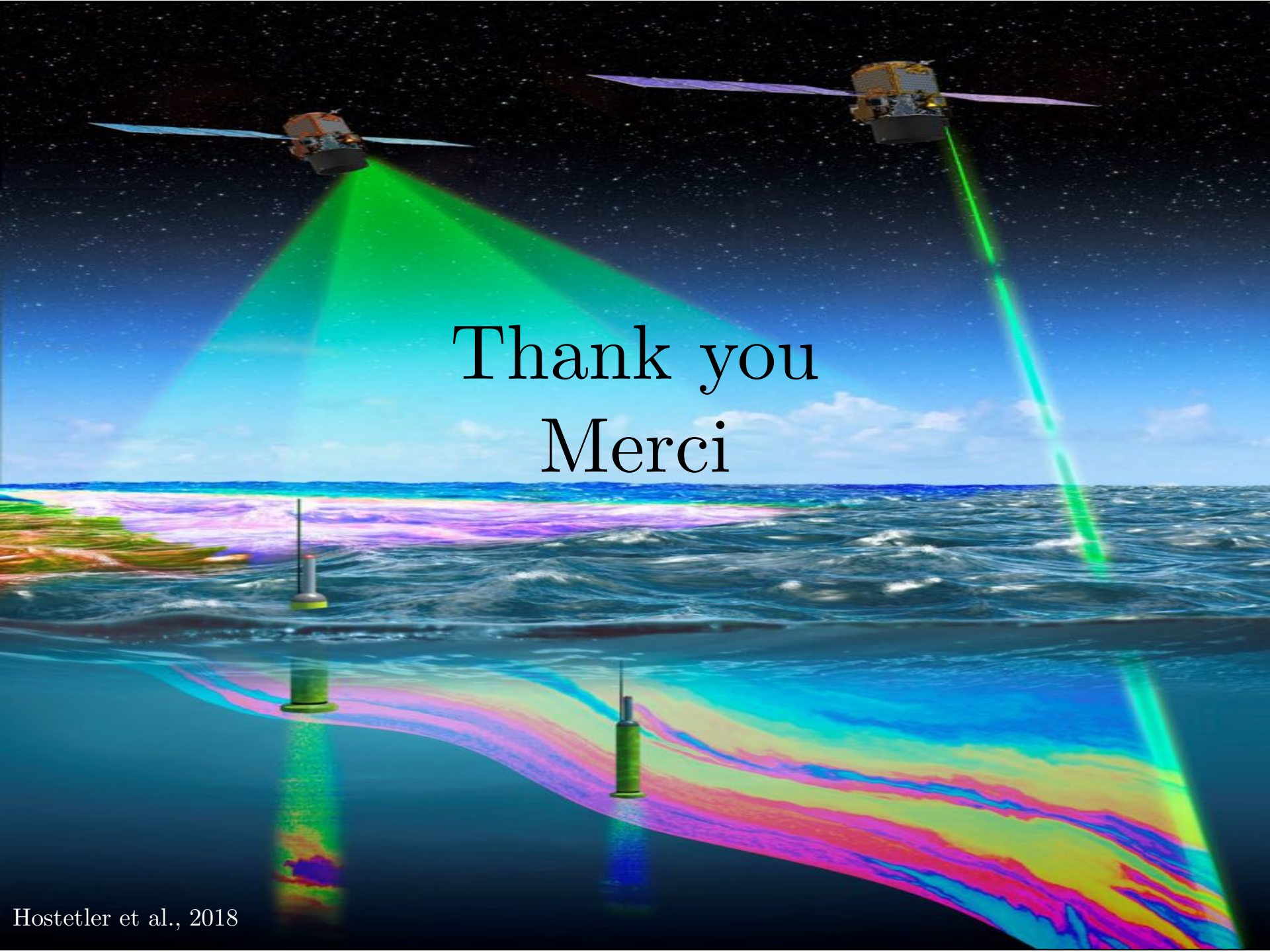


Figure 2 | Polar phytoplankton cycles. a,c. Black symbols: CALIOP monthly mean phytoplankton biomass (C). Blue line: phytoplankton division rates (μ). Green line: phytoplankton loss rates (λ), which are indistinguishable





Thank you
Merci